Report on SES environmental status based on modeling and remote sensing tools

PERSEUS Deliverable D4.12

Project Full title	Policy-oriented marine Environmental Research in the Southern EUropean Seas		
Project Acronym	PERSEUS		
Grant Agreement No.	287600		
Coordinator	Dr. E. Papathanassiou		
Project start date and duration	1st January 2012, 48 months		
Project website	www.perseus-net.eu		
Deliverable Nr.		**Deliverable Date**	
Work Package No	4		
Work Package Title	Developing integrated tools for environmental assessment.		
Responsible	Marco Zavatarelli (CoNISMa-UNIBO)		
Authors & Institutes Acronyms	M.Zavatarelli (CoNISMa-UNIBO), S. Libralato, C. Solidoro (OGS), C.Estournel (UPS-LA), I. Catalan (CSIC), K. Tsagarakis (HCMR), M. Gregoire, A. Capet (ULg), J.Staneva (USOF), B.Salihoglu (METU)		
Status:	**Final (F)**	•	
	Draft (D)		
	Revised draft (RV)		
Dissemination level:	**Public (PU)**	•	
	Restricted to other program participants (PP)		
	Restricted to a group specified by the consortium (RE)		
	Confidential, only for members of the consortium (CO)		

CONTENTS

EXECUTIVE SUMMARY / ABSTRACT

This deliverable collects the working report of all the research units involved in PERSEUS WP4 and concerning the environmental assessment of the marine ecosystem carried out via numerical modeling and remote sensing.

Coherently with the WPO4 general objectives and general framework, the assessment has been carried out by focusing on the basic ecosystem properties that underlies the health of the ecosystem

SCOPE

In PERSEUS WP4 numerical models and remote assessment techniques have been engaged to provide a wide integrated assessment of the Marine ecosystem status of the Southern European Seas encompassing the “ecosystem end to end” framework and based on fundamental ecosystem properties. This on the assumption that such properties are underlying the EU-MSFD vision for the “Good Environmental Status”.

REGIONAL ASSESSMENT

Mediterranean Sea

Northern Adriatic Sea (CoNISMa-UNIBO)

Methodology

The used modelling system is based on the on-line coupling of the general circulation model NEMO (Nucleus for European Modelling of the Ocean; http://www.nemo-ocean.eu, version 3.4) with the lower trophic level biogeochemical Model BFM (Biogeochemical Flux Model, Vichi et al. 2015, http://bfm-community.eu). The system is implemented in the Northern Adriatic Sea with a horizontal resolution of 800 m and 48 vertical z-levels. Surface forcing data were provided from ECHAM5 regional climate simulations (Scoccimarro et al., 2011). Initial conditions and open boundary data and, have been obtained from Mediterranean Sea circulation NEMO based simulations (Lovato et al., 2013), forced with the same atmospheric data used here. Open boundary conditions followed Oddo et al. (2008). The land based river runoff and nutrient load data adopted considers 16 major Adriatic Rivers whose data were obtained from the PERSEUS Deliverable D4.3 Open boundary and initial conditions for BFM state variables were taken from BFM-POM (Princeton Ocean Model-Biogeochemical flux Model) Adriatic Sea simulations. The full NEMO-BFM coupling simulations span the period 1996-2010; here we show the results for the period 1996-2009.

The assessment carried out has been based on the ecosystem properties defining the ecosystem health: Vigor, Organisation, Resilience (Costanza and Mageau, 1999). Here the main emphasis is put on the “vigor” and “organisation” properties, while the “resilience is addressed in the deliverable D4.9.

The “vigor” of a system is simply a measure of its productivity. The organization of a system refers to the number and diversity of interactions between the components of the system.

A model based assessment dictates a preliminary evaluation of the skill of the model in replicating observed feature of the environmental dynamics under analysis. This has been done by comparing the model results with the remotely sensed satellite based observation (1998-2007) of primary productivity and phytoplankton populations structure made available to the PERSEUS project trough deliverable 4.7.

River Forcing

The Northern Adratic Sea runoff and nutrient load is particularly important in determining the variability of the Marine ecosystem. The time runoff and nutrient load time series for the Adriatic Rivers discharging into the Adriatic Sea (fig. 1)

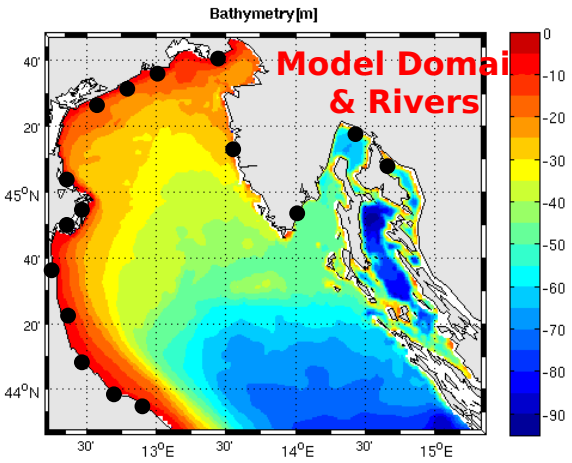

Fig.1: The northern Adriatic Sea models domain and bathymetry. Black dots indicate the location of the rivers discharging into the basin.

taken from PERSEUS deliverable 4.3 are shown in Fig. 2

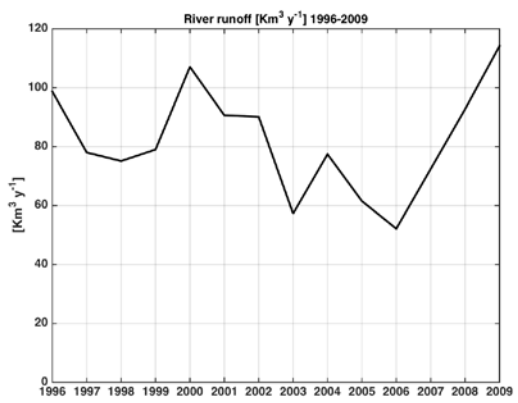

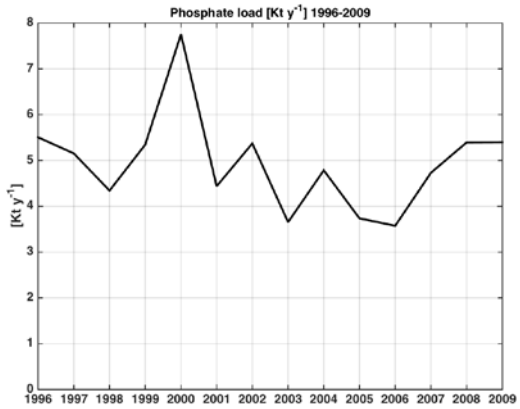

Fig.2: time series 1996-2009 of northern Adriatic Sea river runoff (left) and phosphate load (right). Expressed in annual values.

The runoff time series (Fig. 2, left) show a significant interannual variability of the total fresh water input into the basin with values ranging from about 50 to 115 km^3/y and marked by an overall reduction of the total runoff for the period 2000-2006. After that the runoff started to increase again to reach the maximum value at the end of the period considered. A similar pattern is observed also in the time series of the phosphate load but it has to be noted that despite the strong 2006-2009 runoff increase the phos[hate load show only a moderate increase with waue quite far from the maximum load observed in 2000 and corresponding also to an increase of the runoff.

Vigor of the ecosystem

We start the analysis of the productive capacity of the system by providing a comparison between the simulated surface gross primary productivity with the corresponding remotely (satellite) sensed observations for the period covered by the SeaWifs sensor activity.

Figure 3 provide a visual comparison between model results and satellite annually average distribution of the vertically integrated gross primary productivity (gC $m^{-2}d^{-1}$).

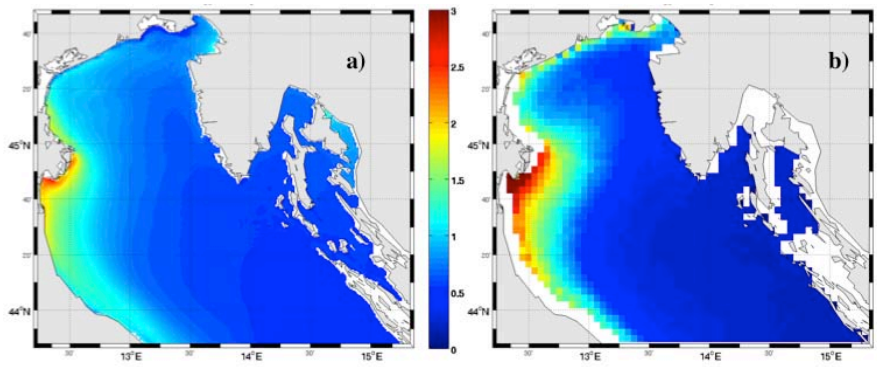

Fig.3: gross primary productivity (gC $m^{-2}d^{-1}$) as simulated by the model (a) and as observed by SeaWifs (b).

The satellite map shows that the most productive areas, are the coastal areas most directly affected by river discharge, notably the Po delta area. Productivity decreases rapidly with a coastal to offshore west-east gradient. This pattern is replicated by the numerical simulation. The overall distribution of the model based productivity is in good qualitative agreement with the observation, however with a degree of underestimation in the coastal areas and a slight overestimation in the offshore regions.

The productivity seasonal cycle described from the satellite observations (fig 4) is

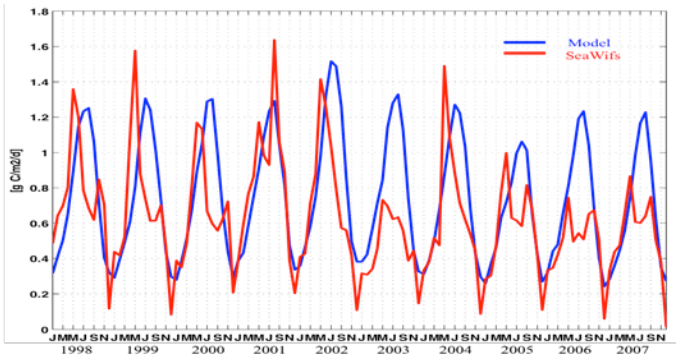

Fig. 4. Time series of gross primary production (g $Cm^{-2}d^{-1}$) from the model and estimated primary production (g $Cm^{-2}d^{-1}$) from satellite data (Marullo et al., 2013) for the period 1998-2007.

characterised by a winter to summer progressive increase, sometimes with a double peak characteristics. The model grossly captures such pattern, with an overall agreement in magnitude (although with a temporal shift in the timing of the peak) for the period 1998-2004. Subsequent years shows a remotely observed seasonal cycle characterised by a double peak, a pattern that apparently the model is not able to capture.

A more objective attempt to evaluate the reliability of the model against the remotely observed data, has been attempted by compiling the Taylor diagram relative to the annually averaged surface chlorophyll concentration and the gross primary productivity (Fig. 5).

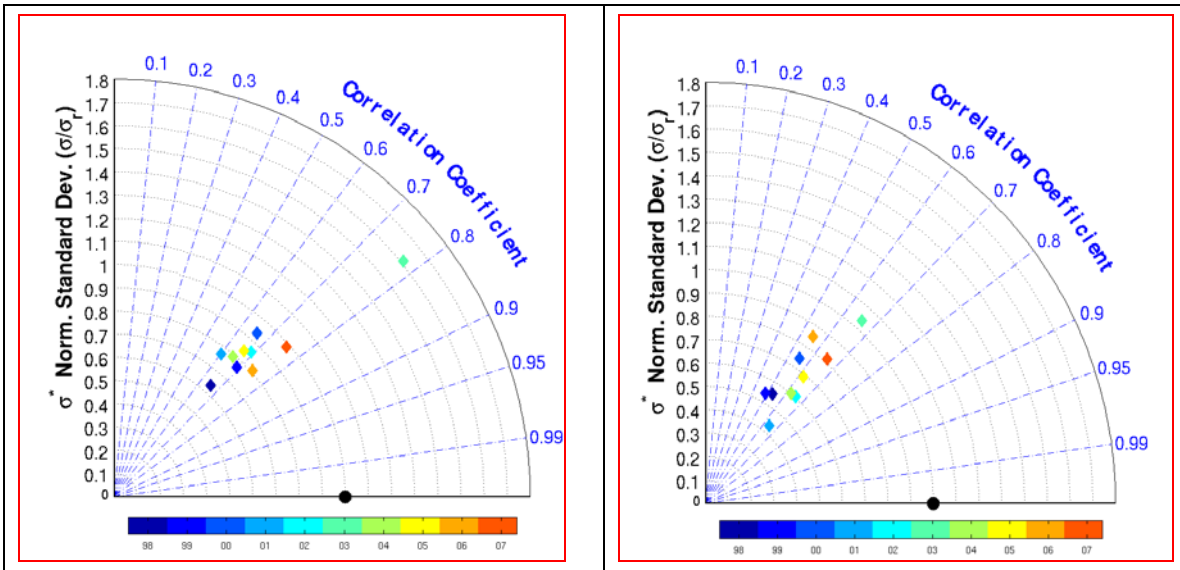

Fig.5: Comparison model-satellite. Taylor diagrams for the annually averaged surface chlorophyll concentration (left) and the gross primary productivity (right).

The comparison show for both properties analysed a relatively high correlation coefficient (about 0.7 for Chlorophyll and about 0.6 for GPP). The variability of the nnually averaged values is also indicated in the diagrams and indicates an overall agreement for chlorophyll while the simulated GPP seems to have a smaller variability with respect to the remote observations.

As a preliminary conclusion it cam be therefore stated that the model has some skill in capturing the overall spatial and temporal variability pf the primary producers dynamics. However the discrepancies between simulations and observations allow a comparison only at the level of spatially and temporally integrated quantities.

The primary production “Vigor” as simulated by the model is now shown at the level of seasonal variability in fig. 6 that show the seasonally averaged distribution of GPP .

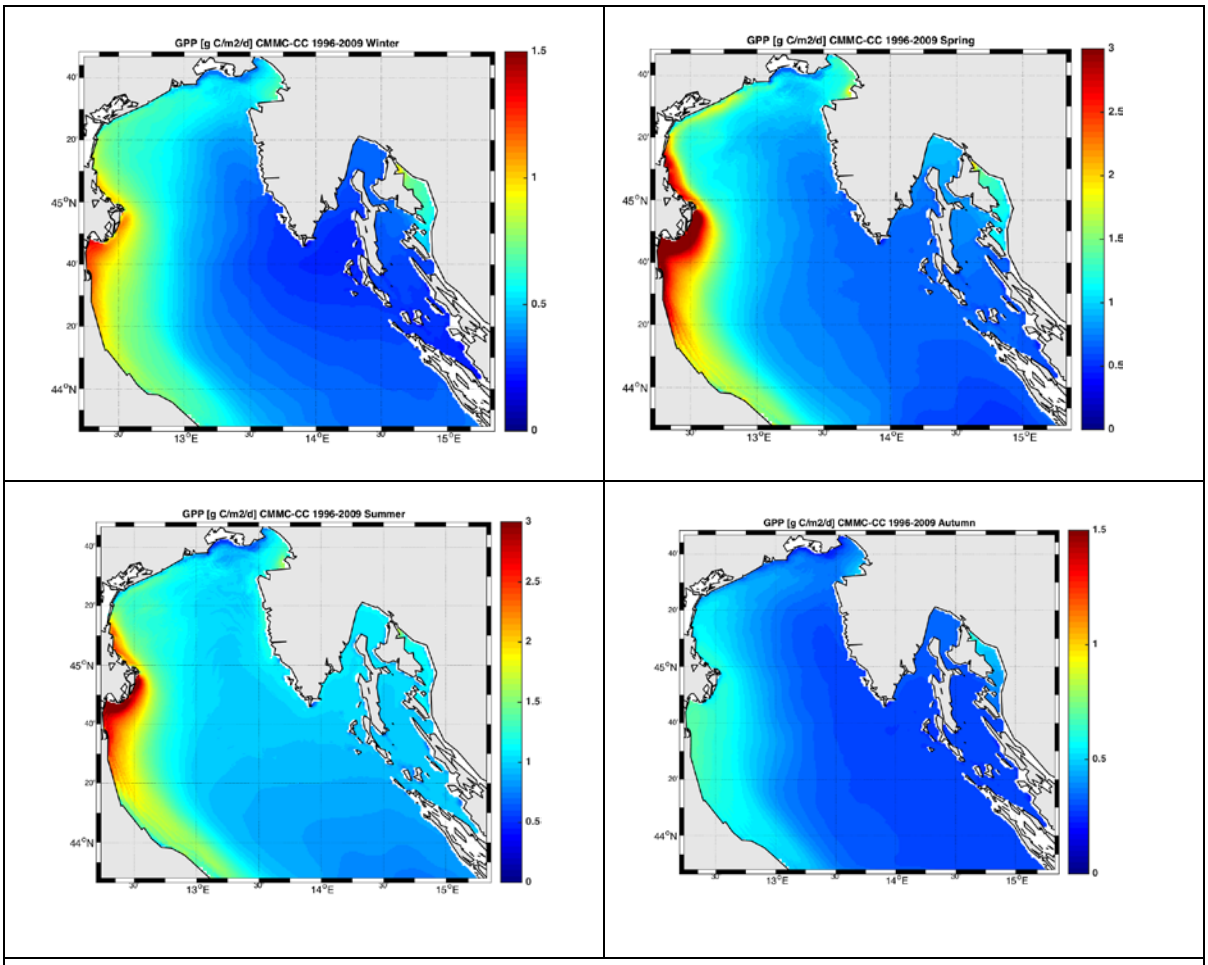

Fig. 6: seasonally averaged gross primary productivity (gC $m^{-2}d^{-1}$). Note the different color scale adopted for winter-autumn with respect to spring-summer.

The seasonal variability of the GPP distribution reflect the patterns described previously about the annual distribution with coastal areas of higher productivity located in proximity of river mouths. Within this almost constant spatial pattern some important seasonal variability can be observed, namely the more intense productivity levels charcterising the spring and summer distribution; soring with a clearly higher GPP levels in the coastal areas and summer with an increase of productivity of the offshore regions in summer.

The interannual variability of the vertically integrated GPP is shown in fig. 7, where

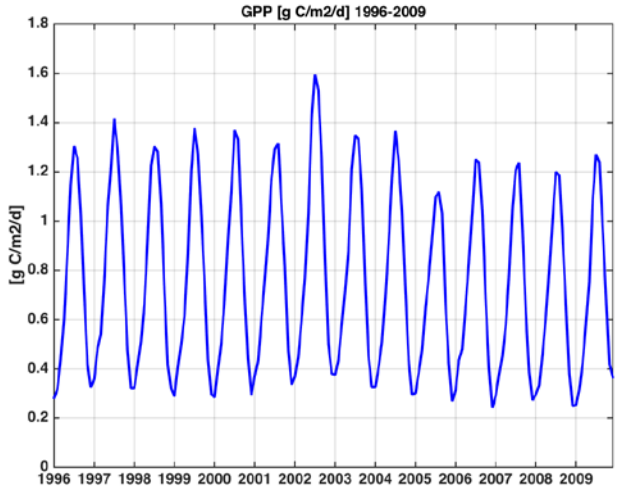

Fig.7: 1996-2009m time series of the basin averaged vertically integrated gross primary productivity

The seasonal pattern described earlier can be noted again and indicating a reduction of de GPP after 2004, despite the relative increase of the nutrient load occurring in the last three year of the simulation period.

We provide now some evaluation of the model derived secondary production "vigor" by considering the meso and microzooplankton gross secondary production.

In figure 8 the seasonally averaged mesozooplankton gross secondary production maps

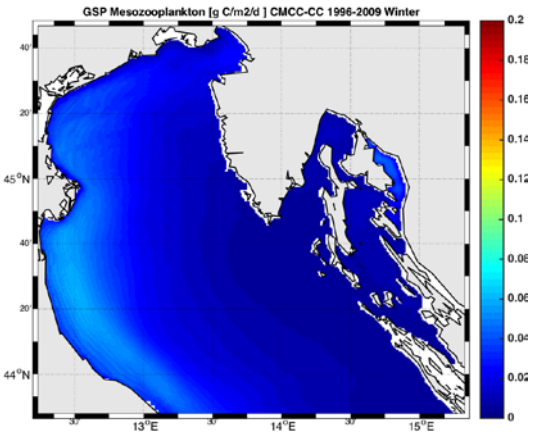

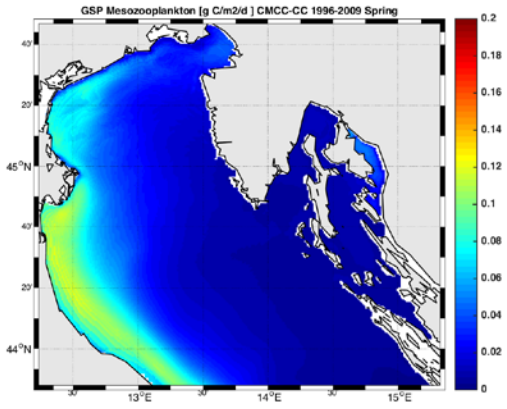

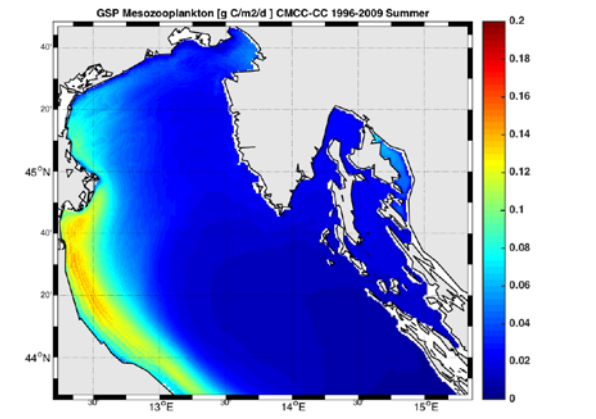

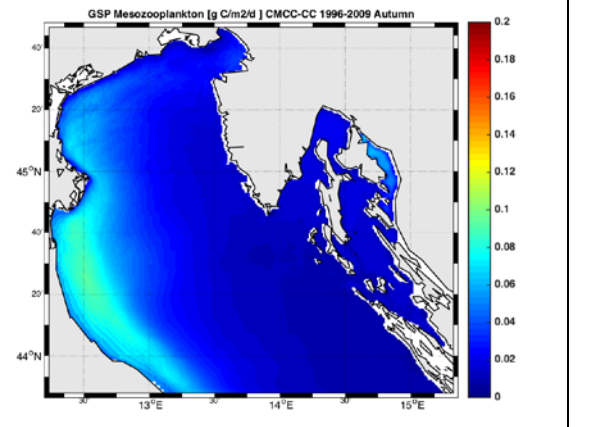

Fig. 8 seasonal distribution of the vertically integrated mesozooplankton gross primary production.

Are reported, while the correspondent microzooplankton distribution is reported in Fig. 9.

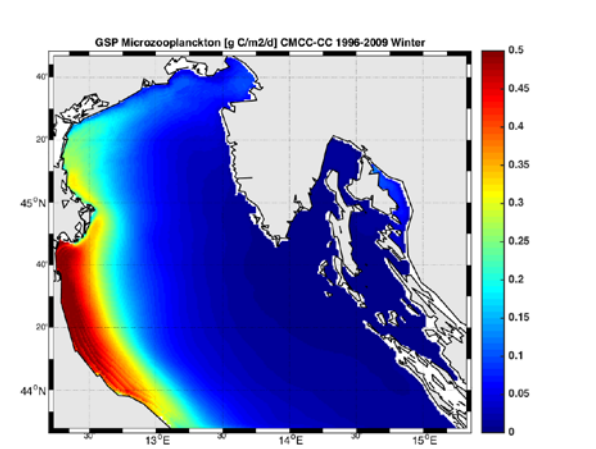

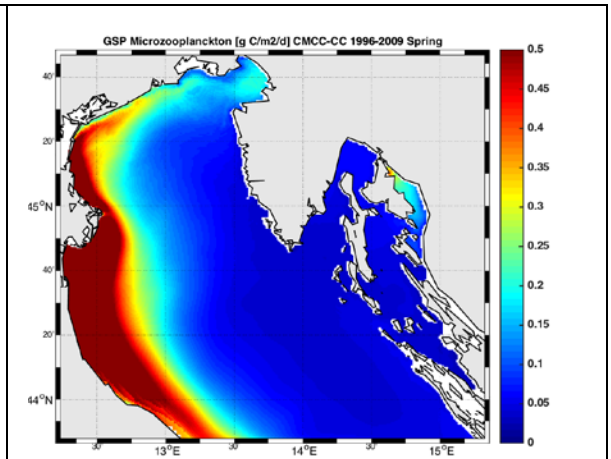

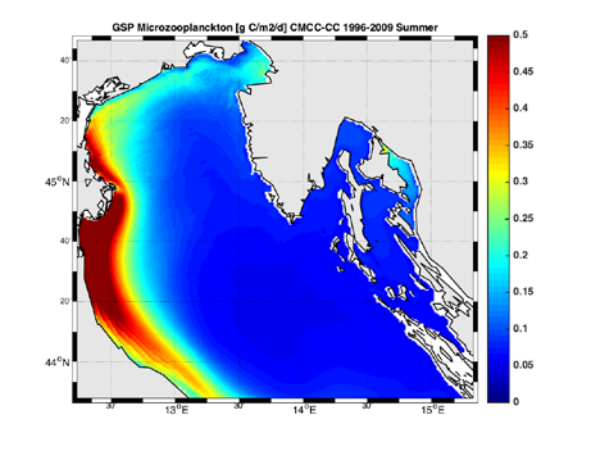

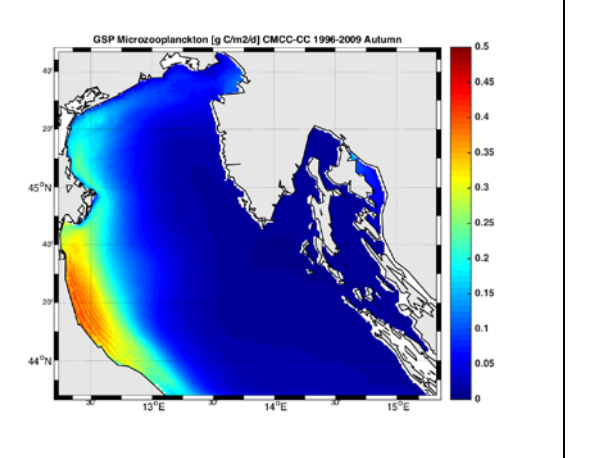

Fig. 9 seasonal distribution of the vertically integrated mesozooplankton gross primary production.

The distribution pattern of both the secondary productivity of the two zooplankters groups classes follows in general the distribution of the GPP with higher values in the coastal areas. However it is worthwhile to note that in the spring-summer period in the offshore regions the microzooplankton productivity is characterized by higher values.

Organisation of the Ecosystem

The organization attribute has been evaluated by following the temporal and spatial evolution of the consistence (biomass) of the three phytoplankton functional types resolved by the model (micro-, nano- and pico-phytoplankton) and comparing the results against the available satellite observations.

Fig 10 show the time series of the basin averaged surface concentration of the functional types along with the correspondent satellite estimates.

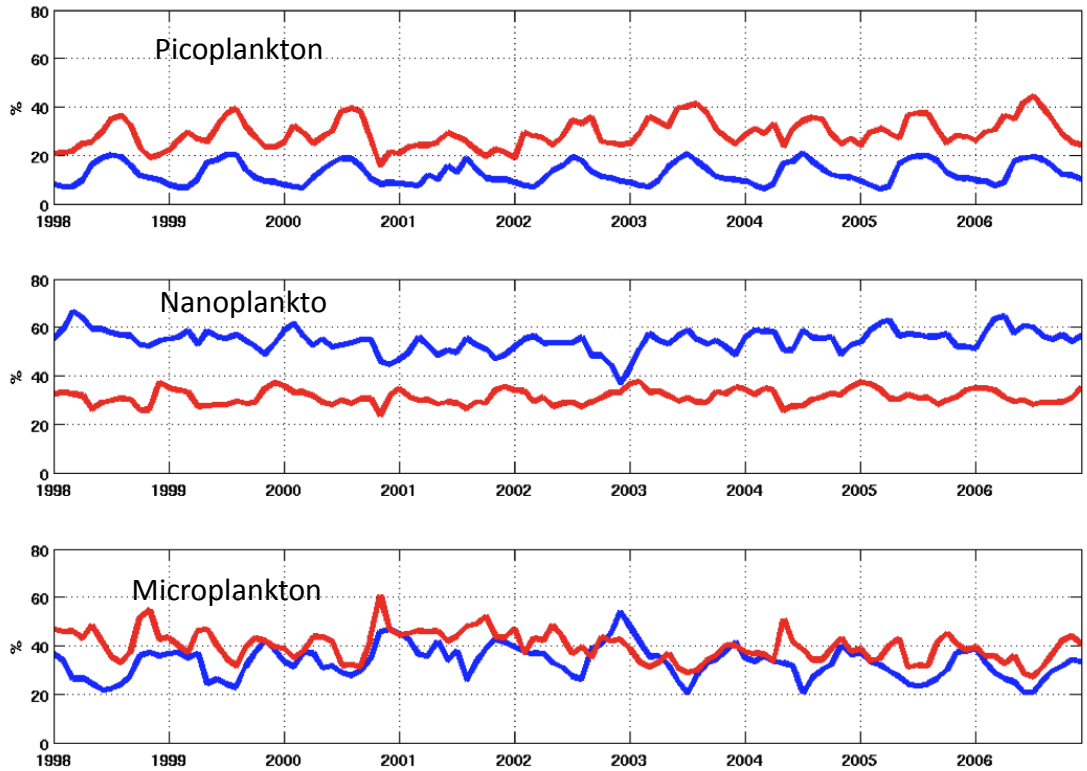

Fig.10: time series of the basin averaged Micro-, Nano- and Pico-phytoplankton in the northern Adriatic sea. Blue: model, Red: satellite observations

It can be clearly seen that while the model produce a Microphytoplankton biomass in agreement with the remote observation a clear discrepancy occure for the Nano- and Pico-phytoplankton biomass, as there is a systematic overestimation of the Nano-functional type and a correspondent under estimation of the pico- functional types. Despati this evident discrepancies, the observed and simulated time series for the three functional types show some elemant of similarities from a qualitative pont of view, such as the timing in achievement of the minimum and maximum concentration. However the differences in resolving the phytoplankton functional types is an issue that deserve close attention in order to improve the model performance, since as can be seen by

inspecting the spatial distribution in fig. 11, such model weakness occur uniformly all over the basin.

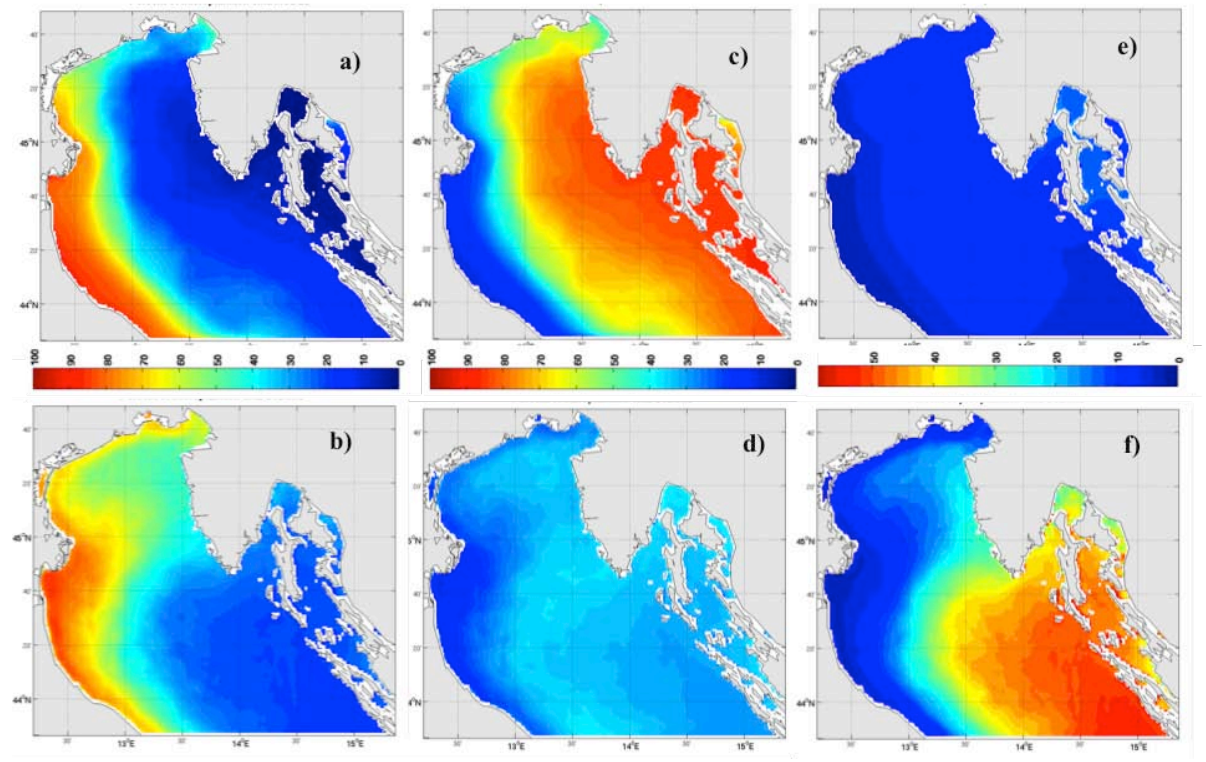

Figure 11: spatial distribution of the annually averaged phytoplankton functional types biomass (mg Chl-a/m^3). Upper row: Model results. Lower row: Satellite estimates. microphytoplankton (a,b), Nanophytoplankton (c,d), Picophytoplankton (e,f).

Despite these discrepancies the model is able to produce reasonable results with respect to the spatial and temporal variability of the trophic web structure. This aspect has been evaluated by estimating the ratio between the microbial and the herbivorous grazing, that is considered an index indicating which trophic chain is dominating: The herbivorous (index>0) ot he microbial (index<0). The results tof this assessment are shown in fig 12, that report the seasonaly average spatial distribution of the index.

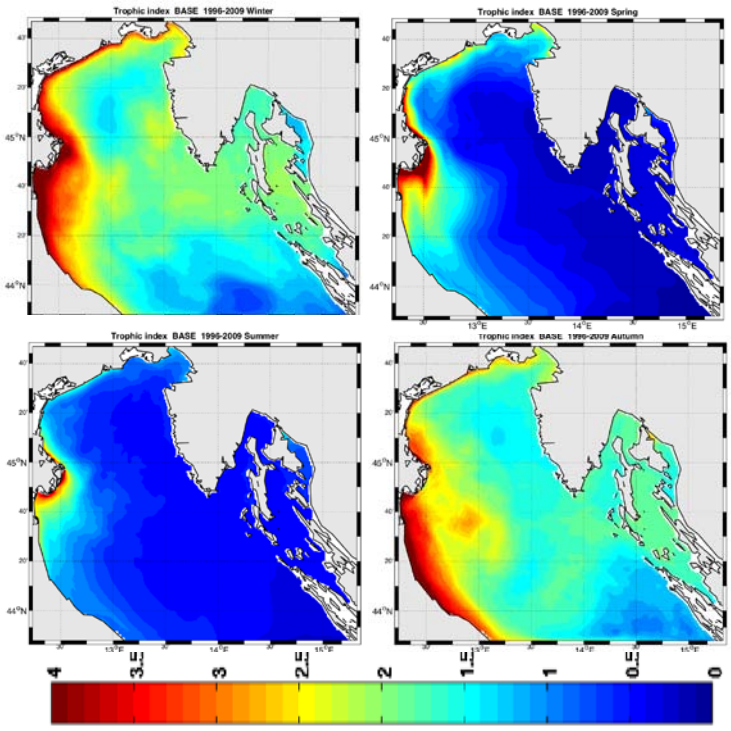

Fig.12. seasonally averaged spatially distribution of the trophic web index: Upper left: winter, Upper right spring, Lower left: summer, lower right: autumn

The figure show how in general coastal areas particularly those directly affected by river runoff have a tendency to maintain all over the year a herbivorous trophic web structure, while the basin appear more structured with an herbivorous web in winter and autumn and with a microbial trophic web in spring summer.

Conclusions

The assessment of the Vigor and oirganisation ecosystem properties for the norther Adriatic Sea has been carried out by constraining the model results with the remote (satellite) observation of surface biomass, gross primary productivity and phytoplankton finctionla types population structure. This severe comparison allowed to understand the limits and the potential skills of the modeling system in predicting the ecosystem properties that are at the base of many MSFD descriptors.

The result therefore indicate that.

1. The model has skill in predicting the surface phytoplankton gross primary production although fails to reproduce the high productivity peaks indicated by the remote observations.
2. Similarly the model appear able to capture the spatial and temporal variability of the trophc web structure (herbivorous Vs microbial) despite a significant weakness in predicting the composition of the population at the functional type level.

Adriatic Sea HTL model (OGS)

The analysis is made by using linked LTL (low trophic level) and HTL (high trophic level) models. The End-to-End approach implemented (detailed in Libralato and Solidoro, 2009; implementation fully explained in Deliverable 4.4 and 4.8 of PERSEUS) is thus connecting hydrodynamic, biogeochemical model for the Mediterranean sea and food web model built with Ecopath with Ecosim for the Adriatic Sea.

The coupled hydrodynamic-biogeochemical model (LTL) for the Mediterranean is the OPATM-BFM (Lazzari et al., 2012) forced with physical outputs produced by the CMCC-MFS16CM Ocean General Circulation model. The simulation carried out spans the period 2000-2020 with a spin-up phase of 5 years. Climatic conditions used for period 2011-2020 are those resulting from application of nutrient loads according to the BAU (Business as usual) conditions as reported in D 4.6 of PERSEUS.

The food web (HTL) model is built with the software Ecopath with Ecosim (Christensen and Walters, 2004) for the Adriatic sea by Coll et al. (2007) that was updated (Libralato et al., 2010; Akoglu et al., 2015) and standardized according to PERSEUS D4.4.

Integration of the LTL and HTL models is done according to methodology described in Libralato and Solidoro (2009), that consists in extending the HTL model to represent also LTL processes in terms of functional groups biomass, production and consumption; the model is extended considering the limiting nutrient (in the case of Adriatic Sea and other Mediterranean systems, nitrogen; Lazzari et al., 2012); then the extended model is adjusted for considering effects of aggregation of detailed OPATM-BFM 3D processes into simplified 0D dynamics (e.g. Solidoro et al., 2010) through an adjusting function. The linked model has been proved to robustly represent ecosystem dynamics under different conditions (see also PERSEUS D4.8).

Indicators applied to assess ecosystem status

The developed End-to-End model for the Adriatic Sea ecosystem permits to determine a series of indicators that are used to synthesize food web properties (Odum, 1969; Christensen, 1995) and often implemented in comparisons (e.g., Heymans et al., 2014; Coll and Libralato, 2013). Therefore, as required by the Marine Strategy Framework Directive (MSFD, EU 2008), some of these indicators are tentatively suggested to measure ecosystem health (e.g. ICES 2014a,b; ICES 2015) although there seems to be quite a great uncertainty on what are the best indicators to assess ecosystem health as a whole, thus under the Descriptor 4 of the MSFD. Moreover, some metrics in the set of indicators are measuring ecosystem properties that are considered to quantify ecosystem health (Costanza and Mugeau, 1999). Overall, given that a large number of the indicators have been connected to good environmental status (GES) (see for example ICES 2014a,b; ICES 2015), we will explore the values of a set of indicators considering however, that according Costanza and Mageau (1999) some are more appropriate for the quantification of ecosystem health (Figure 1).

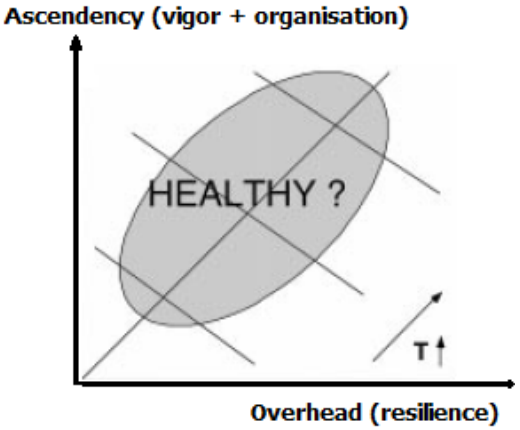

Figure 1. A conceptual diagram of the network analysis-based on quantitative indexes of ecosystem health. The 'healthy' region is indicated by the shaded area, and represents a balance between system vigor, organization, and resilience. Modified from Costanza and Mageau (1999).

The total systems throughput (T), which is the sum of all flows in the model and considered an overall measure of the "ecological size" of the system (Finn, 1976) and is calculated as:

$$T = \sum_{i=1,j=1}^{n} T_{ij} \qquad (1)$$

where Tij is the flow between any two compartments and includes respiration and export flows.

Within the network analysis indicators (Ulanowicz, 1986),the development capacity (C) of the system is the thermodynamic limit of growth in the system and is calculated as:

$$C = -T \cdot \sum_{ij} \frac{T_{ij}}{T} \cdot \log\left(\frac{T_{ij}}{TST}\right) \qquad (2)$$

It scales the T to a measure of the information carried by flows. Capacity is divided between ascendency (A) and the overhead (O). Ascendency is an index of the organisation of a food web (Ulanowicz, 1986) and is defined in terms of flow as the following:

$$A = \sum_{ij} \left(T_{ij}\right) \cdot \log\left(\frac{T_{ij} \cdot T}{T_j \cdot T_i}\right) \qquad (3)$$

and overhead (O, an indicator of the ecosystem's strength in reserve) is calculated as:

O=C-A

(4)

Overhead and Ascendency are divided into export, dissipation and internal flows and the overhead on internal flows has been used as an index of ecosystem redundancy (Ulanowicz, 2000; 2008; Heymans et al., 2012). The redundancy is an indicator of the distribution of energy flow among the pathways in the ecosystem and is calculated as:

$$R = IFO = -\sum_{i=1}^{n}\sum_{j=1}^{n}(T_{ij}) \cdot \log\left(\frac{{T_{ij}}^2}{\sum_{j=1}^{n} T_{ij} \cdot \sum_{i=1}^{n} T_{ij}}\right) \qquad (5)$$

Moreover, the relative overhead, i.e. the difference between capacity and ascendency divided by the throughput, is considered an indicator of resilience (Costanza and Mugeau, 1999):

H-AMI (Entropy - Average Mutual Information) = [(Capacity-Ascencency) / Throughput (6)

The difference between total production and total primary production is considered an ecosystemic Scope for Growth (SfG) and thus calculated as:

SfG = Total production – Total primary production (7)

The Finn Cycling Index (FCI) quantifies the amount of recycling relative to T and is an indication of stress and structural differences (Finn, 1976), and is calculated as:

$$FCI = \frac{T_c}{T} \quad (8)$$

where T_C is the total flow that is recycled.

Other ecological indicators are related to the trophic level (TL) concept, which is the average number of steps for energy to move from primary producers to higher-level consumers and provides an indication of the trophic position of an organism. Thus for a given predator *j* the TL is calculated as:

$$TL_j = 1 + \sum_i DC_{ij} TL_i \quad (9)$$

where TL_i is the trophic level of prey *i* and DC_{ij} is the proportion of prey *i* in the diet of predator *j*. The mean trophic level of the catches (TLc) is calculated as the weighted average TL in the lansings as:

$$TLc = \frac{\sum_i TL_i \cdot Y_i}{\sum_i Y_i} \quad (10)$$

where the weighting factor is the caught biomass of each functional group (Y_i).

The system's omnivory index (SOI) is defined on the basis of the omnivory index (OI) of each food web component. It indicates the variance of trophic levels in the diet, and is:

$$OI_i = \sum_{j=1}^{n} (TL_j - (TL_i - 1))^2 \cdot DC_{ij} \quad (11)$$

So from the OI of each functional group, the SOI for the food web is calculated as:

$$SOI = \frac{\sum_{i=1}^{n} [OI_i \cdot \log(Q_i)]}{\sum_{i=1}^{n} \log(Q_i)} \quad (12)$$

where Qi is the food intake of each consumer (Libralato et al., 2008; Christensen et al., 2005).

The proportion of primary production required for the exploited fishery's catch (PPRc) is defined as:

$$P_{Pred} = \sum_{Prey} \left[Y_{Pred} \cdot R_{Pred} \prod_{r} \frac{Q_{Prey}}{P_{Prey}} \cdot DC_{Prey,Pred} C_{Pred} \right] \quad (13)$$

where P is production, Q consumption, and DC' is the diet composition for each predator/prey interaction in each path from primary production or detritus through the food web to the catch, with cycles removed from the diet compositions . PPRc can be expressed in percentage terms when it is normalized with the primary production (PPRc/PP = PPRc%).

The Fishing in Balance index (FiB) is calculated as follows (Pauly et al. 2000):

$$FiB_k = \log\left(\frac{Y_k \cdot TE^{TLc_k - 1}}{Y_1 \cdot TE^{TLc_1 - 1}} \right) \quad (14)$$

where TE is the mean transfer efficiency of energy between trophic levels (assumed to be 10%; Pauly & Christensen 1995, Libralato et al., 2008), Yk is the total landing for year k, and 1 refers to the first year in a time-series (in this case, the year 1928) used as a baseline.

Kempton index (Q) includes species or functional groups at a trophic level (TL) three or higher (Kempton and Taylor, 1976). Q is a relative index of biomass diversity derived from the Kempton's Q75 index that was also developed as an indicator of biodiversity evenness (Ainsworth and Pitcher, 2006). Decreasing Q would imply in low evenness and richness with higher group dominance. The Kempton Q index is automated in EwE as a dynamic output for simulations (Christensen and Walters, 2004). Some of the above reported indicators are connected with health of the system in terms of vigor, organization and resilience components (Table 2) and used in the following to track changes of health over time.

Table 2. Metrics used to compare the "health" (vigor, organization and resilience) over the time and between of the marine systems Costanza and Mageau (1999).

Vigor	**NPP (net primary production)** **T (Throughput)** **Catch (total catch)**
Organisation	**K's Q (Kempton's Q)** **FiB (Fishing in Balance)** **AMI (Average Mutual Information)** **Ascendency (A)** **FCI (Finn's Cycling Index)** **mPL (Mean Path length)**
Resilience	**H-AMI (Entropy - Average Mutual Information) = [(Capacity-Ascencency) / Throughput]** **SfG (Scope for Growth = Total production – Total primary production)**

Assessment using ecopath conditions

Results reported in D4.4 for synthetic ecosystem indicators for the food web prior and after standardization reveal that model structure has a modest impact on flow-based indicators (see also Angelini and Agostinho, 2005), but some indicators such as connectance and SOI might sensibly change in value also according to model structure. Also network indicators (Ulanowicz 1986) show some minimal differences induced by model structure. For this reason, the End-to-End modelling application in different areas of the Mediterranean has been conducted using a common model structure (see PERSEUS deliverable D4.4).

Nevertheless, one of the problems related with these indicators is the definition of reference values and usually a comparison is implemented to delineate unhealthy situations (e.g. Coll and Libralato, 2012; Costanza and Mageau, 1999). By comparing the results obtained for the three areas of the Mediterranean Sea (Table 3), however, it is quite difficult to delineate the healthy status of the ecosystem in absolute terms, and a more opportune analysis consists in observing trajectories of indicators over time to understand direction of change.

Table 3 . Ecological indicators related to community energetic, structure, flows and information theory for the extendend Ecopath models of the three areas of the Mediterranean Sea at the initial conditions (year 2000 for GoL; year 1993 foe Aegean; year 1990 for Adriatic).

	Gulf of Lion	Northern Aegean Sea	Adriatic Sea	
Sum of all consumption	1286.400	759.330	817.094	mg P/m²/year
Sum of all exports	0.600	0.700	0.627	mg P/m²/year
Sum of all respiratory flows	0.000	0.000	0.000	mg P/m²/year
Sum of all flows into detritus	980.300	605.970	718.697	mg P/m²/year
Total system throughput	2267.200	1365.990	1536.417	mg P/m²/year
Sum of all production	737.500	441.360	461.134	mg P/m²/year
Mean trophic level of the catch	3.900	3.820	3.517	
Gross efficiency (catch/net p.p.)	0.000	1.200	0.640	
Total primary production/total biomass	0.100	0.004	0.002	
Total biomass/total throughput	0.200	0.120	0.261	
Total biomass (excluding detritus)	450.500	158.820	400.361	mg P/m²
Total catches	0,6	0.700	0.639	mg P/m²/year
Connectance Index	0.200	0.320	0.205	
System Omnivory Index	0.300	0.260	0.273	

Assessment using trajectories of indicators

The approach implemented here permits to obtain E2E simulations for the whole food web from biogeochemical variables to high trophic level species and fisheries (Libralato and Solidoro, 2009). Simulation carried out using BAU conditions permits to describe hindcast (2000-2010) and future conditions (2011-2020) using the set of indicators proposed above.

The trajectories of these indicators will be looked in the 2D plane suggested by Costanza and Mageau (1999), delineating: initial conditions (green dot), end of hindcast (dec 2010 ; blue triangle), end of scenario (2020, red dot). Trajectories for hindcast are in black, for future are in red.

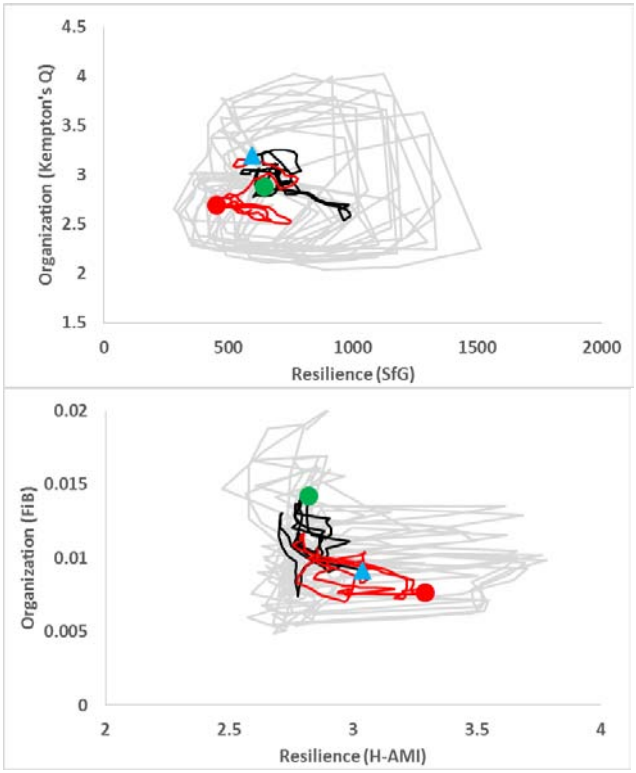

Figure 2. Dynamics of components of ecosystem health, resilience and organization, over time for the Adriatic system. Initial conditions (2000, green dot), hindcast period (2000-2010, black line) and end of hindcast (blue triangle) are distinguished from BAU dynamics (2010-2020; red line) and final situation (red dot; 2020). Values are 12 order moving averages of monthly results (grey line).

Some of the trajectories are reported. For instance resilience indicators (SfG, H-AMI) vs organization indicators (FiB index and Kempton's) (figure 2) clearly shows that the seasonal variability (intra-annual variability) is very large, possibly making long term trends non-significant. Overall Resilience indicators seems to move toward opposite directions: SfG is decreasing during hindcast and BAU scenario (SfG 2000>2010>2020), while H-AMI is increasing over time (H-AMI 2020>2010>2000). Organization measured through Kempton's Q and FiB are also not showing coherent directions.

Plotting trajectories of vigor and organization (Figure 3) shows that dynamics of these two components of health seems to remain within a restricted area, thus possibly these two factors are not changing much in the simulated scenario, at least never moving out of the large range of intra-annual variability.

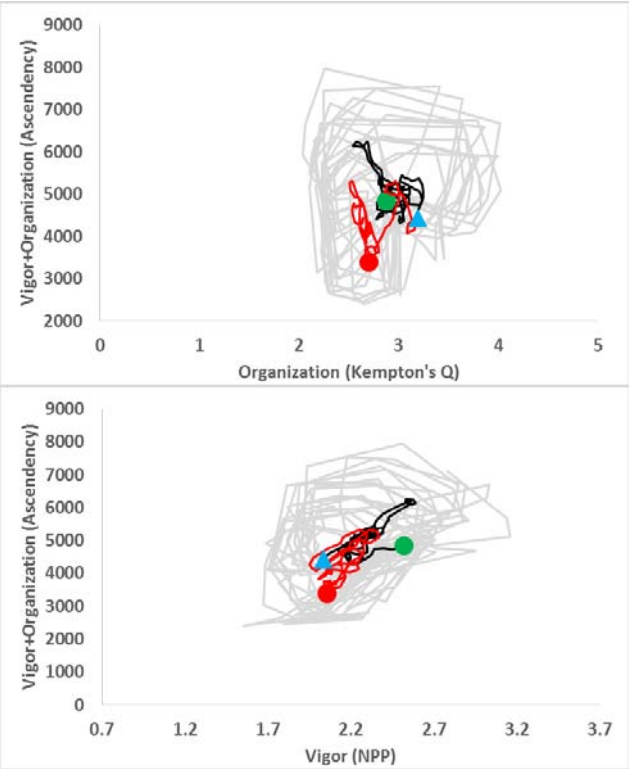

Figure 3. Dynamics of components of ecosystem health, vigor+organization and organization, over time for the Adriatic system. Initial conditions (2000, green dot), hindcast period (2000-2010, black line) and end of hindcast (blue triangle) are distinguished from BAU dynamics (2010-2020; red line) and final situation (red dot; 2020). Values are 12 order moving averages of monthly results (grey line).

However, the system trajectories denote a clear pattern in resilience and in vigor. Thus plotting together these two components of health, also using vigor+organization indicators such as (Ascendency) allows to see that during the BAU scenario the trajectories are deeply moving the system resilience in coordination with changes in vigor.

As can be seen in Figure 4, vigor measured through the Total system throughput (T) and vigor+organization measured by Ascendency (A) are strongly declining through time, both in the hindcast period (2000-2010) and in the future BAU conditions (2011-2020). Importantly these changes seems coordinated by simultaneous and correlated changes in resilience indicators Scope for Growth (SfG) and Entropy - Average Mutual Information (H-AMI). Although these two indicators of resilience show contrasting direction of changes, it seems overall that resilience is strongly related with vigor (and vigor+organization), driving important changes in the system through time under the BAU scenario.

The fact that these changes are not much evident in fisheries-based indicators, such as trophic level of thee catch (Figure 5) suggest that the changes in vigor and resilience are mainly driven by nutrient input modified by climatic changes represented in the BAU 2000-2020 scenarios, that propagates from LTL to HTL (bottom-up effects).

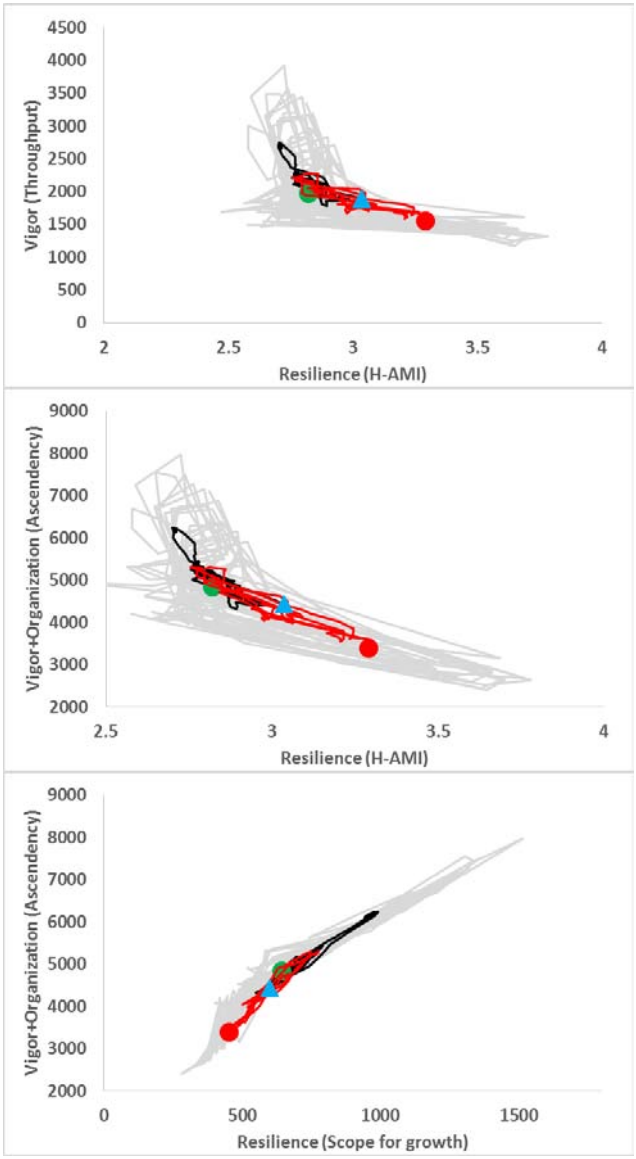

Figure 4. Dynamics of components of ecosystem health, resilience and vigor or resilience and vigor+organization, over time for the Adriatic system. Initial conditions (2000, green dot), hindcast period (2000-2010, black line) and end of hindcast (blue triangle) are distinguished from BAU dynamics (2010-2020; red line) and final situation (red dot; 2020). Values are 12 order moving averages of monthly results (grey line).

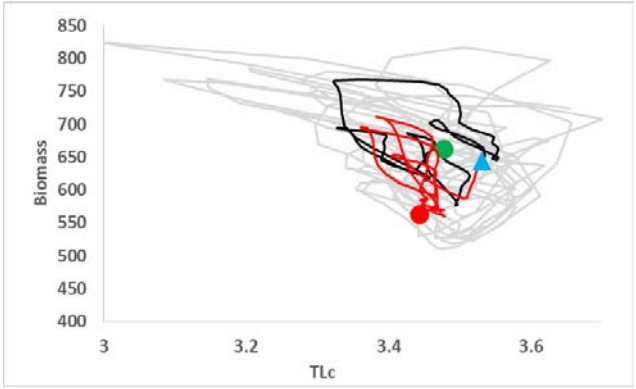

Figure 5. Trajectories of Biomass in the system and Trophic level of the catches over time for the Adriatic system. Initial conditions (2000, green dot), hindcast period (2000-2010, black line) and end of hindcast (blue triangle) are distinguished from BAU dynamics (2010-2020; red line) and final situation (red dot; 2020). Values are 12 order moving averages of monthly results (grey line).

Discussion

State conditions of the Adriatic System are difficult to assess in absolute terms using initial condition (Ecopath). Although results might be influenced also by model structure, standardization (see also PERSEUS D4.4) and comparison between different systems in Mediterranean can be of moderate help. Trajectories of indicators over time, instead can provide insights on direction and magnitude of change in a more comprehensible manner.

The results obtained by looking at condition of a set indicators in the past and looking at their trajectories over time showed that, for the Adriatic Sea, high intra-annual variability can mask some changes that occur in the long term. This seems particularly true for organization component of health. However, measures of Resilience and Vigor show patterns of change that are compatible with a modification of situation over time, by using the scheme of analysis provided by Costanza and Mageau (1999). Climatic changes seems to result in decrease of vigor and simultaneaous increase of resilience if measured with H-AMI. Conversely the other indicator for resilience, scope for Growth (SfG) shows opposite patterns than H-AMI.

The effects of fishing, usually strongly affecting ecosystem dynamics with Ecopath with Ecosim (see also PERSEUS D.4.8) are here possibly resulting in secondary effects while climatic changes appear to dominate trajectories over the period 2011-2020 at least (when fishing is constant). It seems therefore that a coherent pattern of vigor and resilience is evident from climatic modification in the Adriatic system. This bottom-up signal is clearly captured by the End-to-End approach adopted (Libralato and Solidoro 2009) that allows transmission of effects from nutrient discharge in the LTL model up to HTL groups, using the linking approach proposed.

References

Akoglu, E., Libralato, S., Salihoglu, B., Oguz, T., & Solidoro, C. (2015). EwE-F 1.0: an implementation of Ecopath with Ecosim in Fortran 95/2003 for coupling and integration with other models. Geoscientific Model Development, 8(8), 2687-2699.

Angelini, R., Agostinho, A.A., 2005. Food web model of the upper Paranà River foodplain: description and aggregation effects. Ecological Modelling 181, 109– 121.

Christensen, V. 1995. Ecosystem maturity -- towards quantification. Ecological Modelling, 77(1), 3-32.

Coll M, Libralato S (2012) Contributions of food web modelling to the ecosystem approach to marine resource management in the Mediterranean Sea. Fish and Fisheries 13: 60-88.

Coll, M., Santojanni, A., Palomera, I., Tudela, S., Arneri, E., 2007. An ecological model of the Northern and Central Adriatic Sea: analysis of ecosystem structure and fishing impacts. Journal of Marine Systems 67, 119-154.

Costanza, R., Mageau, M., 1999. What is a healthy ecosystem? Aquatic Ecology, 33: 105–115.

EU 2008. DIRECTIVE 2008/56/EC OF THE EUROPEAN PARLIAMENT AND OF THE COUNCIL of 17 June 2008 establishing a framework for community action in the field of marine environmental policy (Marine Strategy Framework Directive)

Finn JT (1976) Measures of ecosystem structure and function derived from analysis of flows. Journal of theoretical Biology 56: 363-380.

Heymans JJ, Coll M, Libralato S, Christensen V (2012) 9.06 Ecopath theory, modelling and application to coastal ecosystems. In: Wolanski E, McLusky DS, editors. Treatise on Estuarine and Coastal Science: Elsevier. pp. 93-113.

Heymans JJ, Guénette S, Christensen V (2007) Evaluating network analysis indicators of ecosystem status in the Gulf of Alaska. Ecosystems 10: 488-502.

Heymans, J. J., Coll, M., Libralato, S., Morissette, L., & Christensen, V. (2014). Global patterns in ecological indicators of marine food webs: a modelling approach. PloS one, 9(4), e95845.

ICES. 2014a. Report of the Workshop to develop recommendations for potentially use-ful Food Web Indicators (WKFooWI), 31 March–3 April 2014, ICES Headquarters, Co-penhagen, Denmark. ICES CM 2014\ACOM:48. 75 pp.

ICES. 2014b. Report of the Workshop to review the 2010 Commission Decision on cri-teria and methodological standards on good environmental status (GES) of marine waters; Descriptor 4 Foodwebs, 26-27 August 2014, ICES Headquarters, Denmark. ICES CM 2014\ACOM:60. 23 pp.

ICES. 2015. Report of the Workshop on guidance for the review of MSFD decision descriptor 4 – foodwebs II (WKGMSFDD4II), 24-25 February 2015, ICES Headquarters, Denmark. ICES CM 2015\ACOM:49. 52 pp.

Lazzari, P., Solidoro, C., Ibello, V., Salon, S., Teruzzi, A., Béranger, K., Crise, A.. 2012. Seasonal and inter-annual variability of plankton chlorophyll and primary production in the

Libralato S (2008) System Omnivory Index. In: Jørgensen SE, Fath BD, editors. Ecological Indicators Oxford: Elsevier. pp. 3472-3477.

Libralato S, Coll M, Tempesta M, Santojanni A, Spoto M, Palomera I, Arneri E, and Solidoro C., 2010. "Food-web traits of protected and exploited areas of the Adriatic Sea." Biological Conservation 143, no. 9: 2182-2194.

Libralato, S., Solidoro, C., 2009. Bridging biogeochemical and food web models for an End-to-End representation of marine ecosystem dynamics: The Venice lagoon case study. Ecological Modelling 220, 2960-2971.

Pauly D, Christensen V, Dalsgaard J, Froese R, Torres FJ (1998) Fishing down marine food webs. Science 279: 860-863.

Solidoro C., Cossarini G., Libralato S., Salon S., 2010b. Remarks on the redefinition of system boundaries and model parameterization for downscaling experiments. Progress in Oceanography, 84: 134–137

Ulanowicz RE (1986) Growth and Development: Ecosystems Phenomenology. Lincoln, NE: toExcel Press. 203 p.

Ulanowicz RE (2000) Toward the Measurement of Ecological Integrity. In: Pimentel D, Westra L, Noss RF, editors. Ecological integrity: integrating environment, conservation, and health. Washington DC: Island Press. pp. 99-113.

Ulanowicz RE (2004) Quantitative methods for ecological network analysis. Computational Biology and Chemistry 28: 321-339.

Ainsworth, C.H., Pitcher, T.J., 2006. Modifying Kempton's species diversity index for use with ecosystem simulation models. Ecological Indicators, 6 (3): 623–630.

Kempton, R.A., Taylor, L.R., 1976. Models and statistics for species diversity. Nature

262: 818–820.

Pauly, D., Christensen, V, Walters, C. 2000. Ecopath, Ecosim and Ecospace as tools for evaluating ecosystem impact of fisheries. ICES J. Mar. Sci. 57: 697-706.

Pauly, D., and Christensen, V. 1995. Primary production required to sustain global fisheries. Nature, 374: 255-257.

North western Mediterranean (UPS-LA)

Vigor of the ecosystem

Methodology

A simulation coupling hydrology and biogeochemistry was done over the period June 2000-June 2013. The hydrodynamic model SYMPHONIE was forced at its lateral boundaries by the NEMOMED8 model described in Herrmann et al., 2010. We use the same atmospheric forcing than this model i.e the ARPERA dataset (Herrmann and Somot, 2008) which is a dynamic downscaling of the ECMWF (European Centre for Medium-Range Weather Forecasts) model reanalysis since 2001. The daily rivers discharges were also realistic for the French rivers and for the Ebro. The biogeochemical model ECO3M-S was previously used to study the Gulf of Lions' pelagic ecosystems impacted by freshwater discharge (Auger et al., 2011) and the pelagic ecosystem dynamics in the offshore areas of the NW Mediterranean basin (Auger et al., 2014). This multi-nutrient and multi-plankton functional types model was forced at the lateral boundaries by the same model that was run at low resolution at the basin scale.

The objective is to understand the spatial and temporal variability of the northwestern Mediterranean ecosystems. Three areas important for the small pelagic fishing activities are considered: the Gulf of Lion, the northern Catalan margin and the southern Catalan margin (Figure 1). These three regions are considered separately as their topographic, hydrologic and climatic characteristics are quite different probably inducing ecological differences.

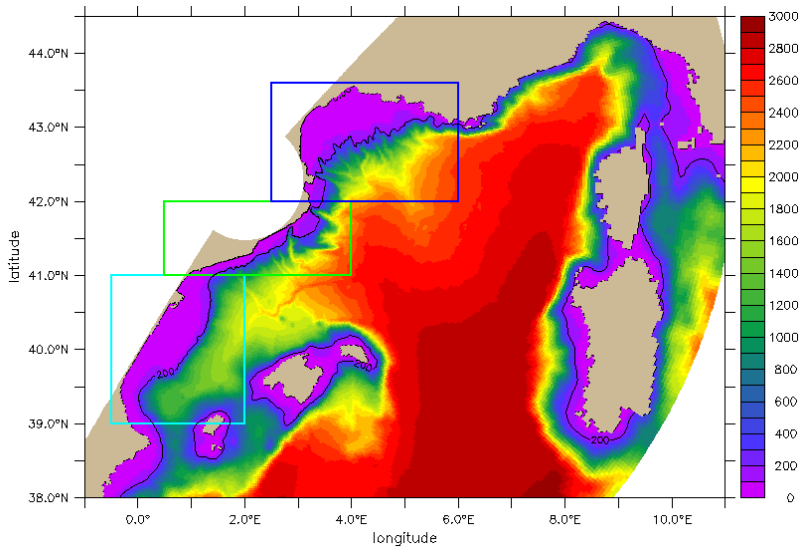

Figure 1: Bathymetry of the numerical domain. The three areas specifically studied are indicated: dark blue, Gulf of Lion; green, North Catalan, light blue, South Catalan. Note that the analysis is restricted to areas shallower than 1000m.

Satellite model chlorophyll comparison

Before looking at the variability of biomass, we need to appreciate the quality of the model. Few data are available except time series of satellite chlorophyll. The comparison with the satellire data indicate that the agreement is generally correct even if the simulated chlorophyll looked too high in late winter early spring especially in the northern Catalan shelf and to a lesser extent in the Gulf of Lion. **New simulations** were done with **improved calibration** as well as the basin scale than with the downscaling at high resolution.

Figure 2 presents the new comparison between surface chlorophyll from MODIS and from the model. Comparisons have been improved. The timing of the seasonal cycle is generally good in the three regions. Same thing for the range of values, the minimum values in summer and maximum values at the end of winter beginning of spring.

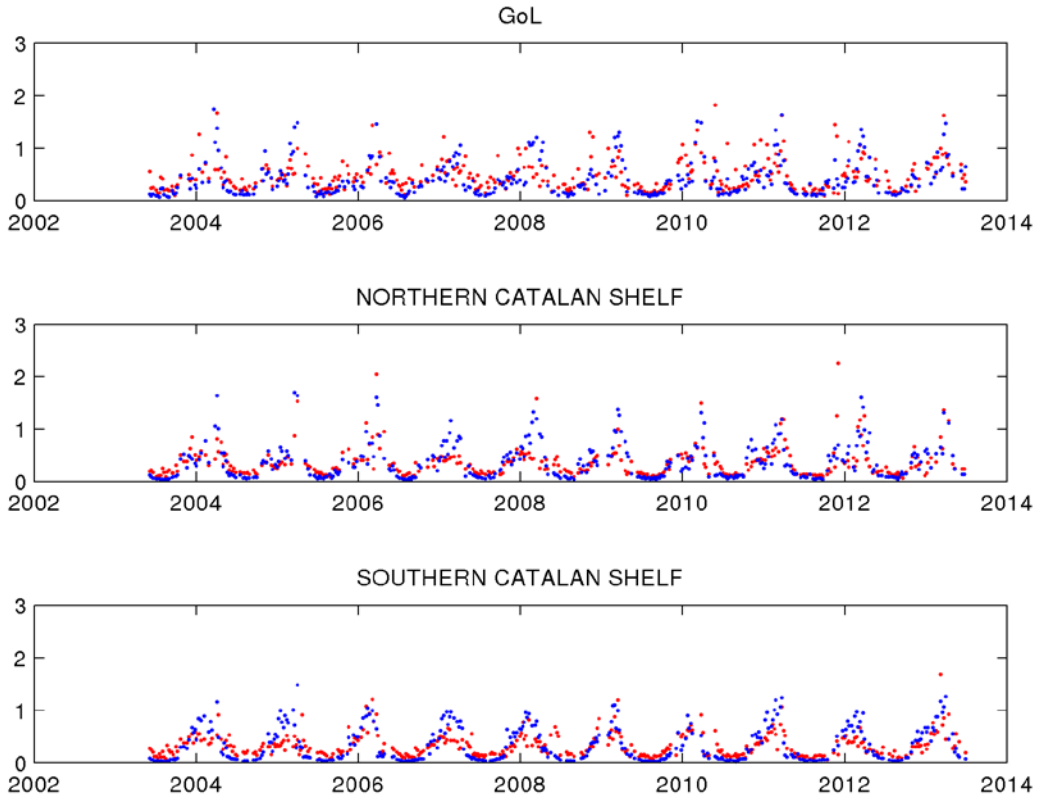

Figure 2: Comparison model satellite of surface chlorophyll in the three coastal regions. blue: model, red : Modis

Simulations were analysed from January 2001 to June 2013. Monthy averages are considered for all the physical and biological variables. Interannual variability is examined and compared for three regions, Gulf of Lion, North Catalan and South Catalan. **Correlations are calculated with meteorological and river forcing to understand this variability and finally the functioning of each region**. As the effect of forcing is not instantaneous on biology, the correlations have been calculated with different time lags (in months).

The variables considered are the biomass in carbon of the three groups of phytoplankton and of zooplankton vertically integrated, the primary production, grazing and bacterial production.

Forcing

For the meteorological forcing, several terms were considered, but clearly the term which explains better the variability of the planktonic ecosystem is the total heat flux. Figure 3 presents the time series of the heat flux for the three regions considered here. The large heat losses characteristic of Mediterranean winters are visible in the three regions but they are maximum in the Gulf of Lion and significantly lower in the two other regions. Interannual variability of winter conditions is high (for example, very cold winter in 2012 and warm winter in 2007). In summer, the lowest heat loss is often in the North Catalan.

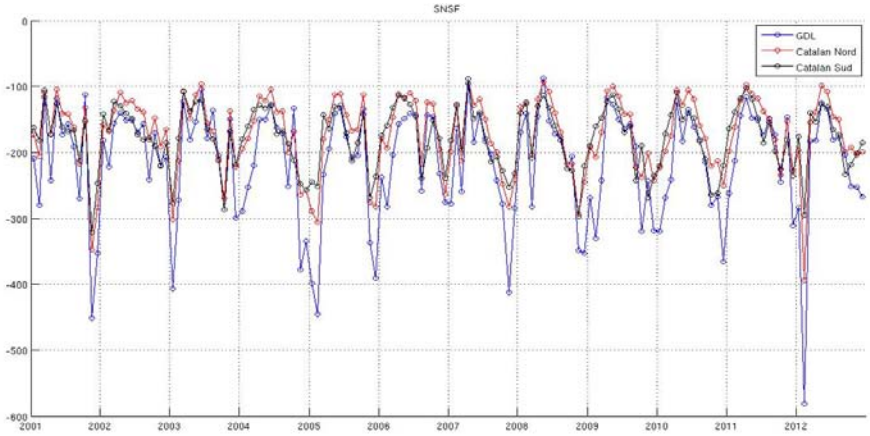

Figure 3 : Total heat flux (in W m^{-2}) for the 3 regions. Negative values correspond to heat losses for the ocean surface.

The rivers discharge are given on Fig. 4 for the Rhône, for the total of the rivers of the western Gulf of Lion and for the Ebro which flows at the boundary between the two Catalan regions (note that for the Ebro, we used climatological values for the three first years). Due to the cyclonic circulation of the region, the Rhone and the rivers of the Gulf of Lion can influence the 3 regions while the Ebro can influence only the two Catalan regions.

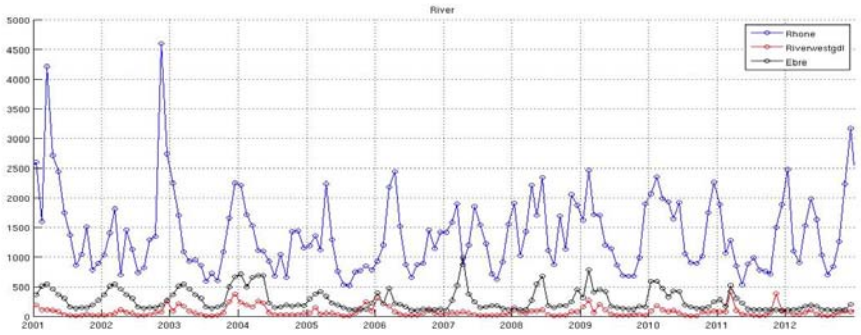

Figure 4 : Monthly averaged rivers discharge in m^3 s^{-1}

Plankton biomass

The phytoplankton and zooplankton biomasses are given on Fig. 5 for the 3 regions.

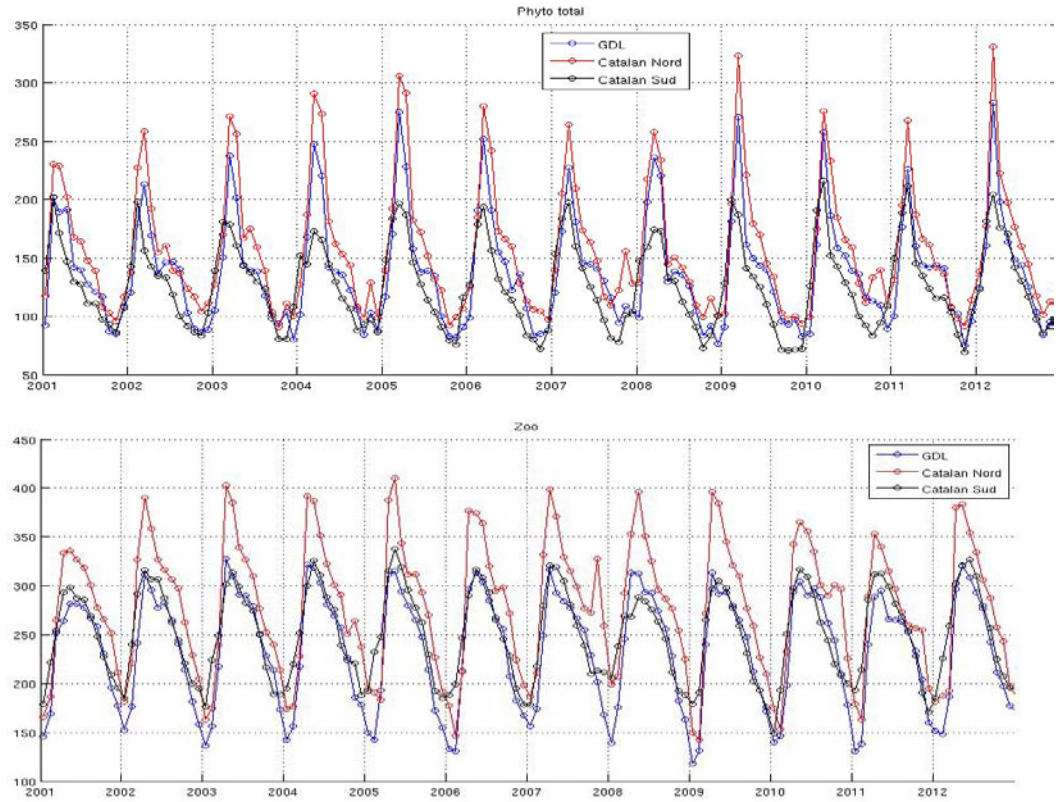

Figure 5. Phyto and Zooplankton vertically integrated biomass expressed in carbon (mmole m^{-2}) in the three regions

The seasonal cycles are marked by a minimum of zooplankton in winter followed by a maximum of phyto and zooplankton in spring and minimum values of phytoplankton in summer.

If the seasonal cycles of the 3 regions are globally similar, some important differences can be noted. First, in summer the phytoplankton and zooplankton biomass increases from the South Catalan region to the Gulf of Lion and the North Catalan. The North Catalan biomass is approximately 1.3 times the South Catalan one. During the spring maximum, the phytoplankton biomass is also clearly lower in the South Catalan. Only during winter, the South Catalan is favoured. For zooplankton, in winter (November-February), the biomass of the South Catalan can be 30% the one of the two other regions. The Gulf of Lion is the poorest in winter especially for zooplankton and the North Catalan is the most favorable region in spring and very obviously in summer.

So to sum up, the table below gives the most important tendencies (no sign means variable). We can keep in memory that **winter is favorable for the productivity of autotrophs and heterotrophs only in the South Catalan and detrimental for the others while spring and summer are always favorable for the autotrophs and heterotrophs in the North Catalan.** These two regions are the most contrasted. The Gulf of Lion works like the North Catalan in winter, and like the South Catalan in summer.

Phyto / Zoo	Late autumn - Winter	Spring (peak)	Summer- Early Autumn
Gulf of Lion	-/-	+/-	+/-
North Catalan	+/-	+/+	+/+
South Catalan	+/+	--/-	-/-

Factors influencing the productivity

The decoupling of the plankton groups and especially for the phytoplankton, results in some compensations between groups which induce a low correlation between the total biomass and the forcing factors. The correlation have therefore to be considered for the different groups separately.

We have found that the phytoplankton winter biomass, is correlated with the heat loss (negative heat flux) with a time lag of 3 months. The total zooplankton biomass as well as its 3 groups are negatively correlated with the heat loss with a time lag between 0 and 2 months (0-1 month for total biomass and 2 months for mesoZk) for the 3 regions.

Productivity in winter

Winter is an essential period to explain the productivity.

The peak of phytoplankton biomass (~March) is highly positively correlated to the heat loss cumulated over January and Fabruary. This is especially true for the Gulf of Lion, a little bit less for the North Catalan. **The zooplankton on the same period has a larger and opposite correlation with meteorological forcing, winter heat losses being detrimental to winter zooplankton for the three regions.** This result emphasizes the importance of the winter meteorological conditions in the Northern Mediterranean which induces a production of large cells of phytoplankton only when winter is over. This result obtained in the coastal ocean is close to what has been obtained by Auger et al., (2014) for the Gulf of Lion open sea. Regions characterized by severe winter conditions produce a strong microphytoplankton biomass in late winter which is allowed by a decrease of the grazing pressure. In the open sea, this relation has been attributed to winter convection which reduces the predators preys interactions. Here, we consider only regions whose depth is lower than 1000 m (with a large part being shallower than 200 m). Further studies would be needed to understand if winter vertical mixing is also responsible of this behaviour through light limitation.

Productivity in summer

We did not find for the three regions a unique relation between the summer biomass and a physical or biological precursor in winter/spring or summer. For the Gulf of Lion only, the phytoplankton biomass averaged over the summer months is positively correlated with the wind stress and negatively correlated with the sea surface elevation (SSH) averaged over the same period while for the North Catalan, the correlation is significant (and strong) only with the SSH (Fig. 6).

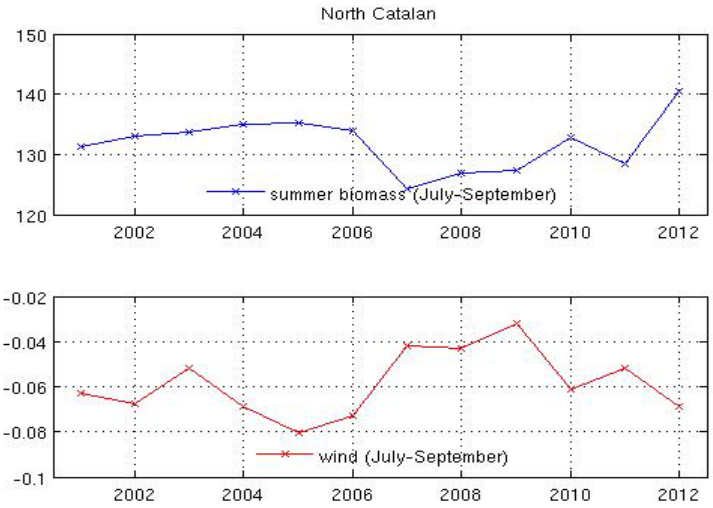

Fig. 6 : Averaged (July September) phytoplankton biomass and sea surface elevation in the North Catalan

These correlations probably reflect an effect of wind on the productivity in summer. The favorable effect of negative ssh indicates that this effect is probably related to upwelling conditions.

For the South Catalan, we did not find a correlation with a physical parameter. For this region, a positive correlation has been found between phytoplanktonic and zooplanktonic biomasses cumulated at the scale of summer. In the same time, the zooplankton biomass is larger than the phytoplankton biomass. These results illustrate how summer is the period of the maximum development of the trophic chain. The energy is efficiently transferred from the primary trophic level to the secondary trophic level and is then recycled. As we will see in the part of this document related to the ecosystem organization, the production is massively regenerated especially in the South Catalan .

Relation of productivity with rivers

A positive correlation has been noted between the phytoplankton biomass and the rivers discharge. The correlation increases from the north to the south. The strongest value (0.55) has been found between in the South Catalan with the Ebro, not far from the North Catalan with the Ebro. The correlation is clearly lower in the Gulf of Lion (0.3 – 0.35 with the Rhône and the rivers of the western Gulf of Lion). The correlation is valid with a time lag between 0 and 2 months depending of regions. In the case of the North and South Catalan, it seems that phytoplankton is first correlated with the Ebro and later with the rivers of the Gulf of Lion which suggests that advection of biogenic components could play a role far from the rivers mouth. More studies should be done to confirm these statistickimg5val results.

Annual productivity

Figure 7 presents the annual biomass of phytoplankton and zooplankton in the three regions. These regions have a contrasted functioning for the two trophic levels. The North Catalan is the most productive for both of them. The South Catalan is favorable to the development of a large biomass of zooplankton (with a low phytoplankton) while in the Gulf of Lion, it is the opposite with a transfer of energy from phytoplankton to zooplankton which is not efficient.

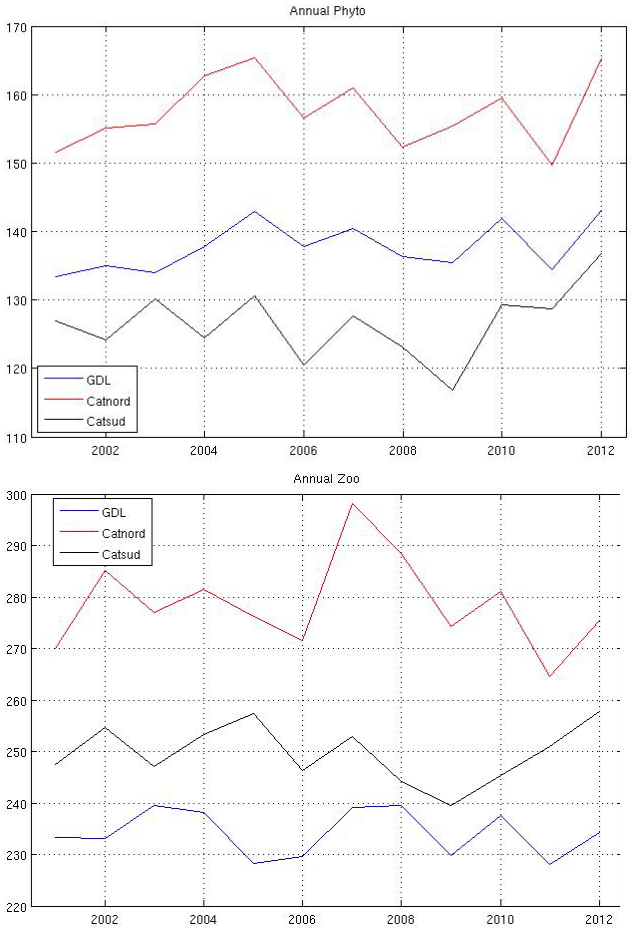

Figure 7 :Mean annual phyto and zoo plankton biomass in the three regions

In the Gulf of Lion, the strong deficit of zooplankton in winter is not counterbalanced in spring and summer as it is the case for the North Catalan. It is very interesting to see that the South Catalan which has an hydrologic behaviour contrasted with the North Catalan has a winter biomass close to summer biomass separated by a moderate spring peak.

The interannual variation of the mean annual phytoplankton biomass is finally also related to the annual atmospheric forcing in the Gulf of Lion and North Catalan. The parameter which is the most correlated to the biomass is the wind stress (correlation of 0.77 in the Gulf of Lion and 0.71 in the North Catalan). This result is in agreement with the good correlation already discussed in winter and in summer. For the South Catalan, such relation does not clearly exist. The productivity is probably in this region a combination of different factors difficult to discriminate.

Conclusion

The seasonal cycle and the interannual variability of three coastal regions of the Northwest Mediterranean have been studied and compared.

The two northern regions (North Catalan and Gulf of Lion) are significantly different from the South Catalan region in winter. The main reason of this difference is likely the vertical mixing induced by the severe meteorological conditions in winter.

The two northern regions where the winter heat loss is maximum are characterized by low zooplankton biomass from December to February. On the contrary, the South Catalan maintains a large zooplankton biomass. An intense bloom of microphytoplankton follows in March, and one to

two months later zooplankton reaches its maximum. The bloom is larger in the northern regions. As in the open ocean, the explosive character of the phytoplankton bloom would be reinforced by the depletion of zooplankton in winter due to prey predator decoupling induced by vertical mixing.

The summer season is very different. The phytoplankton biomass is correlated to the sea surface elevation in the two northern regions probably indicating favorable upwelling conditions. The North Catalan is clearly more productive during this season. Trying to summarize, each one of the three regions have a different functioning :

- The south Catalan is the region with the less intense meteorological conditions. It does not present a clear relation of its biomass with its meteorological or hydrologic conditions. It is the region where the ratio zooplankton/phytoplankton is the largest. The efficiency of the transfer to the upper trophic levels is then high.
- The North Catalan is characterized by intermediate meteorological conditions (but closer to the South Catalan ones). It is the most productive region for the phyto and zoo plankton biomass.
- The Gulf of Lion is characterized by intense meteorological conditions. These conditions are unfavorable to the development of zooplankton while it is rather favorable to phytoplankton. The efficiency of the transfer to the upper trophic levels is poor.

From this analysis, some hypotheses can be drawn. A too intense meteorological forcing is probably detrimental to the development of zooplankton and vice-versa. The strong productivity of the North Catalan region especially for phytoplankton remains to be understood (compared to South Catalan). Maybe moderate wind conditions associated to a privilegiate direction could be a good track to pursue.

Organisation of the ecosystem

We have seen that the productivity is quite different in the northern regions (Gulf of Lion and North Catalan) from the South Catalan and we have related for a part of the year this characteristic to the severe winter meteorological conditions (winter forcing / late winter peak). To understand how the productivity varies at the different trophic levels, it is necessary to consider the organization of the ecosystem, here the composition of the phytoplankton and zooplankton biomass and their variability.

Planktonic groups and seasonality

Figure 8 presents the biomass of the three groups of phytoplankton in the 3 regions. Phyto1, phyto2 and phyto3 represent respectively the pico, nano and micro phytoplankton. The microphytoplanton dominates the biomass from December to April with a peak in March, and is minimum in autumn. At the opposite picophytoplankton which is always low compared to the other groups is relatively high in summer and is very low in winter. The nanophytoplankton is the most complicated group, it presents generally a peak in March-April and then slowly decreases and sometimes increases again in November. These two periods correspond to the spring and autumnal blooms. The South Catalan specificities concern mostly the nanoPk which does not present an autumnal bloom and a minimum in winter but rather a regular increase from October to March. This particularity would indicate that the automnal and spring blooms could be seen as an enrichment by nutrients and induced efflorescence, continuous from autumn to the end of winter. In the case of cold winters as in the other regions, the process is interrupted (in December January) and the two blooms appear as distinct.

The maximum of microPk is shifted to February in the South Catalan (compared to March for other regions) and this is due to a shift in the levels of turbulence between this region and the others.

We have looked for correlations between these 3 groups to understand potential compensations between groups. There is a strong negative correlation (r~0.9) for the three regions between pico and microphytoplankton with a time lag of two months (for example, an increase of picoPk biomass precedes a decrease of microPk biomass by two months). In the two Catalan regions and less in the Gulf of Lion, microPk and nanoPk are positively correlated with a 1-2 month time lag (increase of microphytoplankton precedes increase of nanophytoplankton by 1-2 month). The nanoPk is generally the group which presents the lowest correlation with meteorological conditions at the monthly frequency. We interprete these correlations rather as an opportunistic behaviour of this group dependent of numerous factors and maybe be differing along the year. For example nanoPk generally reaches its maximum when microPk has already declined. In the same way, the positive correlation of nanoPk with heat flux could reveal that this group has benefit of conditions which are detrimental to microPk, for example, mild winters which produce low mixing and reduced nutrients input could favor the development of nanoPk rather than microPk.

Besides the total phytoplankton biomass is highly correlated to microphytoplankton biomass in the three regions without time lag. This is simply due to the major contribution of microPk to the total Phytoplankton biomass

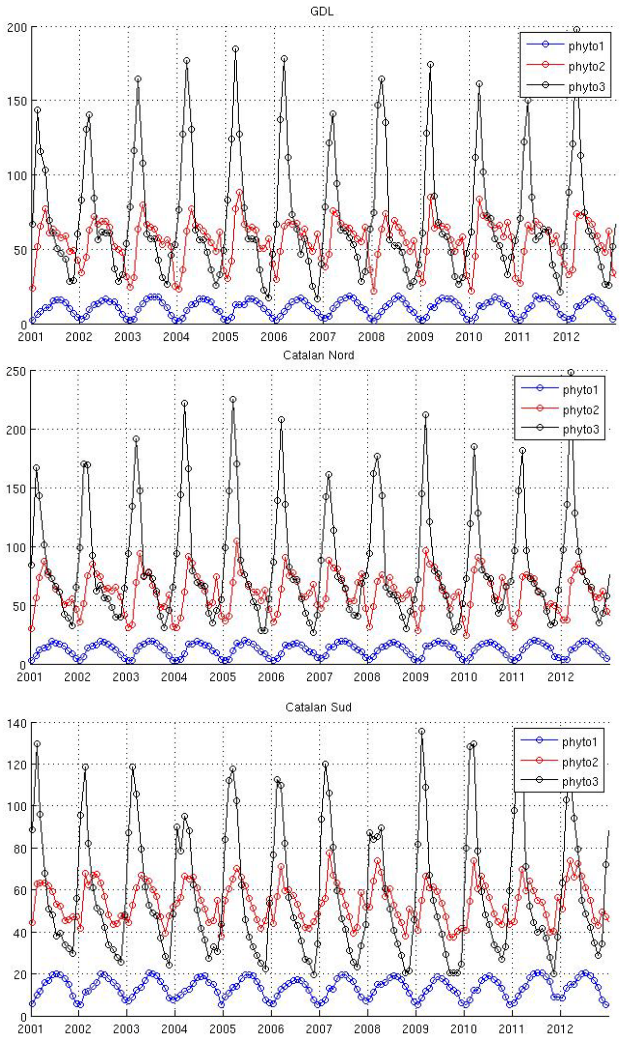

Figure 8 : Biomass of the 3 groups of phytoplankton in the three regions indicated in the frames. Unit : mmolC.m^{-2}

Figure 9 presents the different groups of zooplankton for the same regions. Zoo1, 2 and 3 represent respectively the nano, micro and meso zooplankton groups. The prevailing group is microzooplankton everywhere. The shift between the different regions for the development of the three groups is low. MicroZk is maximum in April, NanoZk in May and mesoZk in June. So the zooplankton groups are more in phase than the phytoplankton groups. In the South Catalan, the annual variation range of microzoopK is lower than in the two other regions. This group is probably more adapted to winter conditions of this region. In the Gulf of Lion and North Catalan, the groups suffer in winter but as soon as winter is over and the phytoplankton starts its development, the zooplankton development is explosive (see the steepness of the ascending part of the curves for microzooPk).

The three groups of zooplankton are generally very well correlated one to the other (r often larger than 0.9). The time lag of these correlations is maximum for microZk and mesoZk, with microZk preceding mesoZk by 1 to 2 months.

Finally the total zooplankton biomass is strongly correlated to the nanoZk and microZk biomasses without time lag. This is due to the major contribution of microZk to the total zooplankton biomass.

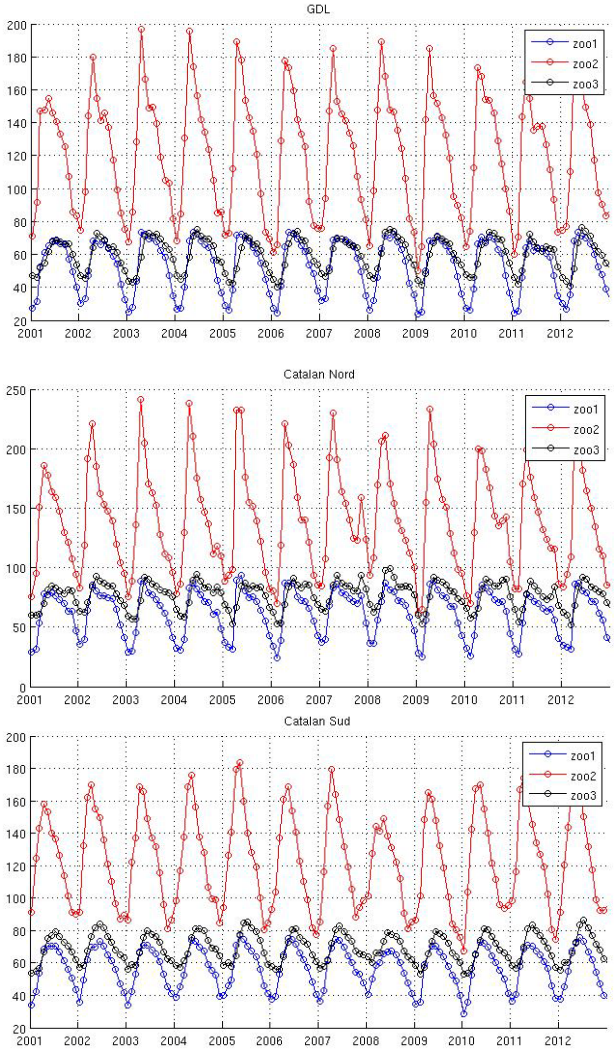

Figure 9 : Biomass of the 3 groups of zooplankton in the three regions

mmolC.m^{-2}

Concerning relations between total phytoplankton and zooplankton biomass, we have found a correlation with a time lag of two months. This correlation is very high in the South Catalan (0.92) and decreases in the two other regions (~0.82). It is probably related to the fact that zooplankton biomass never collapses in South Catalan as it does in winter in the two other regions. The ratio zooPk/phytoPk never falls below 1 as it is the case for the two other regions in winter. So phytoplankton sustains zooplankton production all the year long. The ecosystem is more equilibrated. In the two other regions, climatic factors are probably detrimental to the energy flux between trophic levels at least in winter.

Interannual scale

At the interannual scale, the same relation noted in the first part of this report between summer phytoplankton and wind stress / ssh in the Gulf of Lion and North Catalan has been found only for nanophytoplankton. NanoPk is indeed the main group contributing to the summer biomass. It seems favored by specific wind conditions, probably those inducing upwelling. As for the total phytoplankton biomass, we did not found any relation between individual groups and forcing in the South Catalan. Now if we consider the mean annual biomass, we also found a correlation of different groups with the wind or ssh forcing. The correlation concerns microPk for the Gulf of Lion and North Catalan (it probably reflects the importance of winter) and also nanoPk for the GDL. Once more, no relation was found in the South Catalan with the forcing.

On the other hand, it exists a **high positive correlation for the South Catalan between the mean summer (July-September) biomass of nanoPk and microPk**. Two non exclusive hypotheses can be given. Conditions are much more stationary in summer and then, an equilibrium can be found between groups. The second hypothesis, complementary of the first one, is that the groups are organized relative to each other at smaller scales than the regions considered here and also at different levels on the vertical. For example, we have checked that during summer, the deep maximum of biomass is localized deeper for microphytoplankton than for nanophytoplankton. This could be related to the fact that microphytoplankton needs more nutrient and less light than the other groups. Finally it seems that the nanophytoplankton and microphytoplankton which do not drop abruptly after spring in the North Catalan sustains the zooplankton biomass in summer and then should be responsible of the high zooplankton biomass previously noticed in this region. The reason of this high biological activity in summer has to be found, but we suspect that one reason could be favorable wind conditions able to induce vertical motions as upwelling at the coast or at the shelf break. The Gulf of Lion is more difficult to interprete. On reason could be a spatial heterogeneity, for example the northern coast is generally favorable to upwelling while the western part is favorable to downwelling.

Relation with river discharge

Concerning the influence of **rivers discharge**, the **correlation of the total phytoplankton biomass with rivers is clear** in the South Catalan with the Ebro. The nanoPk and microPk are the groups which respond. In the North Catalan, the biomass is also correlated with the Ebro mainly through the microPk. In the Gulf of Lion, the correlation of microPk is also significant but lower than in the two other regions, this time with the Rhone and West Gulf of Lion rivers. This positive impact on large phytoplankton is accompanied by a clear negative effect on picophytoplankton. **Then, the common point to the 3 regions is the positive correlation of the microPk with the rivers discharge.** This could be due to the strong affinity of microPk with high concentration of nutrients.

Gpp - grazing

Figure 10 presents the gross primary production, the grazing and the bacterial production for the 3 regions. The GPP is maximum in spring summer and minimum in winter. Some remarks done for biomasses are valid for the GPP. The South Catalan is the region presenting the largest GPP in winter and the lowest GPP in summer. The Gulf of Lion has generally the lowest GPP in winter. The North Catalan has the highest GPP in spring summer. The grazing is also maximum in winter in the South Catalan. In spring, the North Catalan presents a peak of grazing, but the three regions are more equilibrated in summer.

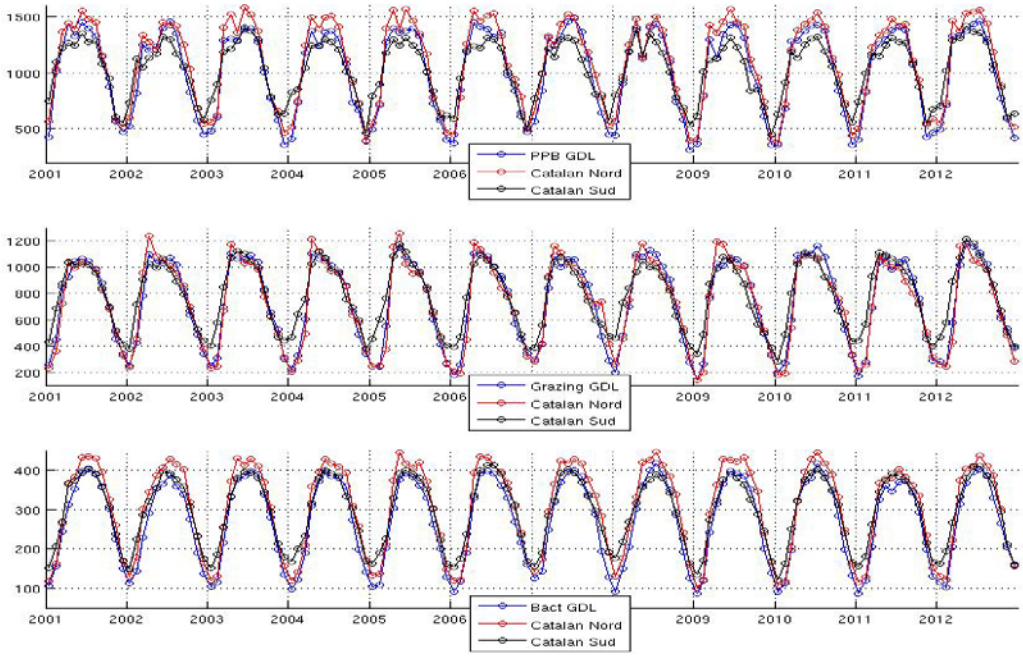

Figure 10 : GPP (top), grazing (middle) and bacterial production (low) in the 3 regions (mg m^{-2} day^{-1})

Figure 11 presents the ratio of these fluxes. These curves confirm that the Gulf of Lion and North Catalan present a strong seasonal dynamics imposed by severe winter meteorological conditions. At the beginning of winter, January is a period of transition in the organization of the ecosystem, the three fluxes are at their annual minimum, but, the PPB is not reduced so much than the heterotrophic production. This fact has been confirmed in the open sea during the Leg1 of the DEWEX experiment which took place during convection. As it is well known, surface chlorophyll becomes very low during convection, but as it was already infered from modelling (Auger et al., 2014), it was observed that the depth-integrated chlorophyll is not low. Second point, the model also shows than the grazing, strongly inhibited by vertical mixing, is more inhibited than the bacterial activity probably stimulated by the exudation of DOM : **the ratio between bacterial production and grazing is then at its maximum in winter**. This effect is as much strong that the winter is severe as shown at two levels : first, by comparing regions, the peak of this ratio does not exist in the South Catalan where winter are mild ; second at the interannual scale, the peak of this ratio is maximum for the Gulf of Lion and North Catalan in 2009 when PPB and grazing are at their minimum and this could be due to a cold pre-winter period (November – December) which durably affected the herbivorous.

Then, March is the period of the bloom. The three fluxes increase very rapidly between February and March. The primary production stimulates the development of herbivorous which makes the Bact/Grazing ratio dropping. May corresponds to the maximum of the zooplankton biomass.

Starting from May June, a new period begins with the change in the phytoplankton population responding to a strong reduction of nutrients. The zooplankton and especially the dominant microZk group decreases but the bacterial activity is maintained leading to a new increase of the ratio Bacterial production/Grazing lasting until December. The Bacterial/Grazing ratio is higher all the year long in the North Catalan than in the Gulf of Lion. This could be a key to understand the large difference of zooplankton biomass (and of phytoplankton in summer) between these two regions which, on the other hand, present similarities in winter.

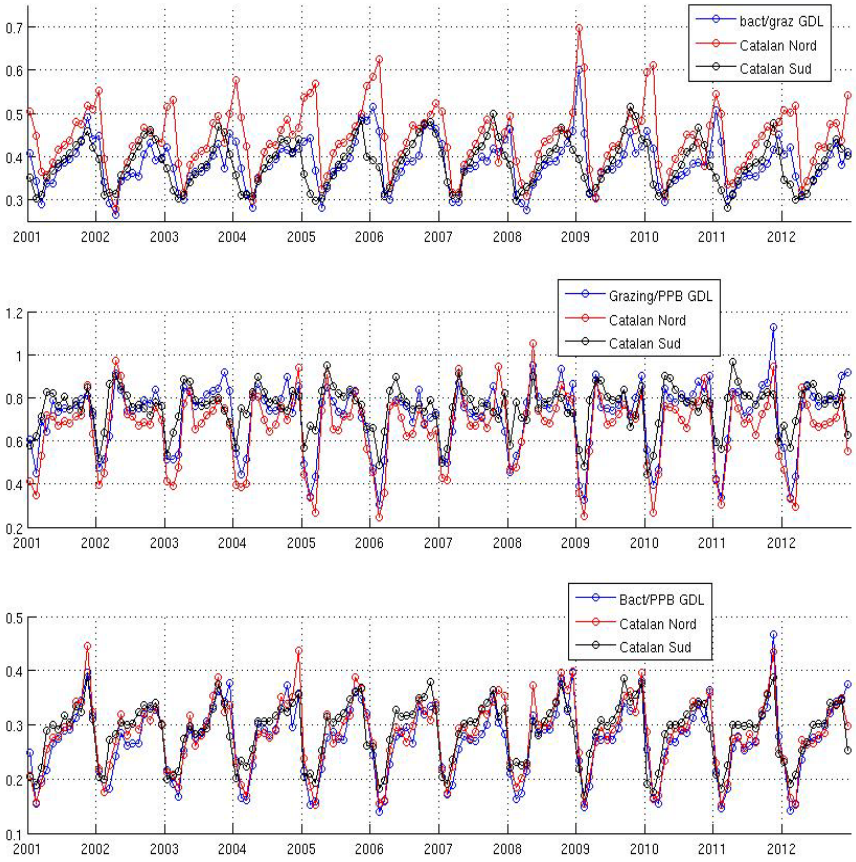

Figure 11

Ratios of biologic fluxes as indicated in the figure

New production – regenerated production

Figure 12 presents the new production (based on nitrate) and the fraction of regenerated production (based on ammonium) over total production. This figure illustrates the difference between the two regions to the North (Gulf of Lion and North Catalan) and the South Catalan. The two northern regions have a large March peak of new production while in the South Catalan the production is more regenerated than in the other regions even in winter (60% vs 40%). Even in summer, new production is more important in absolute and in relative in the northern regions than in the South Catalan.

At the interannual scale, the relation with the forcing is also clear. For calm winters like in 2007, the production in the northern regions is more regenerated.

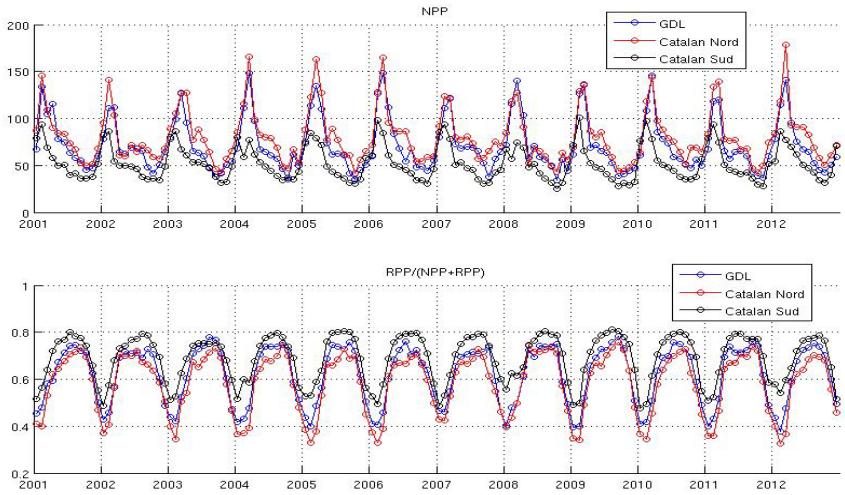

Figure 12 : New production (based on nitrate) and fraction of the regenerated production (f-ratio)

Conclusion

The seasonal cycle and the interannual variability of three coastal regions of the Northwest Mediterranean have been studied and compared.

The two northern regions (North Catalan and Gulf of Lion) are significantly different from the South Catalan region in winter. The main reason of this difference is likely the vertical mixing induced by the severe meteorological conditions in winter.

All the biological fluxes are strongly inhibited by vertical mixing in winter but the processes affecting the secondary trophic level (grazing) are the most affected while PPB and bacterial activity are less inhibited: the ratio between bacterial production over grazing is then at its maximum but drops suddenly when the phytoplankton bloom stimulates the zooplankton growth. During the whole year, the North Catalan is characterized by a relatively high ratio bacterial production / grazing. This could explain the poor efficiency of the transfer to the secondary level of the trophic chain. More research is needed to understand these complicated relations.

The phytoplankton biomass is dominated by microphytoplankton in winter and early pring. Summer is dominated by nanophytoplankton and picophytoplankton. Summer phytoplankton biomasses are higher in the northern regions, while zooplankton biomass is high specifically in the North Catalan. The reason remains to be elucidated.

Rivers affect mainly the microphytoplankton group and the effect is more clear in the South Catalan maybe because nutrients from other sources are more rare.

The new production is larger in the northern regions than in the South Catalan during all the year. The largest value is in the North Catalan region which can be related to the high phyto and zoo plankton biomass in this region. The South Catalan region is characterized by a production that is proportionnaly more regenerated than in the other regions also during all the year.

The three regions have been studied independently from each other. However, advective transfers cannot be neglected between these regions. For example, it would be interesting to consider the potential effect of the advection of nutrients from the Gulf of Lion to the North Catalan that could stimulate new production for example. The Gulf of Lion is probably not easy to understand as it is the addition of at least two contrasted regions (its northern and western parts). A bioregionalization based on hydrologic and biogeochemical variables could help to understand if this hypothesis is pertinent.

Alboran Sea (CSIC)

Investigating vigor through modelling in the Alboran Sea

Introduction

We here calculate vigor through modelling assuming that the analysis through time of biomass of primary and secondary producers is a proxy for the "health" dynamics and productivity of the system. The assumptions in the calculation of ecosystem "vigor" comes from the previous observations (field and satellite data) showing that the functioning of the pelagic system (which cascades down into the benthic compartment) in the Alboran Sea is 1) controlled fundamentally by the strength, position and timing of the Atlantic Jet (AJ) and 2) that AJ is mechanistically tied to the kinetic energy (KE) in the Alboran Sea. As for the first assumption, the paramount controlling role of the AJ in the production of the system has been extensively documented (Ruiz et al. 2001, Macías et al. 2009, Navarro et al. 2011, Oguz et al. 2013). The second assumption has also been documented in PERSEUS work, where the variations in the pelagic HTL (anchovy recruitment) were linked to disruptions of KE, enabling a more stable environment that, despite generating lower primary production, fostered fish recruitment (Ruiz et al. 2013). No abundance time-series for other compartments obtained through modelling exist in the area, so given the peculiar characteristics of this upwelling area, it is reasonable that we adopt an hypothesis-driven approach to the ecosystem dynamics. Within the frame of Perseus, one recent work enabled CSIC to produce model-based biomass estimates for primary and secondary production components in the Alboran Sea, thanks to a Fasham-based biogeochemical model of the type $N_2P_2Z_2D_2$ (Macías et al. 2014). This model thus produces estimates for two forms of nitrogen (NO3 and NH4), which controls productivity in this part of the Mediterranean, two sizes of phytoplankton (nano and microphytoplankton), two sizes of zooplankton (micro and mesozooplankton) and two sizes of detritus.

Objectives

The objectives of this contribution are to provide model-based results of vigor, defining vigor as the variation in system's production for a particular length of time. Within Perseus, we have selected a highly comparable time slices to those indicated in the DoW. Further, we inspect the potential scenarios in 2010-2020 using the available model information and knowledge.

Material and Methods

The coupled biogeochemical model used (Macías et al. 2014) is coupled to a 3D ROMS which has been thoroughly tested in the area (Peliz et al. 2013a, Peliz et al. 2013b). The coupled model spans from 1989 to 2008, with a domain depicted in Fig.1. The hydrodynamical model is a ~2km resolution ROMS-AGRIF model forced with ~9 km winds and air-sea fluxes for all the domain. The details, performance and setup has been described as commented before. The biogeochemical part embedded in ROMS is a modification of (Fasham et al. 1990) following the philosophy of (Kone et al. 2005) and is fully described in (Macías et al. 2014). The conceptual mode is depicted in Fig.2.

We analyzed two time slices (1989-1999 and 2000-2008) to approximate the first two time-slices in Perseus. For the 2010-2020 time slice, and due to the nature of our system, it was judged inappropriate to take as probable the projections. because the forcing functions driving the Kinetic Energy (not only pressure but local wind direction) cannot be adequately projected in the future in a quantitative way (IPCC, 2014) unless an ensemble model for meteo is used, which was not available to us. However, we inspected Perseus projections of Pressure for 2010-2020, but found that projections , with respect to our particular system's functioning, are inadequate. Therefore, we work with alternative scenarios based on KE and Wind regimes and their consequences on the vigor based on the current model-derived knowledge.

The EKE was derived from model outputs so that KE=0.5 *(u_momentum^2 + v_momentum^2). The inspection of pressure was obtained from the ALboran section of forecasted and hindcasted pressure provided by the Perseus Team (M.Vicci).
For each time slice, we here used the model-derived mean monthly values for total phytoplankton and total zooplankton to approximate production. We used two horizontal domains and two vertical calculations. The spatial domain comprised either the whole Alboran (restricted to the area between 5° and 2° W) and the Northern Alboran (same as before but with a lower bound at 36°N (Fig.1). Vertically, we analyzed monthly integrated values at 10 and 100 m. For the integrated 10 m data, we ran preliminary anlysis demonstrating that they were a good proxy for surface (satellite) production) r^2>0.99 compared with Chla at 5 m and with average Chla at 10 m. Using integrated values for production makes sense because the Deep Chlorophyll maximum and associated zooplankton are around 80 m in summer, and surface values do not capture production correlctly (Macias et al. 2011).

The calculation of anomalies was conducted using all the time series, and initial linear fits were adjusted to each time-slice and spatial domain to inspect trends. Trends in vigor were analyzed through General Linear models on the log10-transformed monthly anomalies of biomass measures and for each time-slice, after inspecting the residuals for correct assumptions of the tests.

Results

Calculated past evolution of Vigor in the first two time-slices

Raw model values of total Chla and zooplankton showed, as expected, that integrted biomass is higher in the North Alboran than when all the Alboran Sea is considered (Table 1, Fig.3). This is regardless the time-slice considered. No significant differences were detected in average raw values between time slices when separated by spatial domain (Table 1). Strong seasonal oscillations are observed in spatial and temporal settings (Fig.4), but clearly some anomalies in the time series can be spotted even without further analysis, such as in 1996 and 2001, particularly in the Northern Alboran (Fig.3).
However, if values are integrated over the first 100 m differences between North and all the Alboran Sea are enlarged, particularly for the phytoplankon (Fig.3, Table 1). The analyses of monthly anomalies (thus eliminating seasonal signal) showed that there were no significant differences in average values between time slices (T-tests on log-transformed values, P>0.05).
The average monthly evolution (climatology) of values at each time slice showed the typical annual cycle with different intensities as a function of the spatial coverage (Fig.4). Fig.4 depicts three interesting features. **Firstly**, that the integrated values over the 100 m do differ in average seasonal pattern from the integration at 10 m, reflecting production processes associated with vertical structure such as Deep Chlorophyll maximum. Particularly, the maximum integrated Chla tends to be displaced towards spring, whereas using 10 m values maxima occur earlier in the year. **Second**, that by looking at 10 m-integrated values, the minimum occurs in summer, whereas summer values can be relatively if integrated over the photic zone. And **third**, that although average values tend to be similar between time slices (Table 1), the seasonality (Fig. 4) suggests that the later part of the year**, biomass values tend to be lower in the second time-slice** (e.g. total phytoplankton).
The exploration of anomaly trends in the two time slices (Fig. 5) Showed that no trends were apaprent in most of the relationships (Linear models), except for the period 1998-2008 in values integrated over 100 m. The separate linear models on the anomalies, accounting for a factor 1 autocorrelation showed that the only significant trends were:

1)total phytoplankton anomalies decreased with time in the Northern Alboran if values were integrated over 100 m and only for the time-slice 1999-2008 (anom=84.87 -0.302(se=0.010)*time), r2=0.06, $F_{1,118}$=8.33.
2)The same trend was observed for total zooplankton , where anom=69.29-0.0227(0.010)*time, P<0.05, R2=0.04, $F_{1,118}$=4.96

Estimates for 2010-2020

Under the assumption that KE drives the dynamics of the system, we correlated monthly anomalies for KE with total phytoplankton. A previous autocorrelation analysis showed that lag0 provided the maximum correlations. Table 2 shows that model-based Kinetic energy is directly related to production. The maximum correlation was observed for the North Alboran Sea at the surface (integrating 10 m) (Fig.5).
Under our hypothesis, future changes in the vigor of the system will depend on the dynamics of the AJ (which controls most of the production), which might be measured by KE. We know that KE responds to pressure (Navarro et al., 2011). However, our exploration of the available pressure estimates are either too local (e.g. we tried with the pressure estimates for the pixels in the Alboran Sea produced for 2010-2020 within Perseus) do not provide good correlations with KE anomalies. Using predictions of wind and NAO would ideally provide a more accurate predictor of vigor.
The actual trends in the series indicate a decrease in vigor, but we do not think that these trends can be extrapolated at all. In an scenario frame, and taking into consideration the inverse effect of pressure on production and the direct effect of EKE in production it is expected that primary production (not necessarily fisheries) will be a function of not only KE but when in the year the KE change takes place.

Discussion

Our data have shown the magnitude of model-derived production across time-slices, and some trends that, however, cannot be extrapolated safely into the future. The data offered can beof use in order to compare systems. The model outputs of phytoplankton biomass have already been validated in Macías et al (2014) for some areas in the Alboran Sea. This is not the case for zooplankton, for which few data exist. IN any case, satellite data and model outputs were relatively well correlated in the time series (Macías et al., 2014).
It is clear that spatial correlation exists i our measurements. For example, our separation into the North Alboran Sea and All the Alboran Sea implies that the second contains information of the first one, but by difference it enables to analyze both components. IN any case, the discretization of the North Alboran Sea is crucial for it furnishes most production in the area.
We showed that by integrating production over 100 m we obtain different patterns through the uear, which is extremely relevant for interpreting the system's dynamics. We showed that the model produced anomalies for KE are directly related to production, and thus estimates of KE (by empirical relationships) wull be possible when ensemble model results of AMO and NAO are available.

Figures

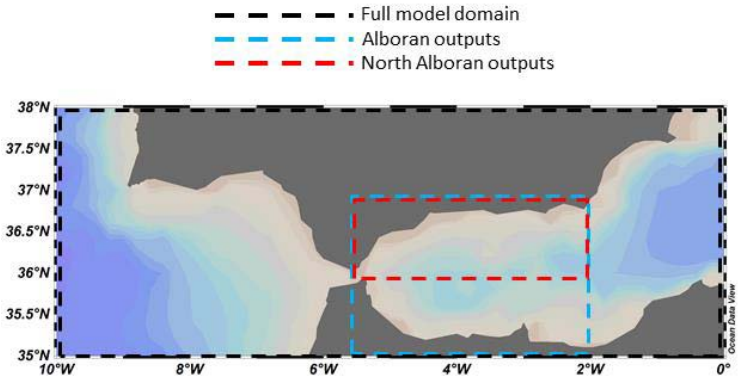

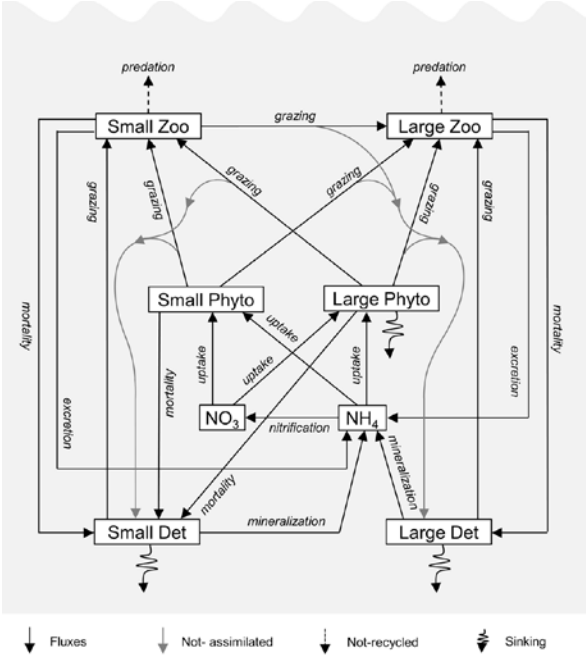

Fig.2 Conceptual diagram of the biogeochemical model used. Boxes represent state variables and arrows are energy and mass fluxes. From Macías et al. (2014)

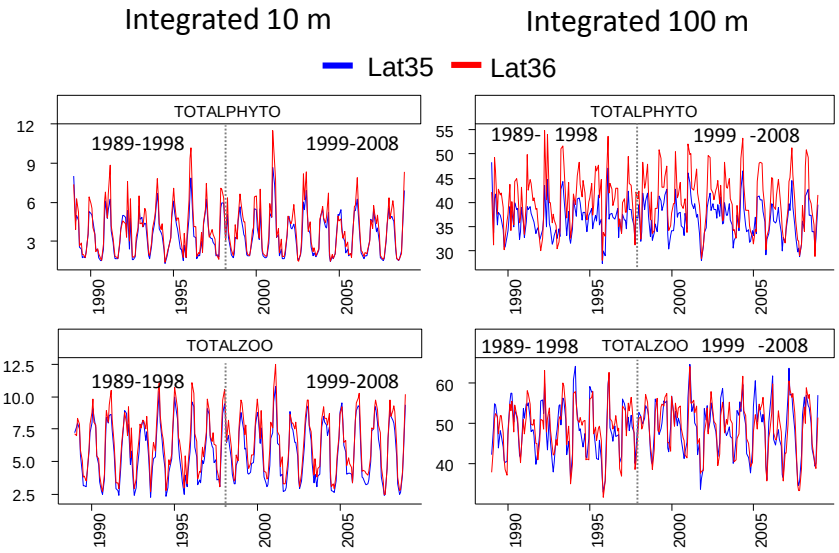

Fig. 3. Raw model-derived Chl a integrated at the top 10 m (A) or integrated at the top 100 m (B). The two spatial domains (all Alboran or North Alboran) and the two initial time-slices are included. SPHYTO=small phytoplankton, LPHYTO=large phytoplankton, TOTALPHYTO=total phytoplankton. Values are mg or ml m^2

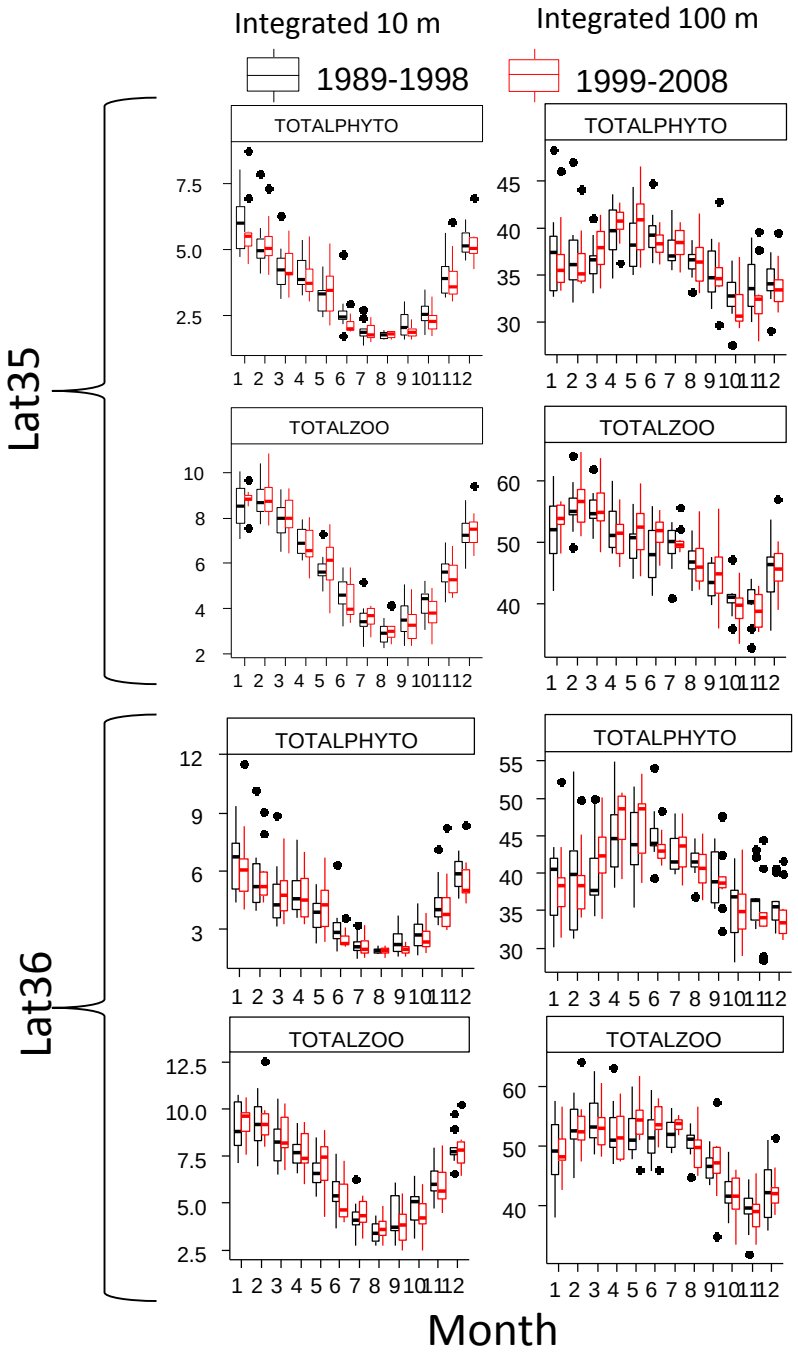

Fig. 4. Model-based Box-plots on monthly data for two calculated time-slices. Data for both spatial domains are included. Note the large differences in the climatology of the integrated values over the first 100 m of the colum. Units as in Fig. 3.

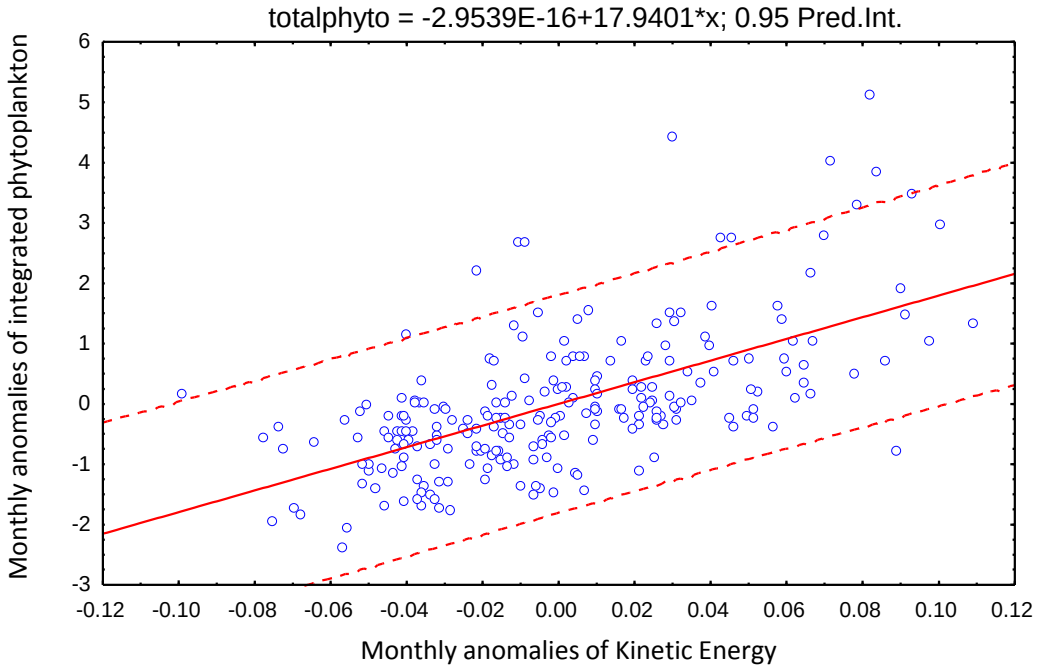

Fig. 5. Regression and 95% prediction intervals between the monthly anomalies of kinetic energy of the North Alboran (average in the first 10 m) and the anomalies in total phytoplankton biomass in the same area and integrated over 10 m.

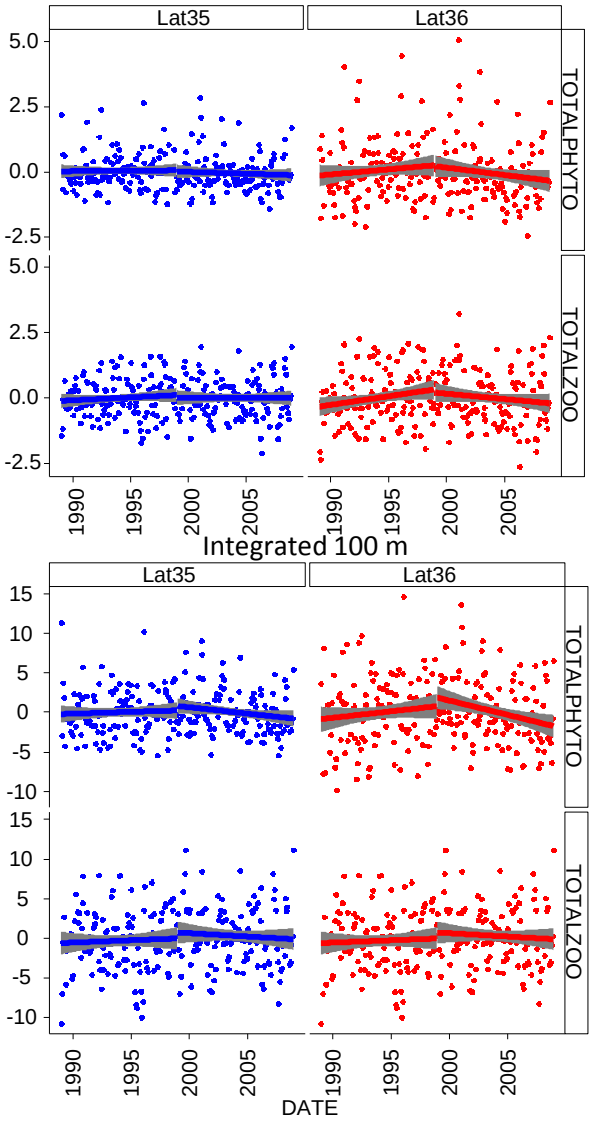

Fig.5. General view of vigor trends by model-derived data for the two time-slices. Note that stats are not displayed as a linear smoother is fit to the raw anomalies, some of which don't fit normality.

Tables

Table 1. Average and standard deviation values of total Chla and zooplankton values for each spatial domain, time slice and vertical type of calculation. Values for phyto are mg/m2, and for zooplankton are are integrated by m2, either mg or ml.

Spatial coverage	time-slice	measurement	Mean Total Phyto	sd	Mean total zoo	sd

Alboran	1989-1998	int10m	3.61	1.536	5.80	2.128
		int100m	36.59	3.544	48.31	6.244
	1999-2008	int10m	3.51	1.574	5.81	2.231
		int100m	36.60	3.840	48.94	6.687
North Alboran	1989-1998	int10m	4.02	1.879	6.45	2.18
		int100m	40.23	5.483	48.82	6.199
	1999-2008	int10m	3.90	1.954	6.45	2.307
		int100m	40.35	5.787	49.07	6.508

Table 2. R^2 values between the average Kinetik energy anomalies (for either 10 or 100 m, and for each spatial domain) with their corresponding anomaly values for integrated total phytoplaknton of zooplankton. values were significant at $p<0.05$. N=239.

Table 3. Scenarios of Vigor contemplated for 2010-20120

Pressure(but related to wind direction)	KE	Biol. production
decrease	increase	increase
increase	decrease	decrease

	Int_10_L35	Int10_L36	Int100_L35	Int100_L36
TOTALPHYTO	0.21	0.37	0.13	0.18
TOTALZOO	0.17	0.26	0.03	0.02

References

Fasham, M. J. R., H. W. Ducklow, and S. M. McKelvie. 1990. A nitrogen-based model of plankton dynamics in the oceanic mixed layer. Journal of Marine Research **48**:591-639.

Kone, V., E. Machu, P. Penven, V. Andersen, V. Garcon, P. Freon, and H. Demarcq. 2005. Modeling the primary and secondary productions of the southern Benguela upwelling system: A comparative study through two biogeochemical models - art. no. GB4021. Global Biogeochemical Cycles **19**:B4021-B4021.

Macias, D., I. A. Catalan, J. Sole, B. Morales-Nin, and J. Ruiz. 2011. Atmospheric-induced variability of hydrological and biogeochemical signatures in the NW Alboran Sea. Consequences for the spawning and nursery habitats of European anchovy. Deep-Sea Research Part I-Oceanographic Research Papers **58**:1175-1188.

Macías, D., C. T. Guerreiro, L. Prieto, A. Peliz, and J. Ruiz. 2014. A high-resolution hydrodynamic-biogeochemical coupled model of the Gulf of Cadiz – Alboran Sea region. Mediterranean Marine Science **15**:759-752.

Macías, D., G. Navarro, A. Bartual, F. Echevarría, and I. E. Huertas. 2009. Primary production in the Strait of Gibraltar: Carbon fixation rates in relation to hydrodynamic and phytoplankton dynamics. Estuarine, Coastal and Shelf Science **83**:197-210.

Navarro, G., A. Vzquez, D. MacÍas, M. Bruno, and J. Ruiz. 2011. Understanding the patterns of biological response to physical forcing in the Alborn Sea (western Mediterranean). Geophysical Research Letters **38**.

Oguz, T., D. Macias, L. Renault, J. Ruiz, and J. Tintore. 2013. Controls of plankton production by pelagic fish predation and resource availability in the Alboran and Balearic Seas. Progress in Oceanography **112-113**:1-14.

Peliz, A., D. Boutov, R. M. Cardoso, J. Delgado, and P. M. M. Soares. 2013a. The Gulf of Cadiz-Alboran Sea sub-basin: Model setup, exchange and seasonal variability. Ocean Modelling **61**:49-67.

Peliz, A., D. Boutov, and A. Teles-Machado. 2013b. The Alboran Sea mesoscale in a long term high resolution simulation: Statistical analysis. Ocean Modelling **72**:32-52.

Ruiz, J., F. Echevarría, J. Font, S. Ruiz, E. García, J. M. Blanco, F. Jiménez-Gómez, L. Prieto, A. González-Alaminos, C. M. García, P. Cipollini, H. Snaith, A. Bartuala, A. Reul, and V. Rodríguez. 2001. Surface distribution of chlorophyll, particles and gelbstoff in the Atlantic jet of the Alborán Sea: From submesoscale to subinertial scales of variability. Journal of Marine Systems **29**:277-292.

Ruiz, J., D. Macías, M. M. Rincón, A. Pascual, I. A. Catalán, and G. Navarro. 2013. Recruiting at the Edge: Kinetic Energy Inhibits Anchovy Populations in the Western Mediterranean. PLoS ONE **8**.

Analysis of ecosystem organization through modelling in the Alboran Sea

Introduction

The dynamics of the system is strongly controlled by the incoming Atlantic jet (angle and strength) and dominating winds. The organisation of the biological components of the system is expected to be similar to a typical upwelling system, and in that respect it is remarkably different to most other areas in the Mediterranean. Although there are no current models that tackle simultaneously all components of the trophic web in the Alboran Sea, several tools have been developed within Perseus and past projects that, within this contribution, will enable to examine both the biological organisation of at least the pelagic realm, its changes in the decades of the 90s and first decade of the 2000's, and how projections of climate force the organisation into 2010-2020. The organisation of LTL through models has been evaluated by Macías et al. (2014) through a $N_2P_2Z_2D_2$, and was the basis to analyze the ecosystem "vigor" in S.4.2.2. In this contribution we work following a hypothesis-driven way to analyze the behaviour of the system organisation and how it may behave in the future. Our basic hypothesis stems from the paper by Ruiz et al (2013) which strongly suggests that the energy of the system, which can be measured as Kinetic Energy (KE), is the main driver of the systems production and is associated with the Atlantic Jet. In that paper, it was shown that the dynamics of the Alboran Sea were particularly disturbed when the Atlantic jet was stopped, and we showed with our model that KE variations can be reproduced in relation to production (Fig.1). In the cases when the AJ is severely disrupted, which occurs only very occasionally, we showed that the weakening of the upwelling (associated to the jet) had inverse consequences on production (reducing it) and positive effects on at least some trophic levels (e.g. anchovy), enhancing an extraordinary high recruitment never described until that AJ disruption. In another paper on the area tackling HTL through modelling in the area (Catalán et al. 2013), it was shown through individual-based modelling (IBM) that indeed the anchovy recruitment is almost always physically-constrained by the permanent existence of the AJ, which constrains the nursery area to a very narrow fringe, thus indirectly supporting the paper by Ruiz et al. (2013). Empirical evidence (Mercado et al. 2007) suggested that the whole planktonic community was affected by the

weakening of the jet in 2001, and they described a change in the LTL and some stages of HTL species, with an increased pressence of cocolitophorids, associated to more stable conditions. Finally, our hypothesis-driven approach implies that meteorological indices associated to air pressure (e.g. NAO) are indeed correlated to changes in the dynamics of the Jet (Ruiz et al. 2013). Therefore, our objective is to link model-based outputs of organization, with empirical models that aid in the understanding of organization responses to the environment.

The organization of the system in the area will be analyzed, for the selected time-slices, through an innovative approach involving the progress in coupled 3D biogeochemical models (see CSIC contribution in subtask 4.1.3. Macías, Guerreiro et al. 2014, Fig.2).

Extrapolations to the future will be explored by first analyzing available proxies for kinetic energy as driver of the system (pressure). Scenarios of potential situations will be utilised as a conservative measure to provide advice on potential changes during 2010-2010.

Material and Methods

The evolution of four compartments of the LTL in the Alboran Sea was modelled for two decades (1989-1998 and 1999-2008) following (Macías et al. 2014b), and described in more detail in S.4.2.2.-CSIC (Fig.2). The two-compartment NPZD model at high (2 km) resolution model yielded, besides detritus (not used herein), small phytoplankton (nanophytoplankton), large phytoplankton (Diatoms), small zooplankton (microzooplankton) and large zooplankton (mesozooplankton). The model has been validated for total phytoplankton and zooplankton in nearby areas. Units were mg m^{-3} for phytoplankton and ml l^{-1} for zooplankton.

For the first two time slices, we analyzed raw monthy data and monthly anomaly time series in search for changes in organisation. As for S.4.2.2.-CSIC, we looked at two spatial domains (Northern Alboran, hereforth L36 (2-5ºW - 36-37ºN), and All Alboran, hereforth L35 (2-5°W - 35-37°N). Previous correlational analyses showed that surface data was well represented by data integrated in the first 10m (hereforth int10) and whole-column production was well represented by data integrated over the first 100 m (hereforth int100). Due to the hypothesis-driven approach of this exercise, we explored for abrupt changes in organisation as those expected to occur when remarkable decrease in KE occured. For that, we first explored for the effect of monthly anomalies of KE on monthly anomalies of organisation indices in the LTL outputs. The KE was analyzed for both spatial domains but average values for 10 and 100 m were used. The organization was explored using two types of related indices. One was based on looking at how the small trophic fractions (small zooplankton/small phytoplankton, SZ/SPH) and the “typical” fractions of the system (large zooplankton/large phytoplankton, LZ/LPH). The second one looked at the relative variation of large vs small primary and secondary producers (large /small phytoplankton, LPHY/SPHY, and large/small zooplankton, LZ/SZ). The indices were explored in their monthly anomalies, and correlations with KE anomalies were screened for both spatial domains. In this contribution, no formal time-series analyses were conducted as only abrupt changes were inspected.

Finally, in an attempt to project changes for 2010-2020, we decided to use a correlational approach first based on the PERSEUS-generated air pressure data over the Alboran Sea, forecasted until 2020, to extract relationships between pressure and KE. As results were not convinvcent, we used a scenario-based approach to analyze potential consequences for the Alboran Sea organization depending on the next year’s evolution of the kinetic energy of the system.

Results

Variation in organisation within the first two time slices.

Oscillation of raw values of the four components of the LTL section showed the expected high seasonality in the LTL components (Fig.3). Absolute values were similar between North Alboran Sea and All Alboran Sea when calculated over the first 10 m, but integrating over 100 m revealed large

spatial differences: The peaks of small phytoplankton and large zooplankton had a maximum when all the Alboran is considered, whereas the large phytoplankton (diatoms, the main production due to upwelling) excels in the northern Alboran Sea (Fig.3).
The seasonal pattern was clearly different in the small phytoplankton, peaking in summer-autumn in both calculated time-slices, whereas the other three components followed the typical spring and toned-down fall production (Figs. 4 and 5).
The individual analyses of anomalies (standardized by each month according to a linear model where the month is consider a factor, and taking the residuals) of the whole series showed some singularities, such as large phytoplankton maxima (the drivers of production as shown in S4.2.2.-CSIC) in 2001 and 1996 (Fig.6), but otherwise similar oscillations between the large and small spatial domains were observed. No decomposition of single components was made as it was an index of organization what this contribution is dealing with.
We used two simple indices to explore how the relative pathways behaved through time. The indices showed, firstly, that **singularities occured when "small phytoplankton" (nanoplankton) was part of the index**. These singularities were different if we integrated over 10 or over 100 m (Fig.7). The indices not using small phytoplankton did not show such order-of magnitude differences, which were due basically to years where small phytoplankton was extremely low. The year 2001 using all the 100 m column came as a **large singularity** in the North Alboran Sea, which, when looking at the raw data, basically corresponds with a peak in small phytoplankton and a low in large zooplakton (Fig.3). The data behaviour prevents from performing typical correlations in the indices with extremely anomalous singularities because linearity and homogeneity of variance are not conformed. We performed however correlations between KE and the indices anomalies, and the results showed evidently that in the indices where small phytoplankton was included, correlations were not significant due to the singularities. On the other hand, correlations between KE and the rest of the indices where small phyto was not included, followed the expected outcome (Table 1): In the **index 1**, high values of kinetic energy tended to be correlated to low index values, mainly attributed to high values in the denominator, the large phytoplankton. Therefore, this supports that higher KE produces higher production due to diatoms. In the **index 2**, what was reflected was that the small zooplankton responded faster to the large phytoplankton (as expected). Indeed, the cross-correlation analyses performed to analyze the lags in the time series between variables (not shown) found that typically the correlation between small zooplankton and large zooplankton was similar at lag 0 and lag1. Further It was clear that the KE in the north Alboran (over Latitude 36) was the KE fraction that best correlated with the observed changes, this reinforcing the assumption that it was linked to the Atlantic jet.
The results above clearly suggested that the analysis of trends was not an option for understanding the changes in organisation of the system. In order to link the LTL results with the HTL results we analyzed the connection between a proxy of the kinetic energy and the response of the HTL, particularly anchovy recruitment in the North Alboran Sea. It was clear from Fig. 8 that extreme events detected by the indices, particularly in 1996 and 2001, were related to strong recruitment of anchovy in those years. The results from Ruiz et al. (2013), also from Perseus, showed that the reason for the coupling between low kinetic energy and high anchovy recruitment was based on: 1) the cessation in the AJ during autumn, coinciding with the postlarval phase of anchovy, 2) the increased stability of the system, which might expand the geographical area in which early juvenile anchovy can develop without being advected by the jet, 3) the expansion of phytoplankton within the basin, possibly enlarging the suitable habitat for postlarval development (Fig. 9). Finally, Mercado et al. (2009) showed empirically that these singularities in 2001 corresponded not only to a decrease in fertilization of the northern coast but to a gradual change in the LTL organization, as revealed by the substitution of the diatom-dominated community by a coccolithophorid and dinoflagellate community.

Projected scenarios:

It is difficult to project scenarios for organization in the system. By assuming an increase or decrease in KE of the system, we will either increase or decrease the probability of disruptions in the AJ, which in turn may be linked to changes into a stable-like small phytoplankton-dominated system. A first exploration on the pressure anomaly (smoothed) over the Alboran Sea provided by Perseus (M.Vicci) showed no relationhips with KE anomalies, probably due to the fact that it is the difference between two areas (e.g. NAO) what should be considered. Unfortunately, an ensemble models of NAO should be used, which were not available at the time, so that uncertainties could be provided. Otherwise, it is ofno use to make any kind of predictions. Further, even if that relationship was found, the changes in organization are extremely punctual and last only until the system has recovered its Aj dynamics, which can occur in less than one year due to the short length of the food web examined. Actually, HTL consecuences were resumed one year after the 2001 anomaly (see the contribution to Resilience).

Table 2 shows that model-based Kinetic energy is directly related to production. The maximum correlation was observed for the North Alboran Sea at the surface (integrating 10 m) (Fig.5).
Under our hypothesis, future changes in the vigor of the system will depend on the dynamics of the AJ (which controls most of the production), which might be measured by KE. We know that KE responds to pressure (Navarro et al., 2011). However, our exploration of the available pressure estimates are either too local (e.g. we tried with the pressure estimates for the pixels in the Alboran Sea produced for 2010-2020 within Perseus) do not provide good correlations with KE anomalies. Using predictions of wind and NAO would ideally provide a more accurate predictor of vigor.
The actual trends in the series indicate a decrease in vigor, but we do not think that these trends can be extrapolated at all. In an scenario frame, and taking into consideration the inverse effect of pressure on production and the direct effect of EKE in production it is expected that primary production (not necessarily fisheries) will be a function of not only KE but when in the year the KE change takes place (Table 2). A change in organization will only be produced when strong disruptions of KE occur, leading to stabilization of the water column and a spatial spread of production (Fig.9). Timing within the year will also determine the velocity of change in organization, and its consequences for HTL (for example through cascading through larval fish growth/dispersion). Only by the use of ensemble models of adequate indices determining KE, it might be possible to have a better proxy for changes in organization. However, being these changes so punctual, we doubt that can be predicted years ahead, and only probabilities of occurrence might be approached.

Discussion

The organization in the area, at least for the pelagic part, is rather stable, forced by the Atlantic Jet (Garcia-Lafuente et al. 2002) and only disrupted under very particular conditions. Based on the hypothesis that the biological organization of the system revolves around the persistence on the AJ (Ruiz et al., 2013), we analyzed both model-derived changes in LTL and observed HTL changes during 20 years. It was clear that at least the most prominent singularities were captured by the model, so that low Kinetic energy singularities produced biological singularities in form of small phytoplankton (and generally low production), that might be related with the observations in the literature and through satellite (Mercado et al., 2009, Ruiz et al., 2013). We are here assuming a causality between the dynamics of the Atlantic Jet and the organization of the system. Although this assumption seems reasonable for LTLs, it is not necessarily true for al HTLs, although anchovy have been shown through modelling and observations to respond to the model-detected singularity.
We postulate that, based only on the available models in the area, disruptions in the organization only occur 1) when the AJ is severely modified during a certain period of time, and 2) that the LTL disruptions are can be linked to HTL disruptions, which is supported by the literature at least for some species.

It has been shown that the increase in dinoflagellates and protists empirically detected in 2001-2002 (Mercado et al., 2007) are preferred prey for anchovy larvae (Catalán et al. 2010). On the other hand, this shift agrees with a less dynamic environment in which diatom-based communities are not favored (Mercado et al. 2005). We contend that the impact of kinetic energy on the system (organization of LTL and its cascading effect on HTL) will only be detectable on singularities of the time series. Therefore, the only way to forecast these singularities will be by better understanding the causes that provoke the rare comlete disruption of the AJ-WAG system in the ALboran Sea, and ensemble models of meteorological indices should be ideally used.

Tables

Table 1. Correlation values between anomalies of KE and the two types of indices. Only significant ones ($p<0.05$) are depicted. Required assumptions were met, except for the indices involving SZ (see text).

	index 1							
	All Alboran				*North Alboran*			
	35	*35*	*35*	*35*	*36*	*36*	*36*	*36*
	SZ/SPHY int10	*SZ/SPHY int100*	*LZ/LPHY int10*	*LZ/LPHY int100*	*SZ/SPHY int10*	*LZ/LPHY int10*	*SZ/SPHY int100*	*LZ/LPHY int100*
KE_L35avt10	*NS*	*NS*	*-0.33*	*-0.31*	*NS*	*-0.36*	*NS*	*-0.34*
KE_L35avt100	*NS*	*NS*	*-0.32*	*-0.29*	*NS*	*-0.35*	*0.16*	*-0.35*
KE_L36avt10	*NS*	*NS*	***-0.46***	***-0.44***	*NS*	***-0.53***	*NS*	*-0.54*
KE_L36avt100	*NS*	*NS*	*-0.39*	*-0.38*	*NS*	*-0.47*	*0.13*	*-0.49*

	index 2							
	All Alboran				*North Alboran*			
	35	*35*	*35*	*35*	*36*	*36*	*36*	*36*
	LPHY/SPHY int10	*LZ/SZ int10*	*LPHY/SPHY int100*	*LZ/SZ int100*	*LPHY/SPHY int10*	*LZ/SZ int10*	*LPHY/SPHY int100*	*LZ/SZ int100*
KE_L35avt10	*NS*	*-0.34*	*NS*	*-0.29*	*NS*	*-0.40*	*NS*	*-0.38*
KE_L35avt100	*NS*	*-0.30*	*NS*	*-0.26*	*NS*	*-0.38*	*0.15*	*-0.38*
KE_L36avt10	*NS*	***-0.42***	*NS*	***-0.33***	*NS*	***-0.54***	*NS*	***-0.52***
KE_L36avt100	*NS*	*-0.35*	*NS*	*-0.27*	*NS*	*-0.49*	*NS*	*-0.48*

Table 2

Potential scenarios for 2010-2020 in case that anomalies with respect to KE occur (not slight trends but abrupt changes).

KE abrupt changes	*LTL total production*	*Stability*	*LTL microbial paths (nanophytoplankton)*	*HTL (anchovy*
increase	*increase*	*decrease*	*decreased*	*decreased*

decrease	*decrease*	*increase*	*increased*	*increased*

Figures

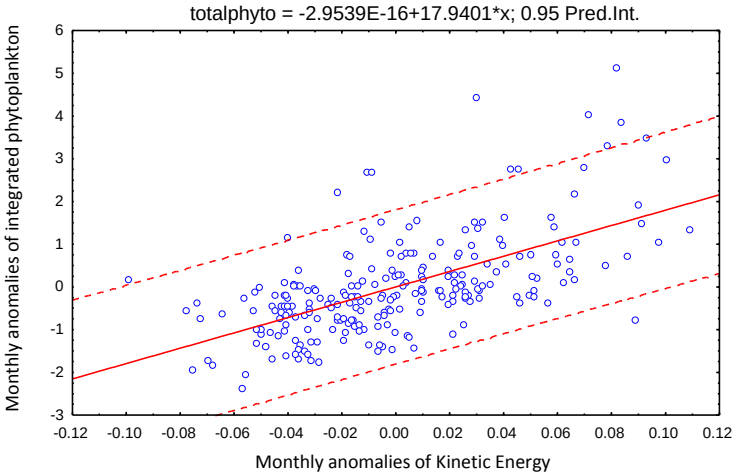

Fig.1 Relationship between monthly anomalies of kinetic energy and production anomalies in the Northern Alboran Sea, for the first 10 m of the water column between 1989 and 2008 (From contribution to subtask 4.2.2.-Vigor).Fig.1. Whole model domain, and restricted domains for the Alboran snf North Alboran Sea used within Wp4

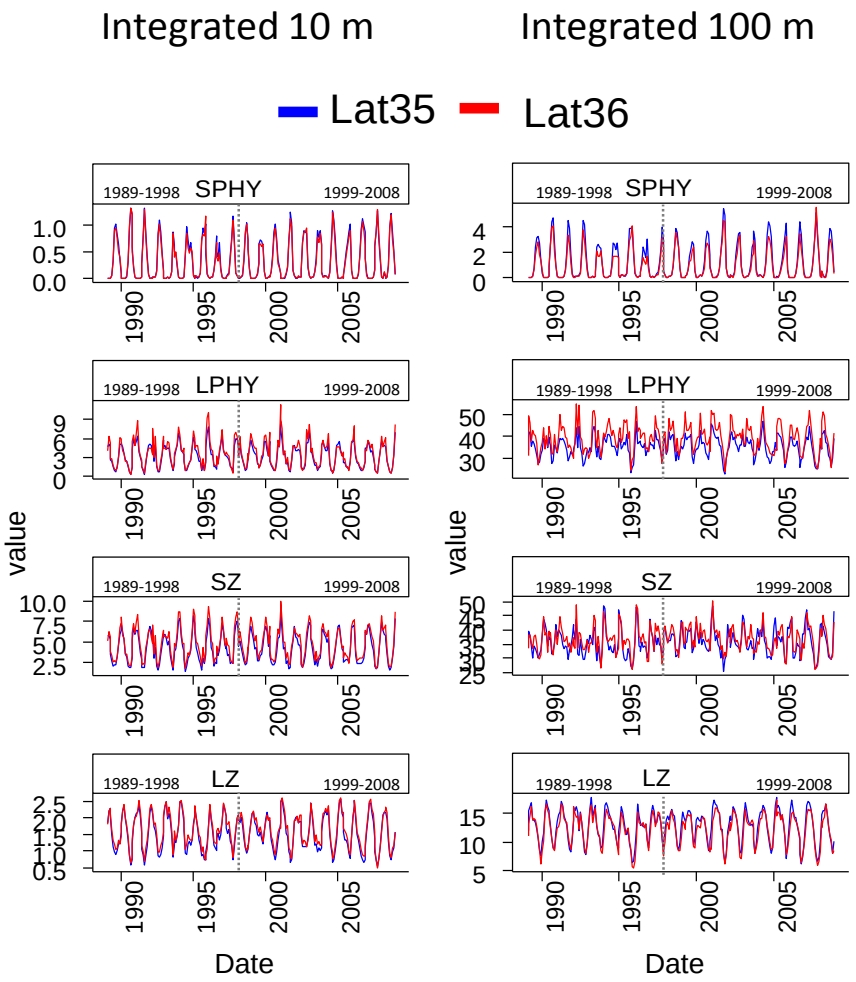

Fig.3. Raw model-derived values for small and large phyto and Zooplankton. Phytoplankton values are measured in g Chla either per m3 or m2(integrated), Zooplankton values are measured in ml/l. The two spatial domains (all Alboran or North Alboran) and the two initial time-slices are included. SPHY=small phytoplankton, LPHY=large phytoplankton, SZ=small zooplankton, LZ=large phytoplankton

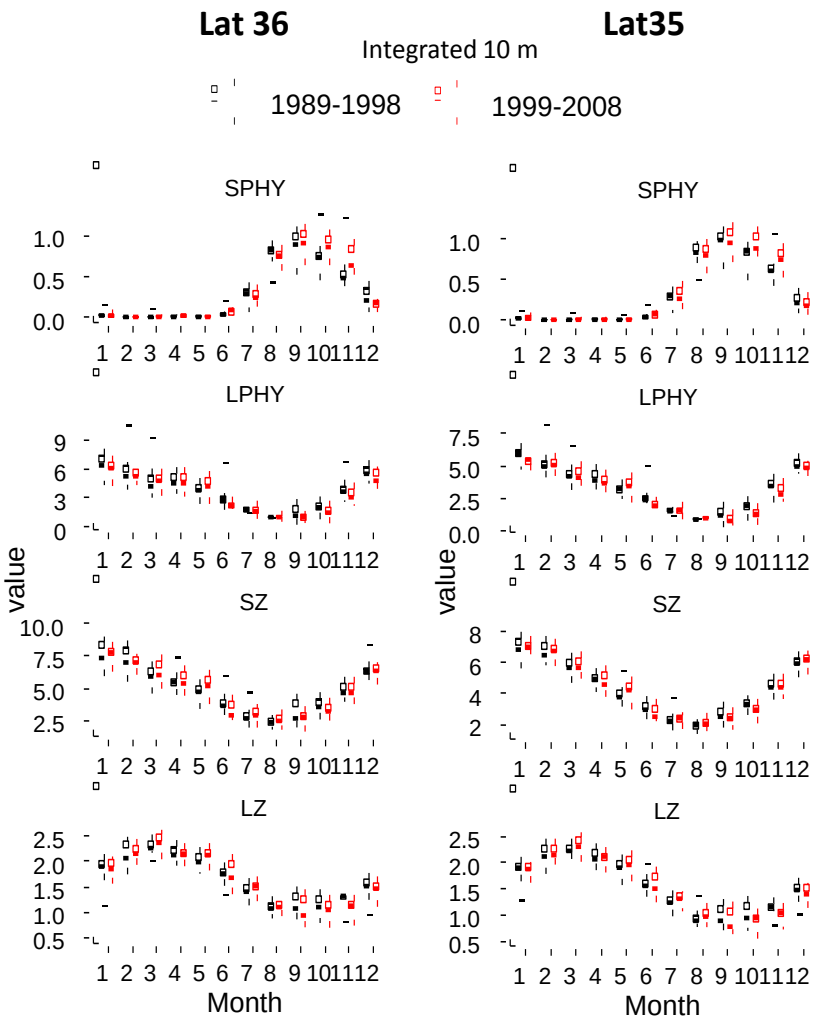

Fig.4 Box-plots on monthly data for two calculated time-slices for integrated depth over 10 m. Data for the two components in the Alboran Sea. Units as in Fig. 1.

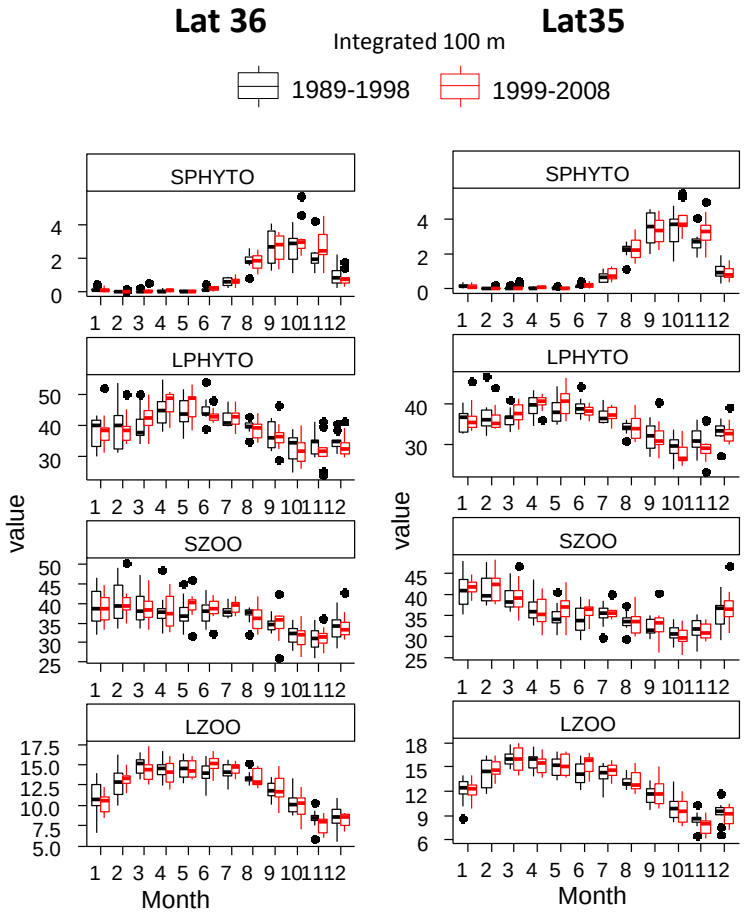

Fig.5. Box-plots on monthly data for two calculated time-slices for integrated depth over 100 m. Data for the two components in the Alboran Sea. Units as in Fig. 1.

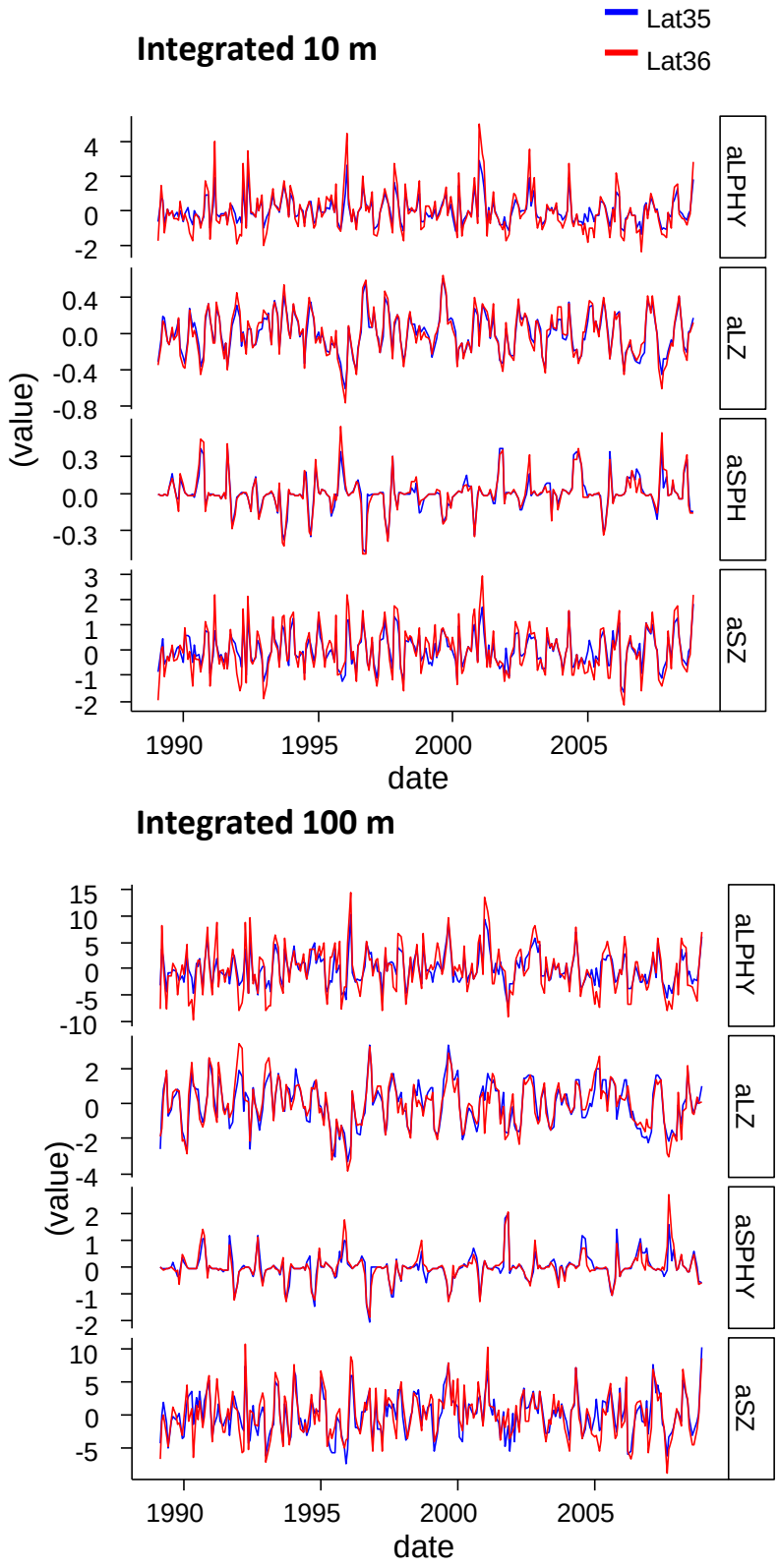

Fig.6. Monthly anomalies time-series for the four trophic components , by spatial domain and type of vertical integration.

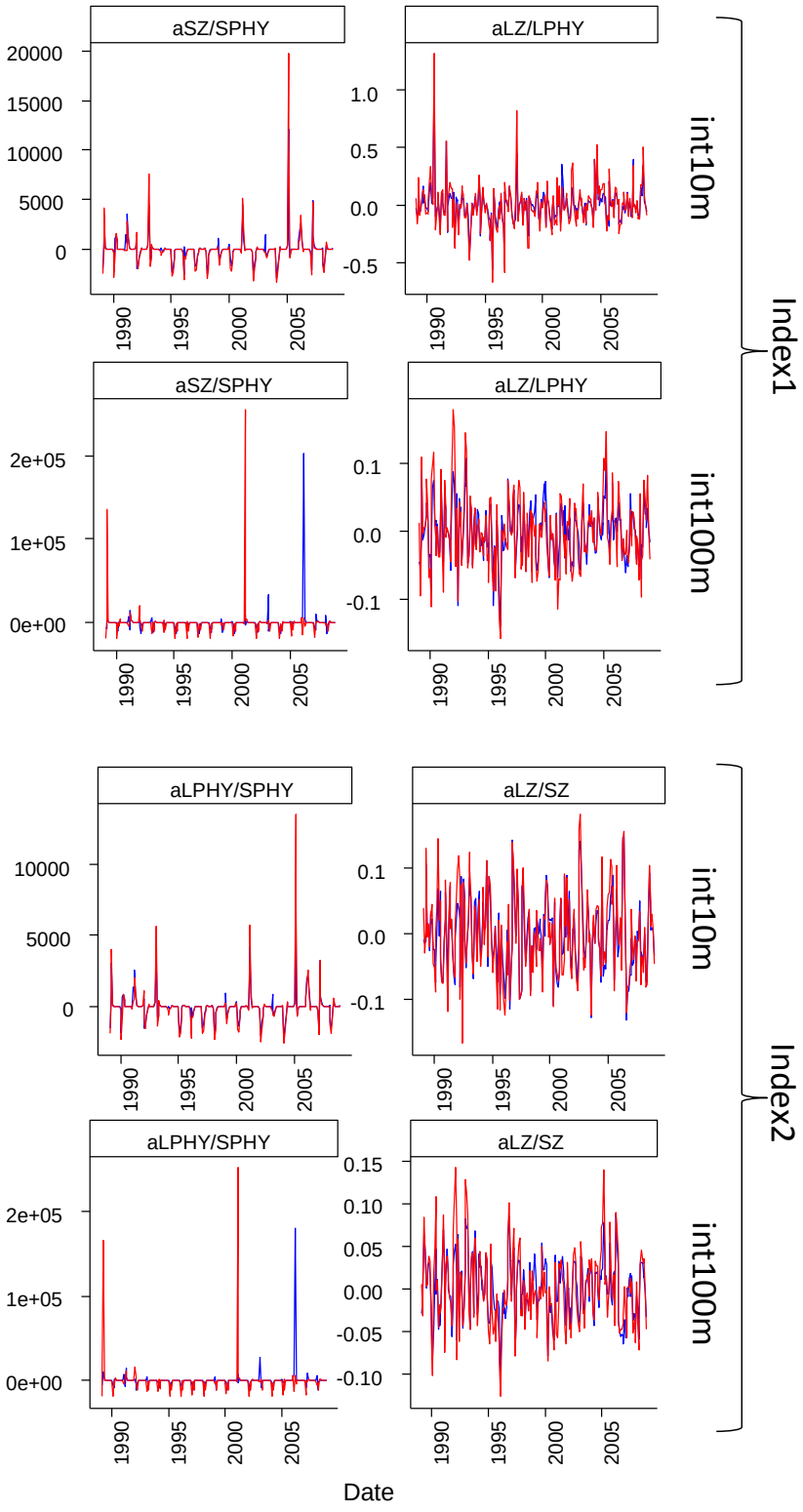

Fig.7. Montly anomaly series for the two indices, at two integrating depths and for the two spatial domains.

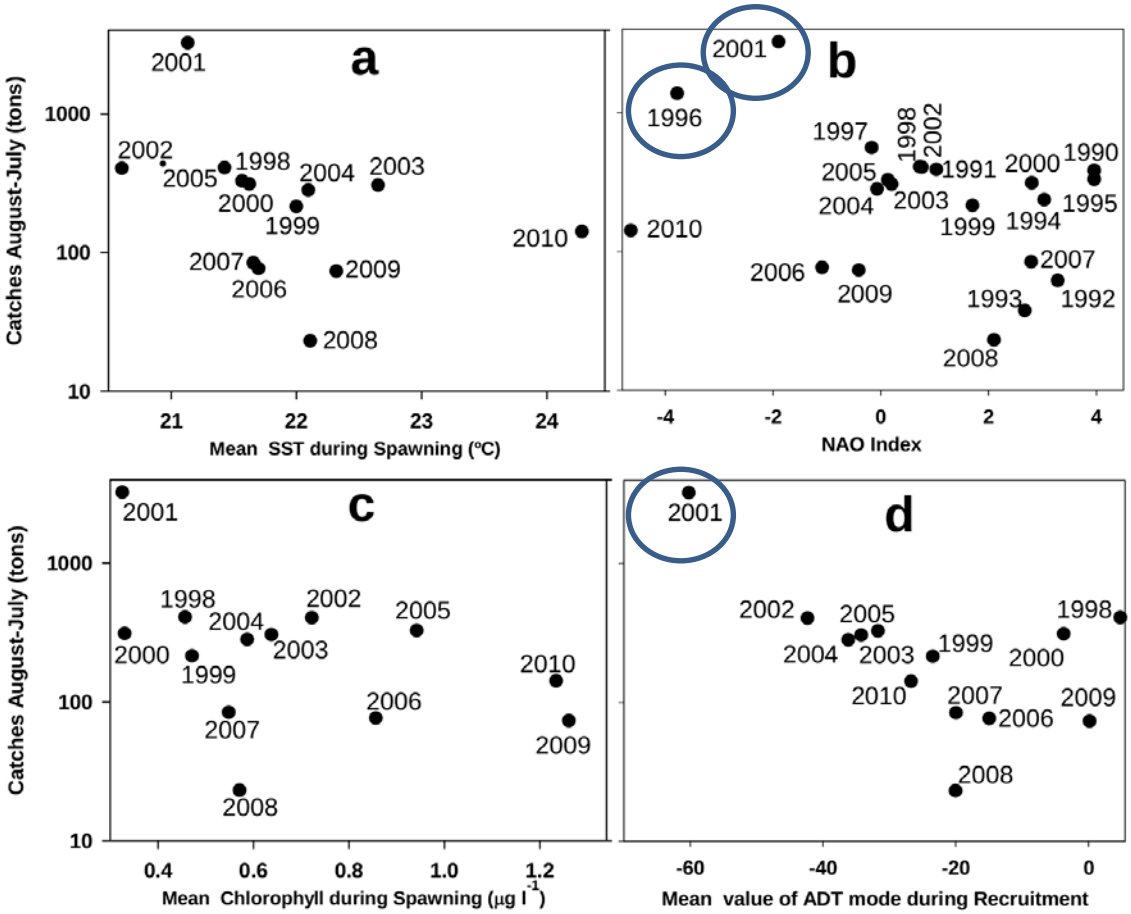

Fig. 8. Relationship between several environmental variables and a proxy for anchovy abundance in the North Alboran Sea (adapted from Ruiz et al., 2013). Circles show how extremes are coincident with the anomalies detected in the organization of the system through models, although we did not have reliable catch data for 1996

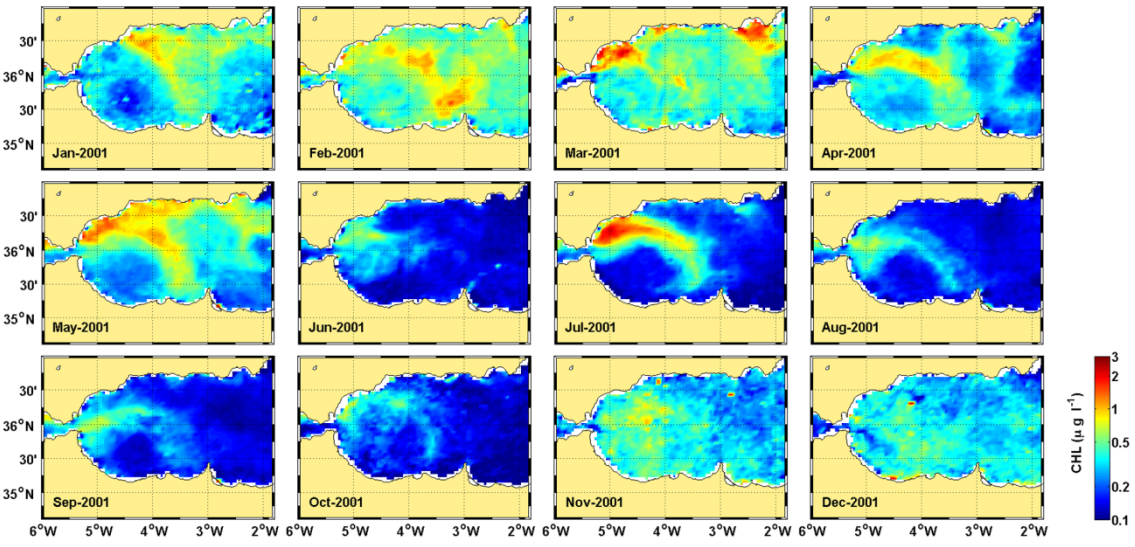

Fig.9. Maps of the consequences that a reduction in the atlantic jet had in 2001. It can be seen that the usual production associated to the jet is stopped and spread in the whole Alboran Sea. From Ruiz et al., 2013.

Northern Aegean HTL model (HCMR)

Introduction

The Mediterranean Sea is an area highly affected by anthropogenic disturbances and climate change causing environmental degradation (Lejeusne *et al*., 2010). For this reason, the goal set by the Marine Strategy Framework Directive (MSFD; EU, 2008) to "..achieve or maintain good environmental status in the marine environment by the year 2020 at the latest" and urges the Member States to take the necessary measures, is particularly important. There is a large debate on what is "good environmental status" and even though descriptors that define it were defined in the Commission Decision 2010/477/EU (EU, 2010), there is not a single answer on this debate. In this framework, the work by Costanza and Mageau (1999) who proposed three ecosystem attributes (vigor, organization and resilience) to characterize the "health" of the marine ecosystem can be particularly useful.

Ecosystem modelling integrates available information to study direct and indirect trophic interactions among ecosystem compartments, including fishing activities and the environment. It is therefore a useful tool for fisheries management (Christensen and Walters 2004). The broad use of the trophic modelling tool “Ecopath with Ecosim (EwE)” (Christensen and Walters 2004) has contributed to complement previous knowledge of the structure and functioning of marine ecosystems and has enabled the proposal of ecological indicators and reference limits based on model outputs and meta-analysis of models’ results (e.g., Christensen, 1995; Libralato *et al.*, 2008; Heymans *et al.,* 2014; Lynam and Mackinson, 2015).

In the current work we used an end-to-end model built for the North Aegean Sea (NAS) ecosystem to simulate a series of nutrient load (related to river runoffs) and fisheries scenarios. The outputs of these simulations were analyzed by exploring trends of ecosystem metrics related to the three ecosystem attributes, vigor, organization and resilience and comparing forecast to past periods in order to assess the status of the NAS ecosystem.

Methods

The coupled NAS model

The end-to-end NAS model area is defined by the 20 m and 300 m isobaths (Figure 1) covering 8374 km^2 in total. This is mainly the area where trawlers, purse seiners and the biggest fraction of artisanal fleets operate.

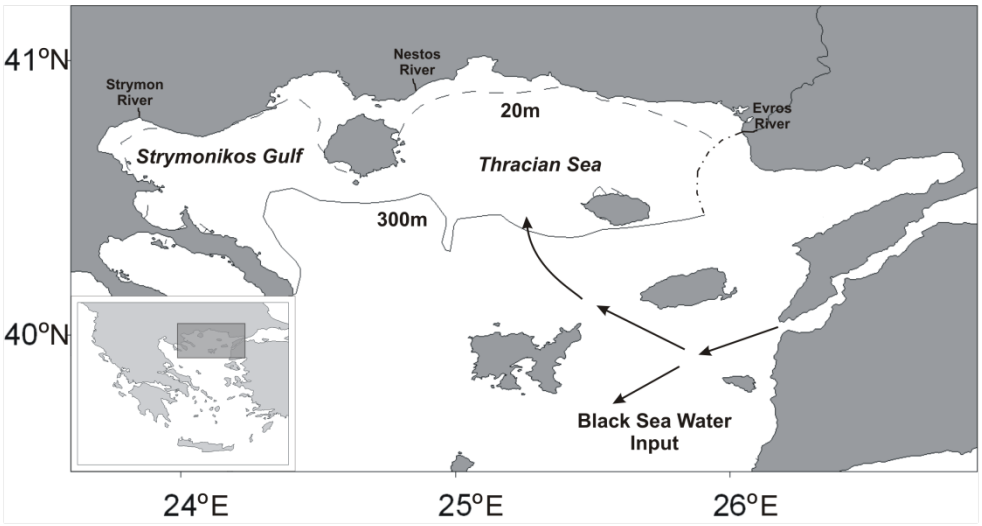

Figure 1. North Aegean Sea (Strymonikos Gulf and Thracian Sea). Isobaths of 20m and 300m which define the model area are shown, as well as the most important rivers of the area. Arrows indicate the direction of Black Sea Water Input.

The structure and the methodology used to build the NAS en-to-end model is described in detail in PERSEUS D4.4 and D4.8. Outputs of the OPATB-BFM LTL (Lazzari *et al*. 2012) were used as input for the biomasses and diet matrix of the LTL groups as well as to drive the LTL components of the model. Flows and biomasses of the model are expressed in phosphorus, P, which is considered the limiting nutrient in the Mediterranean.

The HTL model is based on the previously developed Ecopath model in the area for the period 2003-2006 (Tsagarakis *et al.*, 2010). This model was adjusted to input data from the early 1990s (mainly 1991-1993), averaging data from separate years. The 1990s model followed a standardized structure which was agreed for all the Mediterranean areas (Gulf of Lions, Adriatic, NAS) and which is described in detail in PERSEUS D4.4. In brief, the HTL fraction of the model was represented by 23 living FGs and two detritus groups (detritus and discards). The structure of the food web of the coupled model is shown in Figure 2. For the coupling between LTL and HTL components of the model we followed the methodology described in Libralato and Solidoro (2009). The model simulated the period 1993-2020 using forcing function from LTL input from the BFM (bacteria, pico- and phytoplankton) and time series of fishing effort data. The coupled model was then fitted to LTL and HTL data for the period 1993-2010. For the period 1993-2000, no input from the OPATM-BFM was available thus forcing was based on time series constructed based on climatology using data from the 2000-2010 period.

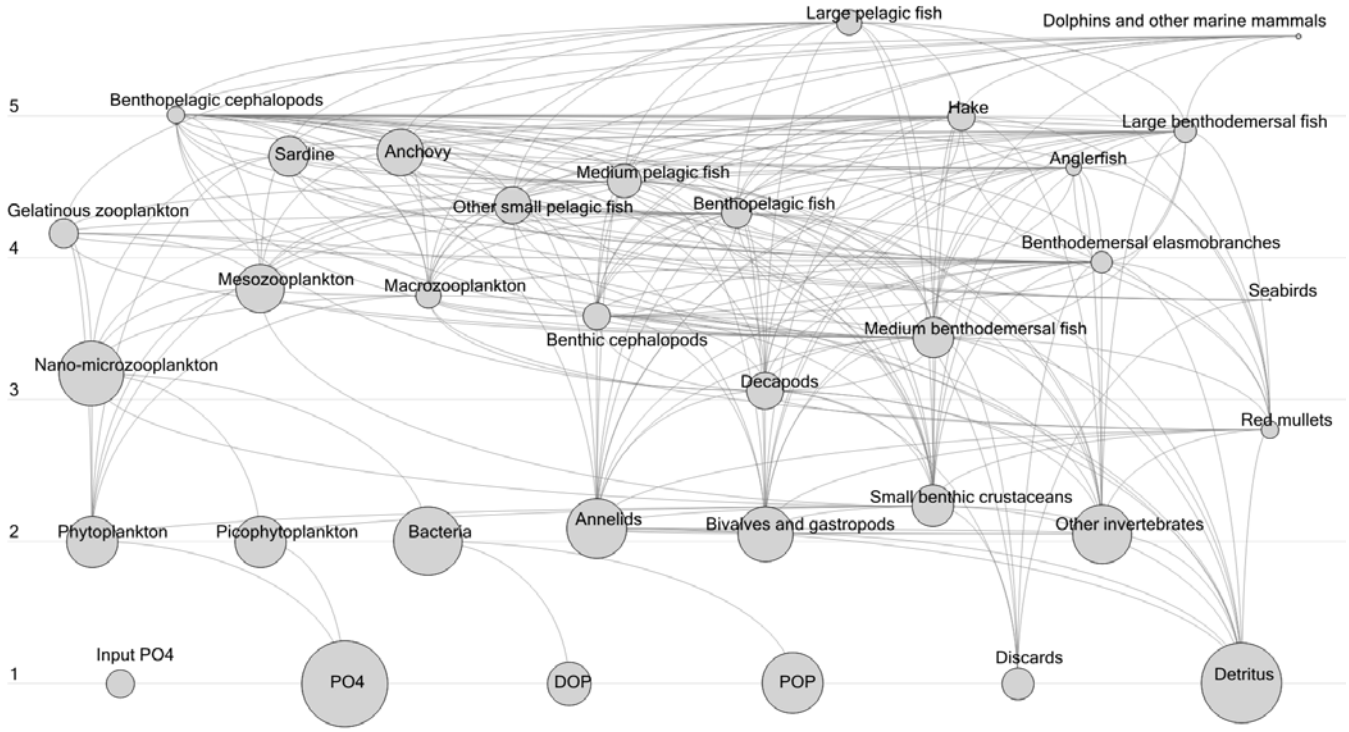

Figure 2. Structure of the foodweb of the end-to-end NAS model. The links between the different compartments show the trophic flows.

Scenarios

The OPATB-BFM LTL simulation used for the end-to-end NAS model were performed using nutrient river run-off scenarios from D4.6 (BAU, BA, MFA, REB, RBE) for the period 2011-2020 which are described in Table 1.

Results of the models using BA, MFA, REB, RBE data were compared to those of the model using BAU (business as usual) scenario considered as the reference one for the period 2011-2020. In all these LTL scenarios fishing pressure was considered constant between 2010 and 2020.

A series of fisheries related (affecting HTL) simulations were explored which used BAU scenario data for LTL. These included decreases/increases of the fishing effort of specific or all gears or changes in the fishing mortality of some functional groups Table 2. Results of the models using the different fisheries scenarios were compared to those of the model using BAU and constant fishing effort between 2010 and 2020 (BAU).

The ecosystem metrics extracted from the NAS coupled model which were used to assess the "health" (vigor, organization and resilience) of this system over the time under different scenarios (LTL and HTL) are presented in Table 3. Two other indices related to exploited systems were estimated: catch over biomass (C/B) and trophic level of catch (TLc).

The 2000-2010 period was considered as the reference one and for the needs of this work, year 2010 (last year of the reference period) was compared with the output of the last year of the scenarios period (2020). The comparison was in terms of values of the metrics as well as in terms of biomasses of the model's functional groups (FGs). Trends of the indices were also constructed to comparably assess the status of the ecosystem.

Table 1. Low trophic level model scenarios used in this report (from PERSEUS Deliverable 4.6)

IMAGE model parameter	Scenario				
	Business as Usual	Regional Expanding Block	Market for All	Regional Blue Economy	Blue Archipelago
	BAU	REB	MFA	RBE	BA
Per capita food consumption	High, high meat	High, high meat	Low	High, low meat	Low, low meat
Agricultural productivity increase	Same as 2010	High	Low	Medium-high	Medium
Fertilizer use and efficiency	No change in fertilizer use efficiency after 2010	No change in countries with a surplus; rapid increase in N and P fertilizer use in countries with soil nutrient depletion (deficit)	No change in countries with a surplus; slow increase in N and P fertilizer use in countries with soil nutrient depletion (deficit)	Rapid increase in countries with a surplus; rapid increase in N and P fertilizer use in countries with soil nutrient depletion (deficit)	Moderate increase in countries with a surplus; slow increase in N and P fertilizer use in countries with soil nutrient depletion (deficit); better integration of animal manure

Table 2. High trophic level model scenarios related to fisheries used in this report

Code	Scenario
P10All	Increase by 10% the fishing effort in term of number of boats for all the fleets for the period 2010-2020 compared to 2009
M10All	Decrease by 10% the fishing effort in term of number of boats for all the fleets for the period 2010-2020 compared to 2009
P10Btwl	Increase by 10% the fishing effort in term of number of boats for the benthic trawls for the period 2010-2020 compared to 2009
M10Btwl	Decrease by 10% the fishing effort in term of number of boats for the benthic trawls for the period 2010-2020 compared to 2009
P10SPF	Increase by 10% the fishing mortality for commercial small pelagic fish species (sardine and anchovy) for the period 2010-2020 compared to 2009
M10SPF	Decrease by 10% the fishing mortality for commercial small pelagic fish species (sardine and anchovy) for the period 2010-2020 compared to 2009
P10LPF	Increase by 10% the fishing mortality for large pelagic fish species for the period 2010-2020 compared to 2009
M10LPF	Decrease by 10% the fishing mortality for large pelagic fish species for the period 2010-2020 compared to 2009

Table 3. Metrics used to compare the "health" (vigor, organization and resilience) over the time and between of the marine systems Costanza and Mageau (1999)

Vigor	NPP (net primary production) T (Throughput) Catch (total catch)
Organisation	K's Q (Kempton's Q) FiB (Fishing in Balance) AMI (Average Mutual Information) Ascendency (A) FCI (Finn's Cycling Index) mPL (Mean Path length)
Resilience	H-AMI (Entropy - Average Mutual Information) = [(Capacity-Ascencency) / Throughput] SfG (Scope for Growth = Total production – Total primary production)
Exploitation	C/B (catch over biomass) TLc (trophic level of the catch)

Results

Comparison of reference (2010) with target (2020) period

Results of the comparison of the reference year (2010) with target (2020) one in terms of vigor, organization and resilience ("health" ecosystem metrics) as well as in terms of indices of exploitation are detailed in Table 4 both for LTL (nutrient load) and HTL (fisheries) scenarios. Important changes were identified in year 2020 compared to 2010 under all scenarios. The only metrics not showing changes were H-AMI and TLc which obviously had lower sensitivity. All other metrics increased or decreased and it is interesting that the direction of change was the same in almost all scenarios (Table 4). Specifically, all metrics related to vigor (Net Primary Production, Throughout and total Catch) seem to deteriorate up to 14% in 2020 in all scenarios (only Catch reduces in few of them). This is also true for SfG which is related with resilience. Indices of organization showed mixed responses with Kempton's Q and Ascendency being lower in 2020 and Fishing in Balance, Finn's Cycling Index and mean Path Length generally higher (Table 4). However in three out of five nutrient load scenarios (MFA, RBE, REB) FCI was lower. Despite these, the indices linked to exploitation (C/B but also FiB) generally increased, without though having increased catches (Table 4).

The exploration of the changes at the FG level showed mixed results (Table 5). The biomass of picophytoplankton, bivalves and gastropods as well as anglerfish was lower in all scenarios. Even though negative effects were recorded for both LTL and HTL organisms, LTL ones seemed to be affected more. On the other side, positive effects were shown for many invertebrate and fish FGs (e.g. Benthodemersal elasmobranches, Hake, Benthopelagic fish, Other invertebrates). The response also differed in the scenarios examined, with MFA, RBE and REB showing the most negative result on FGs' biomasses.

Table 4. Comparison of indices related to vigor, organization, resilience and exploitation for the nutrient load and fisheries scenarios of the North Aegean Sea. Absolute values are presented for the reference and scenarios periods, while relative changes are reported for year 2020 in the remaining scenarios. Significant differences (> 5%) between reference year (2010) and 2020 in all scenarios are indicated in bold and in shaded cells (red for lower values and green for higher values compared to 2010).

metrics	Vigor			Organisation						Resilience		Exploitation	
	NPP	T	Catch	K's Q	FiB	AMI	A	FCI	mPL	H-AMI	SfG	C/B	TLc
BAU in 2010	1.26	1405.96	0.57	7.60	0.00	1.98	2780.56	50.28	8.68	2.66	370.04	0.00	3.79
LTL scenarios													
BAU 2020-past (2010)	-7.44	-10.47	-2.10	-6.23	22.21	0.23	-10.28	12.80	21.97	-0.87	-17.34	3.38	-1.11
BA-past (2010)	-6.27	-10.00	4.85	-10.38	-6.83	0.55	-9.53	12.51	20.65	-0.55	-16.72	7.87	-0.99
MFA-past (2010)	-9.22	-13.58	-11.26	-31.91	39.82	0.74	-12.90	-24.87	25.98	-2.74	-22.79	6.10	-1.79
RBE-past (2010)	-9.19	-13.14	-10.67	-31.60	37.12	0.68	-12.50	-17.48	24.71	-2.65	-22.06	6.17	-1.70
REB-past (2010)	-9.16	-13.28	-10.75	-31.78	37.30	0.72	-12.61	-31.56	24.97	-2.66	-22.29	6.23	-1.71
Fisheries scenarios													
p10All-past (2010)	-7.46	-10.50	3.72	-3.36	-3.87	0.24	-10.30	2.41	21.72	-0.94	-17.42	9.98	-1.39
m10All-past (2010)	-7.41	-10.44	-8.21	-11.26	45.80	0.30	-10.19	12.90	22.25	-0.86	-17.26	-3.52	-0.80
p10Btwl-past (2010)	-7.44	-10.47	-0.48	-5.97	16.45	0.22	-10.30	12.80	21.91	-0.88	-17.36	5.17	-1.19
m10Btwl-past (2010)	-7.43	-10.47	-3.74	-6.54	27.86	0.24	-10.27	12.81	22.03	-0.87	-17.33	1.56	-1.04
p10SPF-past (2010)	-7.46	-10.49	-0.01	-6.48	10.68	0.19	-10.34	12.80	21.81	-0.88	-17.40	5.92	-1.17
m10SPF-past (2010)	-7.42	-10.45	-4.31	-5.99	32.95	0.27	-10.22	12.81	22.14	-0.86	-17.29	0.70	-1.04
p10LPF-past (2010)	-7.44	-10.47	-2.28	-5.05	22.03	0.23	-10.28	12.86	21.90	-0.88	-17.35	3.25	-1.18

m10LPF-past (2010)	-7.44	-10.47	-1.96	-7.60	22.44	0.23	-10.29	12.75	22.05	-0.87	-17.34	3.45	-1.05

Table 5. Comparison of the FGs' biomasses under different LTL and HTL scenarios. Absolute values are presented for year 2010, while relative changes (%) in year 2020 are reported for BAU and the remaining scenarios. Significant differences (> |5%|) between 2010 and 2020 for all scenarios are indicated in bold and in shaded cells (red for lower values and green for higher values compared to 2010).

		Nutrient load scenarios					Fisheries scenarios							
Functionl group	201	BAU	BA	MFA	RBF	RFB	P10al	M10a	P10Bt	M10Bt	P10SP	M10SP	P10LP	M10LP
Phytoplankton	6.67	-0.74	2.33	**-5.12**	-4.74	-4.87	-0.81	-0.66	-0.75	-0.73	-0.79	-0.69	-0.74	-0.74
Picophytoplankton	8.03	**-5.35**	**-5.46**	**-7.70**	**-7.09**	**-7.12**	**-5.37**	**-5.32**	**-5.35**	**-5.34**	**-5.36**	**-5.33**	**-5.35**	**-5.35**
Bacteria	33.8	0.68	1.48	-0.03	-0.02	-0.03	0.66	0.70	0.68	0.68	0.66	0.69	0.68	0.68
Nano-microzooplankton	23.0	-4.94	-4.34	**-8.92**	**-8.10**	**-8.21**	-4.99	-4.88	-4.95	-4.93	-4.97	-4.90	-4.94	-4.94
Mesozooplankton	4.44	-2.34	4.66	**-**	**-9.87**	**-**	-2.49	-2.18	-2.36	-2.31	-2.44	-2.23	-2.34	-2.33
Macrozooplankton	0.62	-3.39	-2.54	-1.79	-1.39	-1.44	-3.85	-2.85	-3.36	-3.42	-3.39	-3.39	-3.67	-3.09
Gelatinous zooplankton	0.75	-0.70	**12.8**	**-7.25**	**-6.26**	**-6.41**	-0.06	-1.38	-0.66	-0.74	-0.82	-0.58	-0.61	-0.81
Annelids	14.2	2.25	**8.07**	-3.84	-3.35	-3.44	2.35	2.18	2.38	2.13	2.12	2.39	2.27	2.22
Bivalves and gastropods	7.58	**-9.63**	**-8.45**	**-**	**-**	**-**	**-**	**-8.67**	**-9.73**	**-9.53**	**-**	**-8.91**	**-9.48**	**-9.78**
Benthic cephalopods	0.50	**5.36**	2.30	**-**	**-**	**-**	-2.03	**13.42**	4.39	**6.33**	4.45	**6.33**	**5.49**	**5.25**
Benthopelagic cephalopods	0.24	**-10.82**	-0.79	**-**	**-**	**-**	**-7.19**	**-**	**-11.51**	**-10.13**	**-**	**-11.00**	-2.22	**-20.01**
Small benthic crustaceans	3.24	-2.92	-1.00	**6.81**	**6.95**	**6.97**	-1.79	-4.09	-2.72	-3.10	-2.91	-2.92	-2.85	-3.02
Decapods	2.14	**-5.64**	1.58	**7.96**	**7.99**	**8.04**	-2.80	**-8.48**	**-5.16**	**-6.10**	**-5.67**	**-5.62**	**-5.21**	**-6.14**
Other invertebrates	12.2	**14.14**	**15.0**	**-**	**-**	**-**	**13.9**	**14.27**	**13.89**	**14.40**	**13.36**	**14.97**	**14.00**	**14.32**
Sardine	2.28	-2.39	**12.3**	-4.28	-3.66	-3.76	**-6.04**	1.90	-2.38	-2.40	**-6.90**	2.55	-3.25	-1.33
Anchovy	4.50	**-6.78**	**8.54**	-1.16	-0.60	-0.67	**-5.47**	**-8.62**	**-6.81**	**-6.75**	**-8.07**	**-5.51**	**-5.23**	**-8.78**
Other small pelagic fish	1.74	-0.58	**8.03**	**-9.24**	**-8.67**	**-8.76**	-1.03	-0.10	-0.39	-0.76	-0.22	-0.94	0.66	-1.77
Medium pelagic fish	1.42	2.58	**10.7**	-4.95	-4.46	-4.54	**-5.15**	**11.69**	1.90	3.27	2.66	2.51	2.06	3.31
Benthopelagic fish	1.05	**6.64**	**13.2**	**-**	**-**	**-**	**7.85**	**5.31**	**6.58**	**6.66**	**6.62**	**6.66**	**6.51**	**6.77**
Large pelagic fish	0.58	**36.58**	**36.4**	**-**	**-**	**-**	6.08	**74.33**	**35.37**	**37.81**	29.56	**44.12**	11.12	**67.11**
Red mullets	0.32	-3.69	3.68	**6.57**	**6.68**	**6.70**	**-5.64**	-1.58	-4.66	-2.72	-3.60	-3.79	-4.28	-3.05
Medium benthodemersal fish	2.95	**5.25**	**6.50**	**-**	**-**	**-**	2.40	**8.20**	4.63	**5.85**	4.99	**5.54**	4.47	**6.14**
Hake	1.00	**7.83**	**5.98**	**-8.81**	**-8.49**	**-8.58**	2.38	**13.45**	4.86	**10.84**	**7.12**	**8.57**	**8.26**	**7.36**

Anglerfish	0.07	**-49.05**	-	-	-	-	-	-	**-56.12**	**-40.83**	-	**-48.15**	-	**-48.79**
Benthodemersal	0.54	**5.23**	**5.45**	-4.31	-4.07	-4.14	2.57	**7.91**	3.00	**7.53**	4.99	**5.47**	4.91	**5.55**
Large benthodemersal fish	0.55	4.38	**6.30**	-	-	-	-1.73	**11.13**	2.47	**6.29**	3.65	**5.16**	4.06	4.73
Seabirds	0.00	**7.20**	**12.1**	-	-	-	**15.4**	-1.37	**11.79**	2.55	3.65	**10.95**	**7.81**	**6.43**
Dolphins and other marine	0.03	-1.52	-1.18	-	-	-	-4.12	1.14	-1.82	-1.22	-2.35	-0.66	-1.11	-1.98

Trends in metrics related to ecosystem attributes

The time series of the estimated metrics showed high seasonality but allowed to detect trends in time and differences among the scenarios. Regarding indicators related to **vigor**, higher changes among nutrient load scenarios were observed for the catch than for NPP and Throughput (Figure 3). In contrast, fisheries scenarios did not differ compared to BAU, with the exception of Catch (Figure 4). There were large variation throughout the forecast period with negative trend especially in Throughout and Catch (but only in 3 scenarios).

As regards time series of indices related to **organization** they were very similar for MFA, REB, RBE which deviated from BAU especially after 2017. These changes were more apparent for Kempton's Q, FiB, FCI and Ascendency (Figure 5). Fisheries related scenarios changed mainly for Kempton's Q, FiB and FCI (Figure 6). There was a large change in the values of some metrics after 2017 (Kempton's Q decreased but FiB and Ascendency increased) but values were restored after a while to values close to the reference year.

In time series of indicators related to resilience the situation was similar to the two other ecosystem attributes. LTL scenarios MFA, REB and RBE differentiated from BAU again after 2017 (Figure 7) at lower values overall but these indicators were not sensitive in fisheries scenarios (Figure 8). A decreasing trend for SfG was observed.

Catch over Biomass ratio as well as mean Trophic Level of the Catch, which are considered metrics of **exploitation**, deviated a lot from BAU in LTL scenarios (Figure 9), and a slightly positive trend was observed. In fisheries related scenarios, Catch over Biomass ratio was higher when fishing effort and mortality was increasing while mTL didn't show apparent changes (Figure 10).

In general many indices showed temporal increases for part of the period 2015-2020 but they were forecasted to decrease around 2020 at levels usually lower than in 2010, or the opposite for few indices.

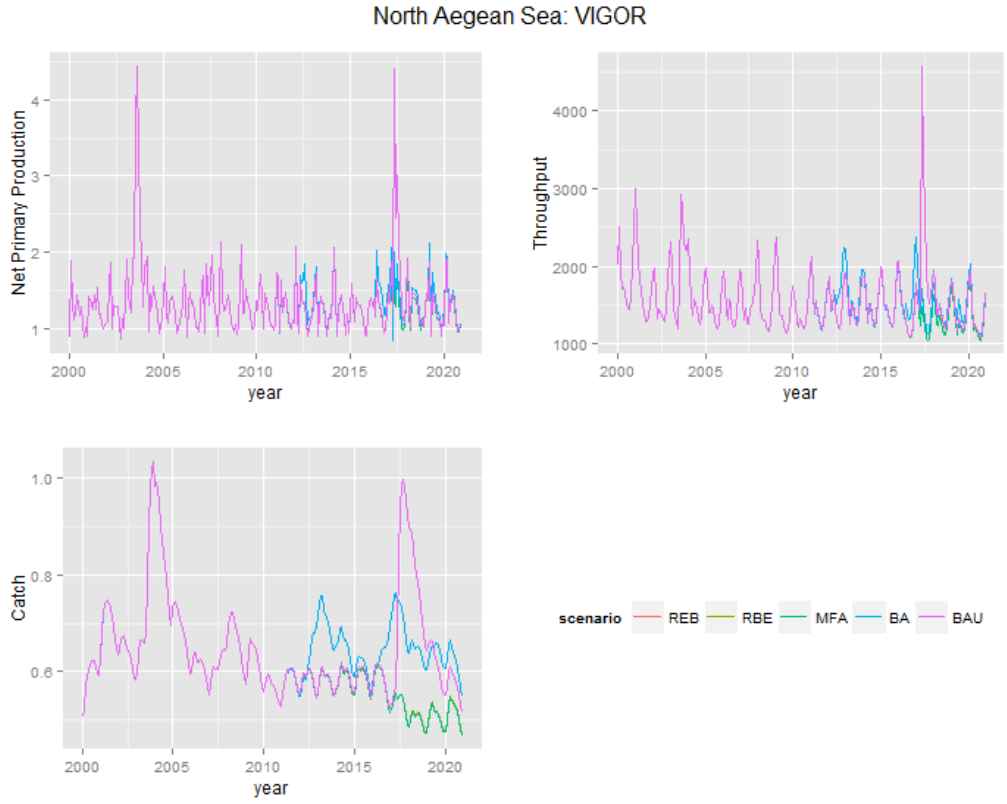

Figure 3. Vigor estimated metrics for the nutrient load scenarios applied for the period 2011-2020. The 2000-2010 period corresponds to the coupled model fitted to data.

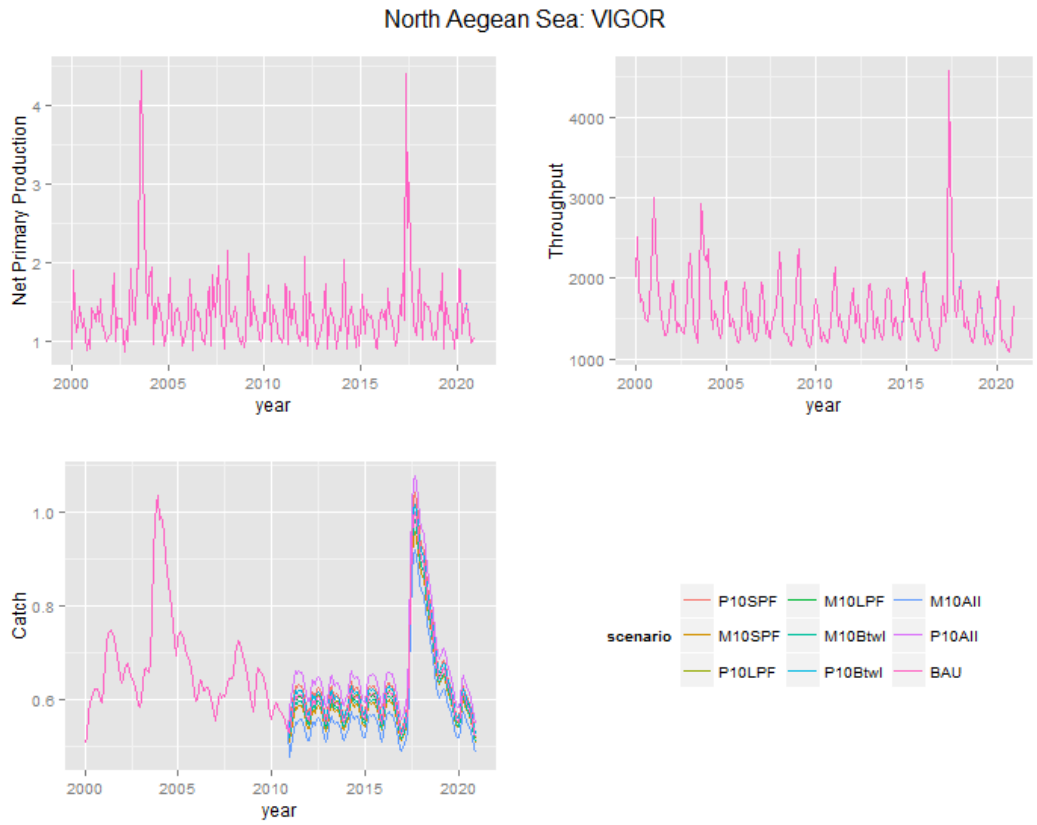

Figure 4. Vigor estimated metrics for the HTL (fisheries) scenarios applied for the period 2011-2020. The 2000-2010 period corresponds to the coupled model fitted to data. All the HTL scenarios in the coupled model used the same BAU scenario LTL data.

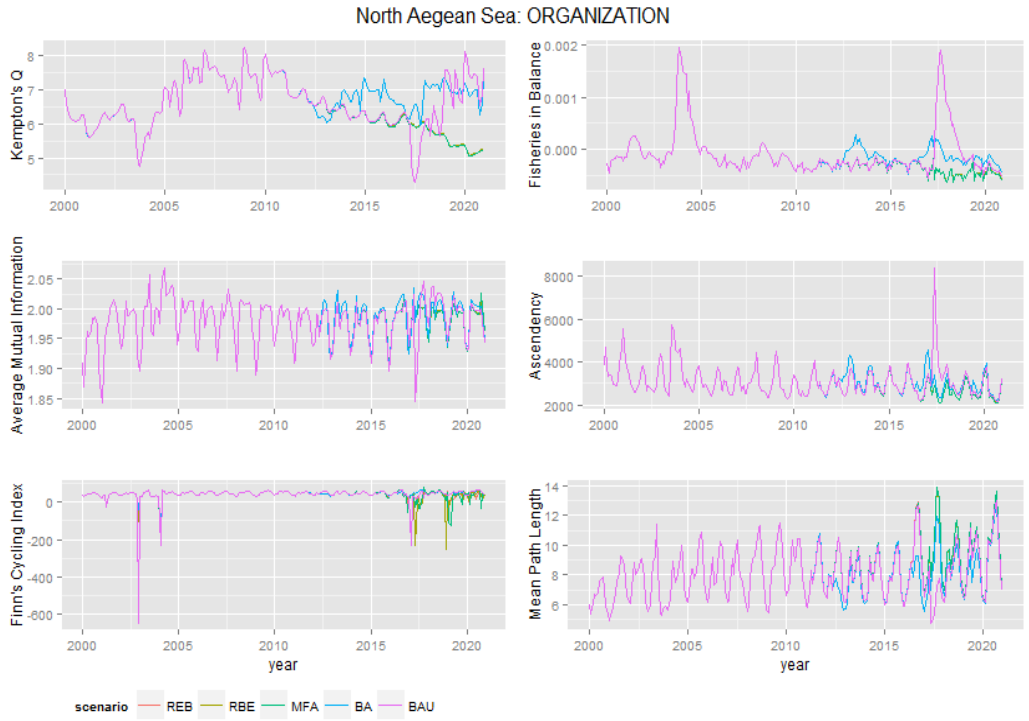

Figure 5. Organisation estimated metrics for the nutrient load scenarios applied for the period 2011-2020. The 2000-2010 period corresponds to the coupled model fitted to data.

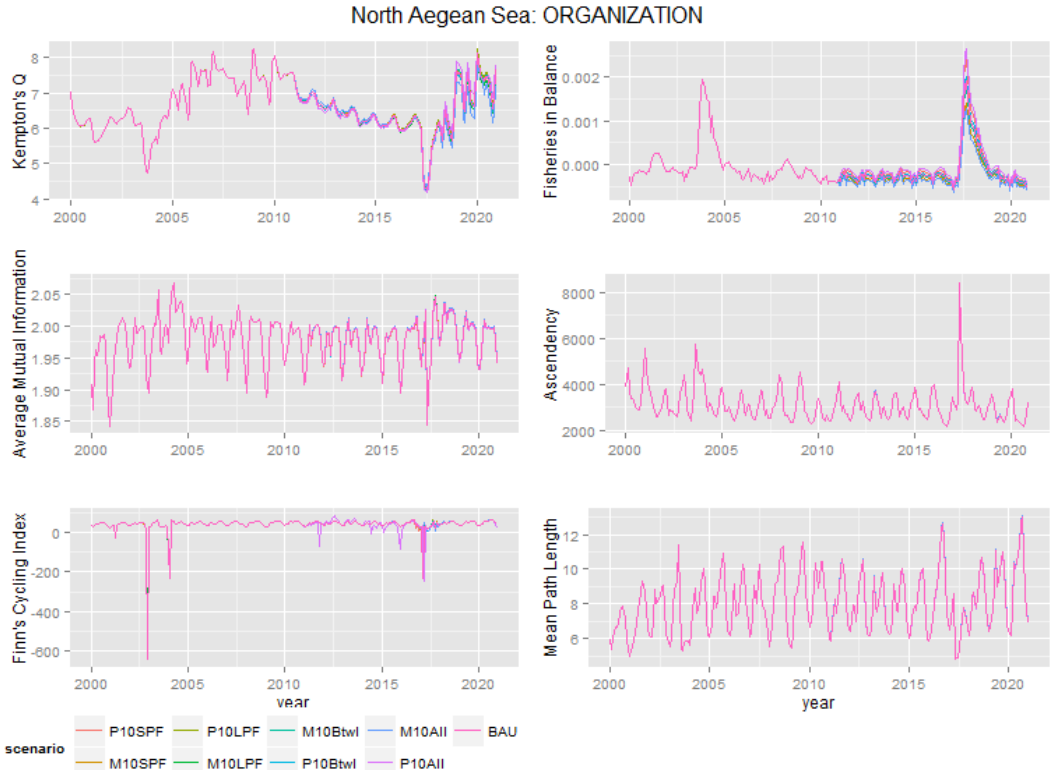

Figure 6. Organisation estimated metrics for the HTL (fisheries) scenarios applied for the period 2011-2020. The 2000-2010 period corresponds to the coupled model fitted to data. All the HTL scenarios in the coupled model used the same BAU scenario LTL data.

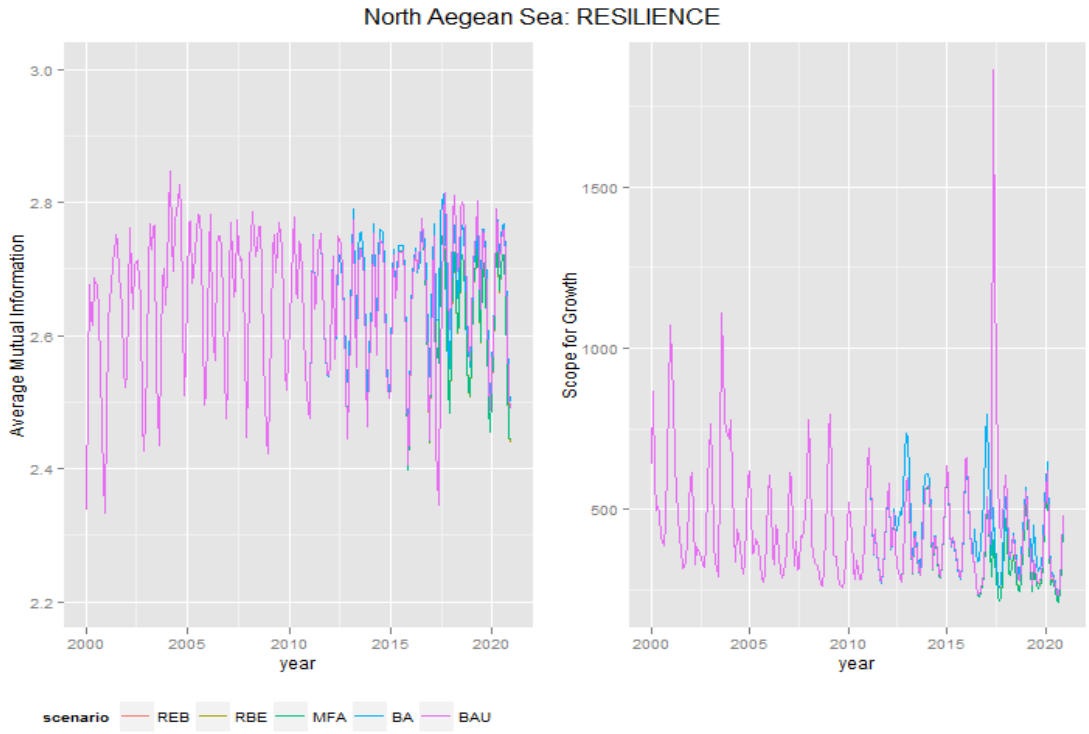

Figure 7. Resilience estimated metrics for the nutrient load scenarios applied for the period 2011-2020. The 2000-2010 period corresponds to the coupled model fitted to data.

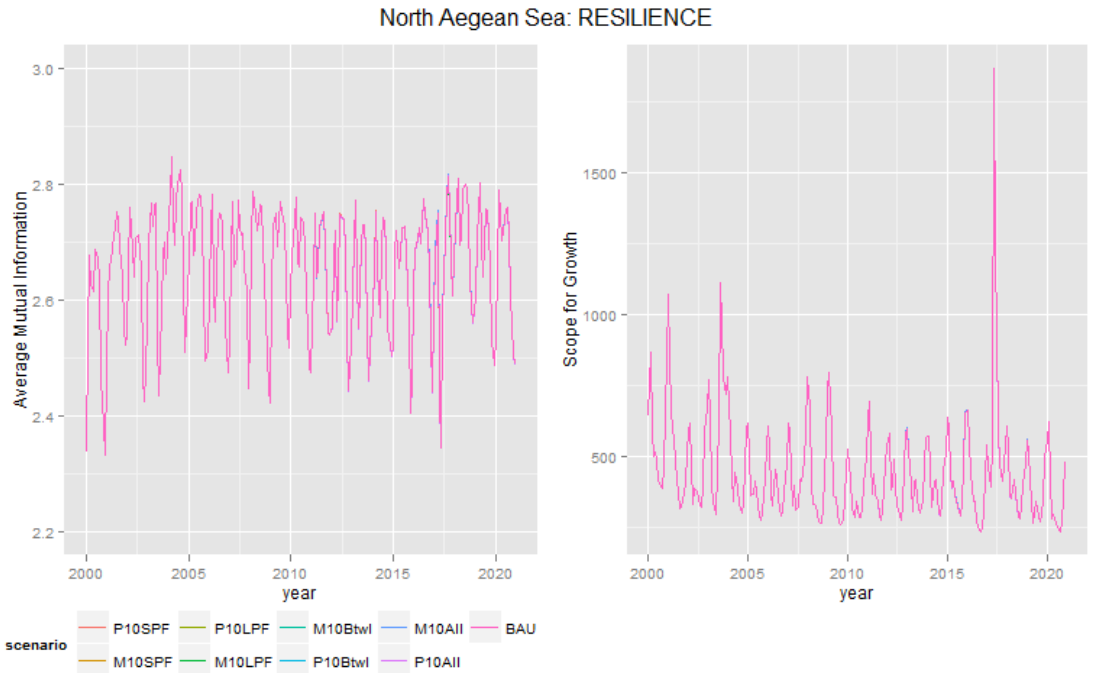

Figure 8. Resilience estimated metrics for the HTL (fisheries) scenarios applied for the period 2011-2020. The 2000-2010 period corresponds to the coupled model fitted to data. All the HTL scenarios in the coupled model used the same BAU scenario LTL data.

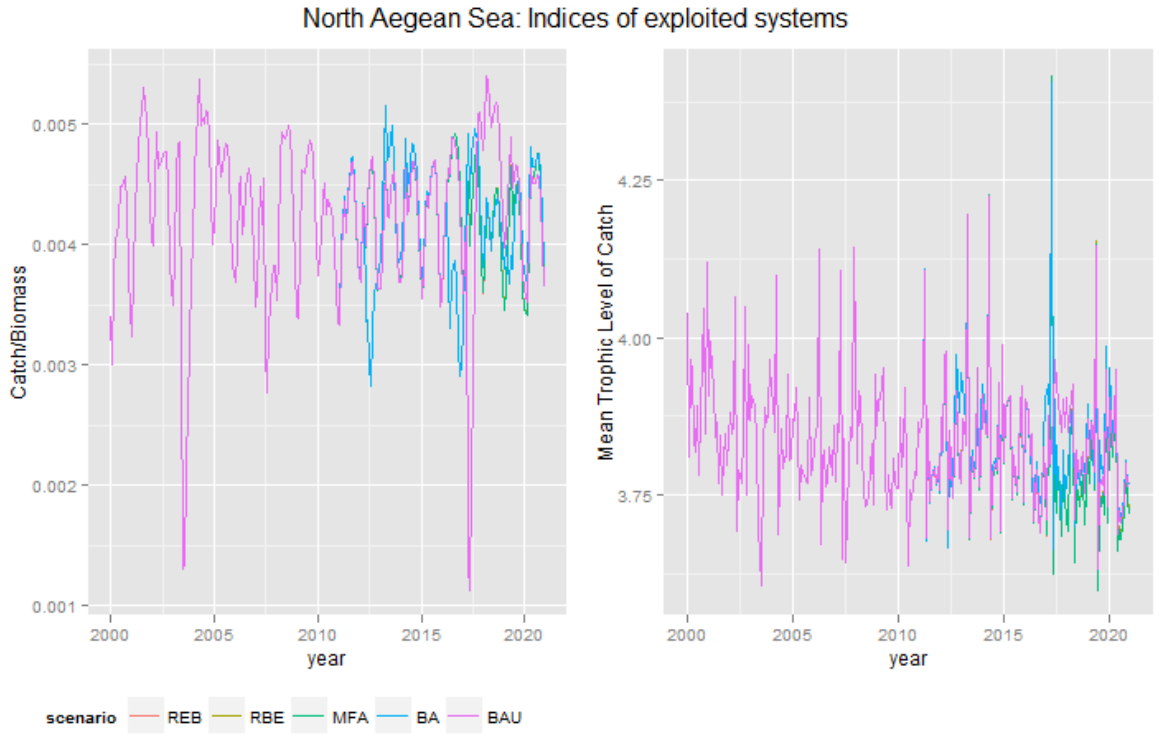

Figure 9. Indices of exploited systems estimated for the nutrient load scenarios applied for the period 2011-2020. The 2000-2010 period corresponds to the coupled model fitted to data.

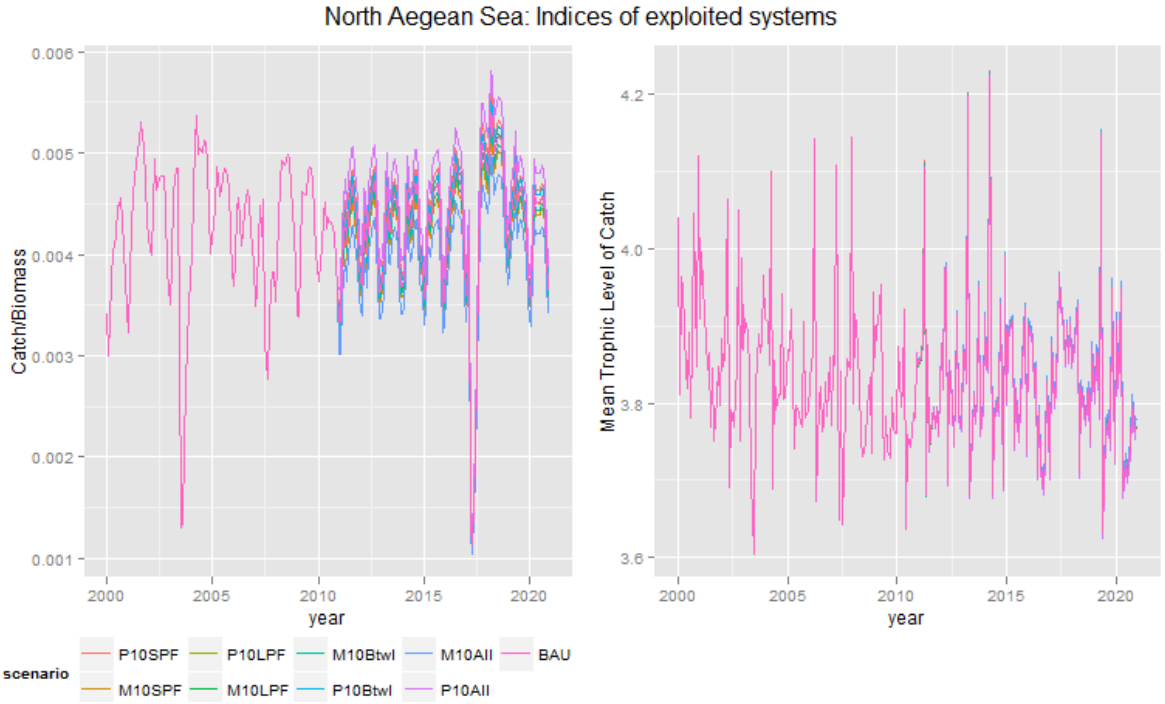

Figure 10. Indices of exploited systems estimated for the HTL (fisheries) scenarios applied for the period 2011-2020. The 2000-2010 period corresponds to the coupled model fitted to data. All the HTL scenarios in the coupled model used the same BAU scenario LTL data.

Discussion and conclusions

The simulated changes in the nutrient inputs and fisheries had a negative effect on the system Vigor as seen by the reduction in the Throughput, Net Primary Production and Catch. Similar effect was found for Resilience (specifically Scope for Growth) while the pattern of Organisation related metrics was mixed with some descending (Kempton's Q, Ascendancy,) and other ascending (Fishing in Balance, mean Path Length, Finn Cycling Index). The large number of changes detected in FGs' biomasses also imply that the organization of the ecosystem is probably affected. These changes affect, among other some key groups along the whole spectrum of the food web such as phytoplankton (LTL), small pelagic fish (medium TL) and anglerfish (top predator).

Indices related to the exploitation also reveal changes and specifically deterioration of the fisheries in terms of catches. However, the fact that FiB and C/B ratios were positively affected shows that there is a change in the catch composition of the fisheries in a way that the sustainability of the exploited part of the community is maintained.

In general the level of change in 2020 compared to 2010 as well as in the whole time series was higher for three of the nutrient load scenarios. The time series and changes in metrics under the fisheries related scenarios followed similar patterns with BAU but were positively or negatively shifted, depending on the change in fishing effort/mortality. The catch increased as a direct effect of increasing fishing effort/mortality (and vice versa), however the effect on FiB index was opposite implying that there was an impact on fisheries sustainability. The most apparent effects were when changing the fishing effort of all gears (+/- 10%) followed by the scenarios that fishing mortality of small pelagic fish (SPF) was altered. The latter was probably due to the fact that SPF dominate mid-trophic levels and may affect both higher and lower trophic levels, which is known as wasp-waist control (Cury *et al.*, 2000) and impacts several ecosystem components, as reflected in the values of the metrics

Not all metrics showed sensitivity to the examined scenarios. For example AMI, H-AMI and TLc showed very little sensitivity. In addition, even the sensitive metrics showed contrasting trends in some cases. This highlights the need to use several metrics for the assessment of ecosystem status, as already proposed by several authors (e.g., Christensen, 1995; Coll *et al*., 2016). Still, in general it can be said that the nutrient load scenarios under study do not contribute to MSFD goals of achieving good environmental status in the NAS, at least not for the two descriptors that are most relevant to this analysis, D4 food webs and D3 exploited species. The reduction of fishing effort/mortality is a positive management scenario towards this direction but a larger reduction is probably needed for substantial improvement.

References

Christensen, V. 1995. Ecosystem maturity -- towards quantification. Ecological Modelling, 77(1), 3-32.

Christensen, V., Walters, C. J. 2004. Ecopath with Ecosim: methods, capabilities and limitations. Ecological Modelling, 172, 109–139.

Coll M., L. J. Shannon, K. M. Kleisner, M. J. Juan-Jordá, A. Bundy, A. G. Akoglu, D. Banaru, J. L. Boldt, M. F. Borges, A. Cook, I. Diallo, C. Fu, C. Fox, D. Gascuel, L. J. Gurney, T. Hattab, J. J. Heymans, D. Jouffre, B. R. Knight, S. Kucukavsar, S. I. Large, C. Lynam, A. Machias,

K. N. Marshall, H. Masski, H. Ojaveer, C. Piroddi, J. Tam, D. Thiao, M. Thiaw, M. A. Torres, M. Travers-Trolet, K. Tsagarakis, I. Tuck, G. I. van der Meeren, D. Yemane, S. G. Zador and Y. J. Shin, 2016. Ecological indicators to capture the effects of fishing on biodiversity and conservation status of marine ecosystems. Ecological Indicators, 60, 947-962.

Costanza, R., Mageau, M., 1999. What is a healthy ecosystem? Aquatic Ecology, 33: 105–115.

Cury P, Bakun A, Crawford RJM, Jarre A, Quinones RA, Shannon LJ, Verheye HM. 2000. Small pelagics in upwelling systems: patterns of interaction and structural changes in ‘‘wasp-waist’’ ecosystems. ICES Journal of Marine Science 57: 603-618.

EU 2008. Directive 2008/56/EC of the European Parliament and of the council. Establishing a framework for community action in the field of marine environmental policy (Marine Strategy Framework Directive). Official Journal of the European Union.

EU 2010. Comission Decision on criteria and methodological standards on good environmental status of marine waters 2010/477/EU. Official journal of the European Union.

Heymans, J. J., Coll, M., Libralato, S., Morissette, L., Christensen, V. 2014. Global Patterns in Ecological Indicators of Marine Food Webs: A Modelling Approach. PLoS ONE, 9(4), e95845.

Lazzari, P., Solidoro, C., Ibello, V., Salon, S., Teruzzi, A., Béranger, K., Crise, A., 2012. Seasonal and inter-annual variability of plankton chlorophyll and primary production in the Mediterranean Sea: a modelling approach. Biogeosciences, 9(1): 217-233

Lejeusne, C., Chevaldonné, P., Pergent-Martini, C., Boudouresque, C. F., Pérez, T. 2010. Climate change effects on a miniature ocean: the highly diverse, highly impacted Mediterranean Sea. Trends in Ecology & Evolution, 25(4), 250-260.

Libralato, S., Coll, M., Tudela, S., Palomera, I., Pranovi, F. 2008. Novel index for quantification of ecosystem effects of fishing as removal of secondary production. Marine Ecology Progress Series, 355, 107-129.

Libralato, S., Solidoro, C., 2009. Bridging biogeochemical and food web models for an End-to-End representation of marine ecosystem dynamics: The Venice lagoon case study. Ecological Modelling, 220(21): 2960-2971.

Lynam, C. P., Mackinson, S. 2015. How will fisheries management measures contribute towards the attainment of Good Environmental Status for the North Sea ecosystem? Global Ecology and Conservation, 4, 160-175.

Tsagarakis K, Coll M, Giannoulaki M, Somarakis S, Papaconstantinou C, Machias A. 2010. Food-web traits of the North Aegean Sea ecosystem (Eastern Mediterranean) and comparison with other Mediterranean ecosystems. Estuarine, Coastal and Shelf Science 88: 233-248.

Black Sea

HNW-Black sea LTL coastal modelling (ULg-MARE)

The GHER model implemented in the Black Sea northwestern shelf (BS-NWS) includes hydrodamics (Capet et al, 2012), pelagic biogeochemistry (Grégoire et al., 2008; Capet A., 2014) and benthic biogeochemistry (Capet et al, 2015). It has a horizontal resolution of 15 km, and used a double-sigma vertical coordinate systems (terrain-following, 20 layer from 0-120 m + 11 layers below). Although the focus is on the BS-NWS, this implementation considers the entire BS basin in order to avoid boundary conditions problems at the shelf break. More details on the model and validation results can be found in associated deliverable D.4.4. Forcings for the HTL models were derived using projections of river runoff and nutrient load (D.4.6) and atmospheric conditions (D.4.2). A base simulation covered the years 1980-2010. From 2010 to 2020, five different sets of riverine load scenarios were used to extend the simulation initialized from the base simulation. The simulations results were used to provide an assessmebnt of the environmental state of the region based on the ecosystem properties defining the "health of the marine ecosystem.

Vigor :

Vigor is addressed here as the productive capacity of the system through net primary production.

Primary production in the Black Sea is higher in the northwestern shelf region (NWS) under direct influence of large riverine nutrient loads (Fig . 1). In the open basin two patterns superposes : (1) a cycle originating from nutrient brought upwards by winter mixing with higher intensity in the central basin where isopycnals are shallower., and (2) plumes of primary production originated from materials exported from the shelf, south of Crimea in the summer months and along Anatolian coast in autumn-winter.

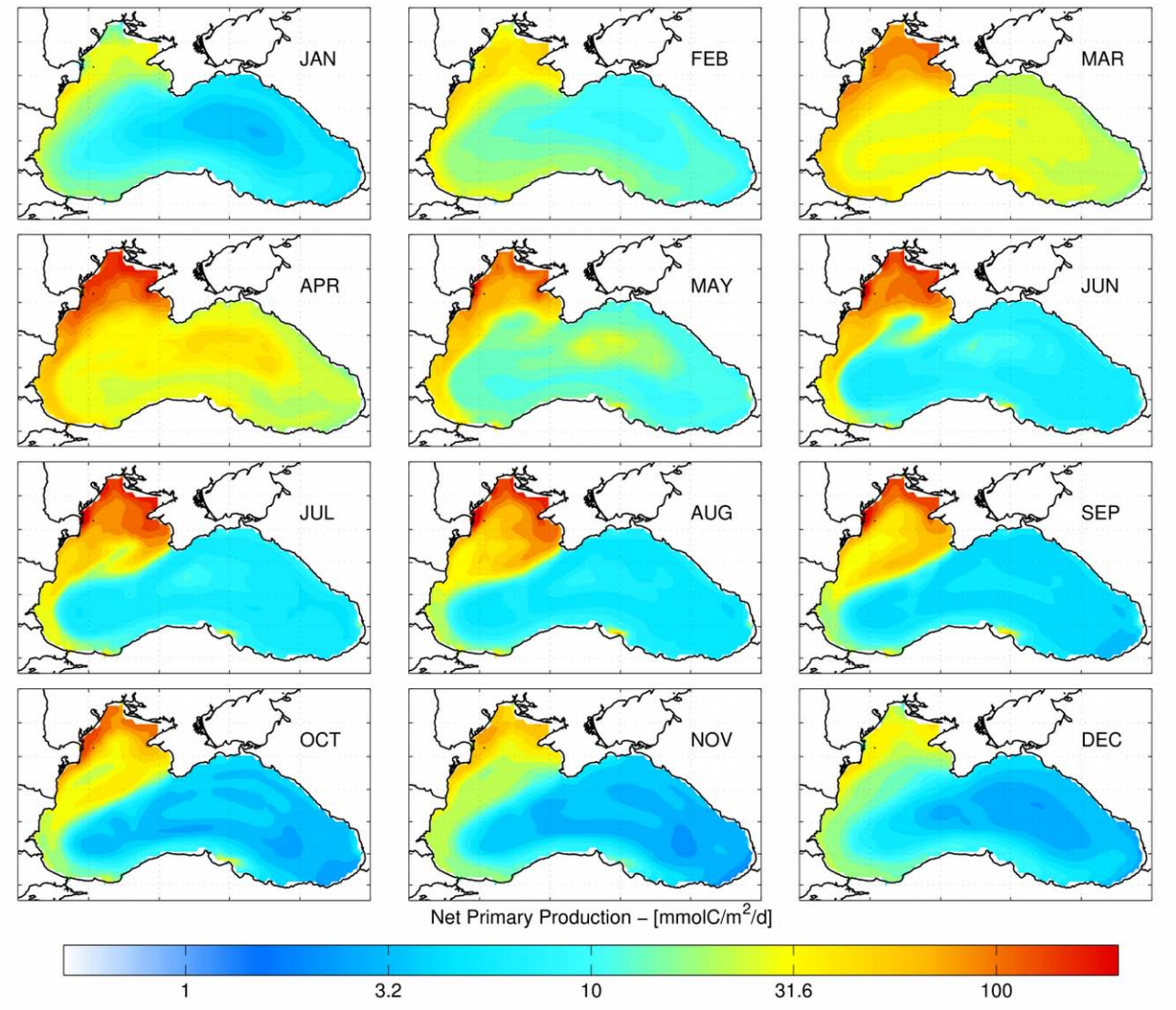

Fig 1.: Climatology of net primary production over the period 1985-2015.

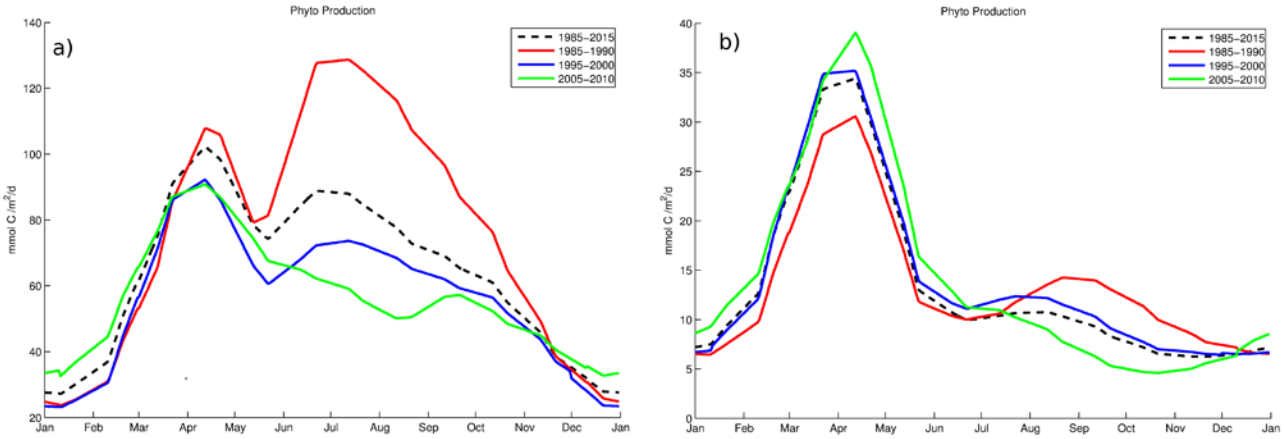

Fig 2: Net Primary production in (a) the northwestern shelf, and (b) the open basin. Different periods are depicted.

On a seasonal scale, primary production presents two peaks (spring and summer) both on the NWS area and in the open basin. In the open basin area the spring bloom, triggered by nutrient uplifting, overpasses the summer bloom, triggered by export from the shelf. In the NWS, Spring bloom is dominated by diatoms, while summer bloom is mostly due to flagellates (see model description in Grégoire et al., 2008; Capet A., 2014). Therefore the respective importance of spring and summer blooms is dependent on the ratio between silicate and other nutrients. In these simulations, an increase of the silicate content in the surface waters entailed a reduction of the summer bloom in the last decades.

Organization:

Considering the Black Sea northwestern shelf as a system operating the transfer of terrestrial inputs towards the open basin we investigate the different pathways of this transfer. In this framework, it is relevant to evaluate which part of the shelf biogeochemical cycling is operated via the sediment layer. Because mineralization in the sediments occurs in a chemical environment that differs from the pelagic (ie., much less oxygen), it involves redox reactions at different rates. In particular, denitrification in the sediments has the capacity to remove a considerable fraction of fixed nitrogen from the system by producing gaseous forms of nitrogen.

Three biogeochemical provinces were identified in the Black Sea northwestern shelf showing contrasting benthic mineralization rates, relative importances of mineralization pathways and ensuing benthic fluxes (Fig 3). In the shallower region, characterized by high organic matter settling rates, high seasonal variability of bottom water conditions and seasonally affected by bottom water hypoxia, benthic mineralization is mainly achieved anoxically. In the intermediate region denitrification is maximal (compared to the other regions). In the third region, along the shelf break, where organic matter settling rates and seasonal variability of bottom water conditions are minimal, benthic mineralization is mainly achieved oxically.

The benthic contribution to the NWS biogeochemistry is considerable. During the stratified period, benthic respiration accounts for 30\% of the oxygen consumption below the mixed layer depth (Capet et al. , 2013). The benthic release of reduced compounds and ammonium causes further oxygen consumption through their pelagic oxidation, which contributes by an additional 10% to the oxygen consumption below the mixed layer during the stratified period. Benthic oxygen consumption is therefore a critical factor in the dynamics of the bottom water hypoxia, which is further emphasized by the close correspondence between the spatial distribution of benthic oxygen consumption and the spatial extension of seasonal hypoxia in the BS-NWS (Capet et al. , 2013).

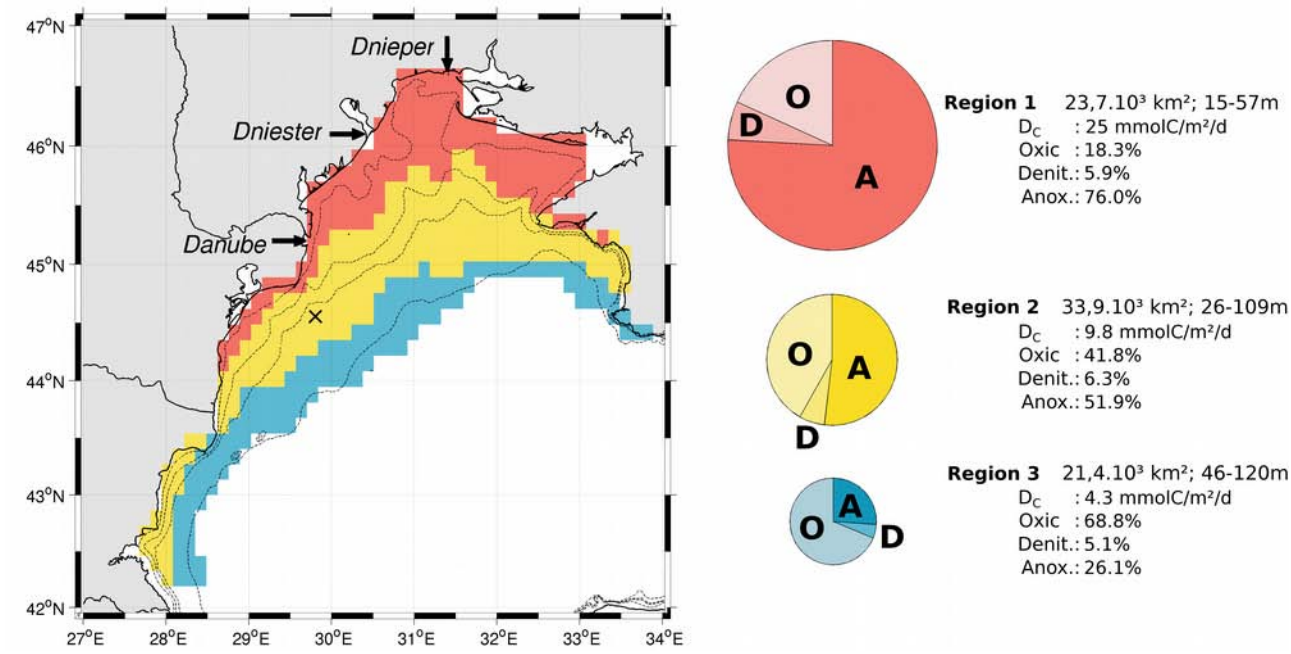

Fig :

The loss of bio-available nitrogen through denitrification and burial represents 47% (or 34% for denitrification alone) of the total N input to the shelf area, which includes the riverine inputs of nitrate and nitrite (27 Gmol N/yr), ammonium (5 Gmol N/yr) and organic forms (10 GmolN/yr) and the atmospheric nitrogen deposit (4.5 Gmol N/yr). For comparison, the nitrogen loss toward gaseous forms in the pelagic layer through denitrification and anaerobic ammonium oxidation is three time smaller. The significant sedimentary nitrogen sink in the NWS-BS resolves the apparent conflict that primary production in the outer shelf region might be limited by nitrogen, while still the N:P ratio of riverine waters indicates phosphorus limitation (Oguz et al, 2006).

About 75% of the annual carbon mineralization arises from the organic matter with slow decay rates (~10 year) . Since this type of mineralization uses organic matter produced during previous years, this introduces an uncoupling between the amount and timing of nutrient delivered by the rivers and the consequences of eutrophication in

the Black Sea. Riverine nutrients are temporarily stored as organic matter in the sediment, and are released with a time delay as nutrient fluxes across the sediment water interface. This uncoupling explains why bottom water hypoxia is predicted to continue in the Black Sea several years after riverine nutrient loading has been reduced (inertia of ~10 years, Capet et al. , 2013). These results stress that any monitoring of nutrient reduction policies in shelf areas should take into account benthic-pelagic coupling in general and this inertial behavior in particular.

Sediment accumulation determines the horizontal distribution of diagenetic rates and benthic-pelagic fluxes. Shallow regions are generally more productive, but are also exposed to stronger wave and current influences, and hence experience higher bottom shear stresses. Particles uplifted by resuspension events are exposed to lateral advection. As higher bottom stress restrains sediment accumulation in the shallower region, successive deposition and resuspension events result in a lateral transfer of sedimentary materials from the coastal locations with highest productivity to deeper offshore areas. We noticed that the calibration of sediment resuspension is a very sensitive issue since it bears a large impact on biogeochemical cycling on the shelf but also beyond the shelf break on the entire basin, as it controls the flux of nutrient and organic materials towards the open sea. Ignoring bottom stress effects enhanced the benthic oxygen consumption and carbon sequestration in the whole BS-NWS by 45\% while removal of bio-available nitrogen was increased by 30% (Fig. 3 d).

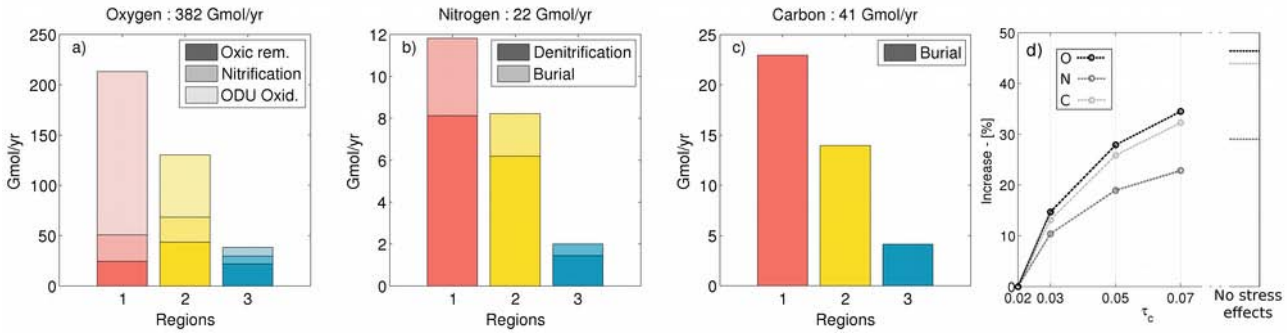

Fig. 3: Net annual benthic cycling of (a) oxygen, (b) nitrogen and (c) carbon in each biogeochemical region in the BS-NWS (averages computed over 1995-2005).The different color shades in each bar indicate the contribution of different processes. (d) Relative increases in the net benthic consumptions of oxygen, nitrogen and carbon integrated over the BS-NWS, for different values of τ_{dep} .(a), (b) and (c) have been computed with the reference value of τ_{dep}=0.02 N/m^{-2}.

Enhancing the sensitivity to bottom stress (i.e., reducing the critical deposition and erosion thresholds) increases the transfer of organic matter from the shallow to the deep parts. This entails a reduction of benthic mineralization rates in the shallower part of the shelf (Fig. 4e) and a reduction of the ratio of net primary production being mineralized locally in the shelf sediments (Fig. 4f). The associated higher transfer of nutrients and organic matter to the open sea results in a basin-wide increase of primary

production of 10% (comparing the best estimate for critical bottom stress deposition thresold τ_{dep} =0.02 N/m^{-2} to the still realistic case of τ_{dep} =0.05 N/m^{-2} ; Fig. 4d).

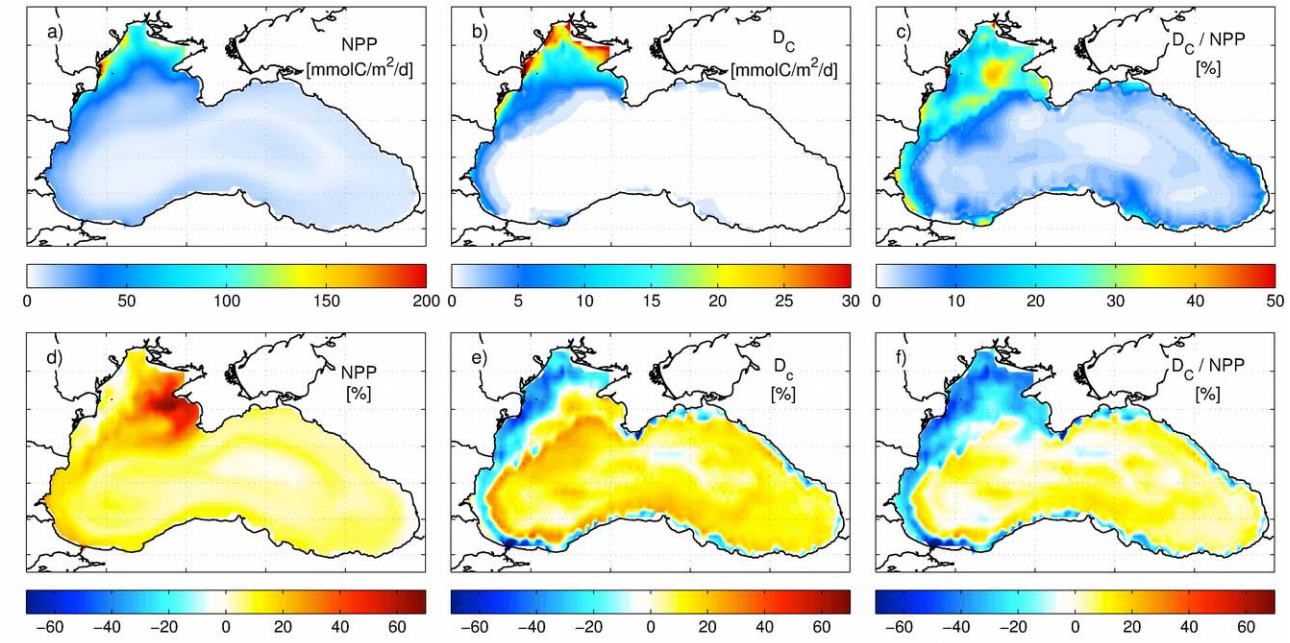

Fig 4. : Upper panels: annual averages of (a) net primary production, (b) benthic mineralization rate and (c) ratio of net primary production being mineralized locally. Lower panels: relative increase comparing the baseline simulation (τ_{dep}= 0.02 Nm^{-2}) to the case with reduced sensitivity to bottom stress (τ_{dep}= 0.05 Nm^{-2}): (d) net primary production, (e) carbon benthic mineralization rate, (f) ratio of net primary production being mineralized locally.

Resilience

Given the short projection time considered, the riverine forcing data provided for different socio-economical scenario showed only very small differences. As could be expected, the differences between LTL simulations obtained using these different forcing sets are similarly very smalls.

Impacts on trophic networks have been reported in the associated deliverable D. 4.8.

A particularity of the Black Sea is the occurrence of hypoxic ([O2] < 60 mmol/m^3) and anoxic ([O2] < 10 mmol/m^3) conditions. Deoxygenation dynamics responds to eutrophication (as nutrient loads fuel high organic matter production and degradation in the lower water column) and climatic drivers (as physical ventilation is restrained by the warming of surface waters). Two cases are considered in the following: (1) the case of seasonal hypoxic events affecting the northern part of the northwestern shelf and (2) the case of the anoxic deep water in the open basin, and in particular, the vertical stability of the depth of transition from oxic to suboxic waters.

Hypoxia on the northwestern shelf : The NWS is seasonally affected by bottom water hypoxic events (Capet et al., 2013). The different processes which, together, constitute the seasonal mechanism of these hypoxic events have been detailed using the 3D coupled model. This allowed to identify the key factors controlling the intensity of hypoxic events on an inter-annual scale by acting on those processes (Fig. 6). The factors that support hypoxia are (1) high nitrogen load that enhance the flux of organic matter to bottom waters, (2) accumulation of benthic carbon content, that enahnces benthic oxygen consumption, (3) Warm springs that reduce the ventilation of bottom water before the summer thermocline isolate these waters from the atmopshere and (4) warm summers that delay the extend of the stratification period.

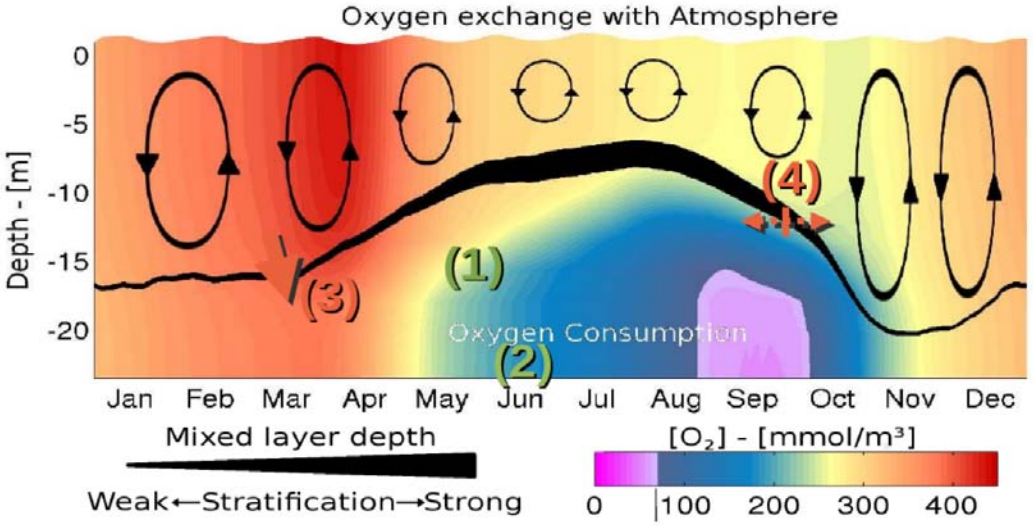

Two aspects are relevant to the issue of resilience. First, because of the slow decaying rate of organic matter accumulated in the sediments, a transition period of approximately 10 years is expected before hypoxic intensity correspond to new levels of riverine nutrients loads (eg. set in the framework of environmental management directive). Second, atmospheric warming alters the hypoxic response to a given level of nutrient loads, and as such restrain the ability of the system to recover pristine conditions if nutrients load are reduced to their pristine levels (Fig 7).

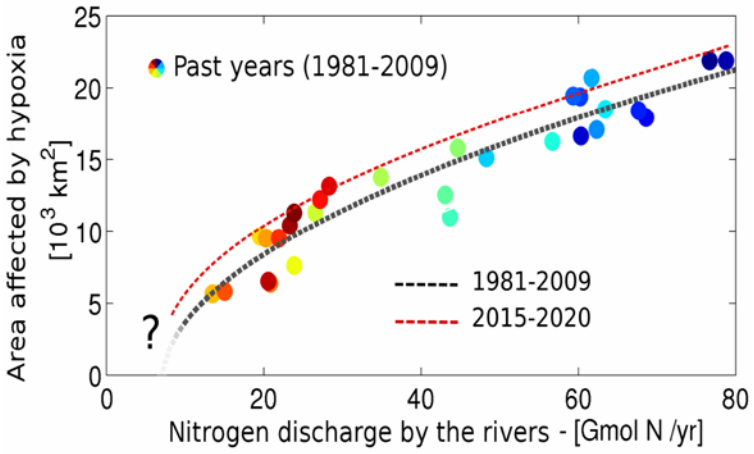

Shoaling of the Black Sea Oxycline : The second study case concerns the vertical stability of the transition interface between oxic and suboxic waters in the Black Sea open basin (Capet et al . 2015). It has been shown that the oxygen penetration depth has shoaled in the past concordingly with high nutrient loads in the eutrophication period (~ 1970-1990). In this case the resilience of the system is assessed through the vertical migration of oxygen penetration depth after nutrient reduction in 1990. We investigated the evolution of oxygen penetration depth (over which [O2]>20 mmol/m^3) and oxygen inventory (integrated above this limit) during the past 60 years using in-situ oxygen profiles (Ship-based casts and ARGO profilers, no model involved in this study).

Our results shows that oxygen penetration depth has shoaled from 140 m in 1955 to 90 m in 2013 (Fig 8), and that oxygen inventory was reduced by 36% over the same period.

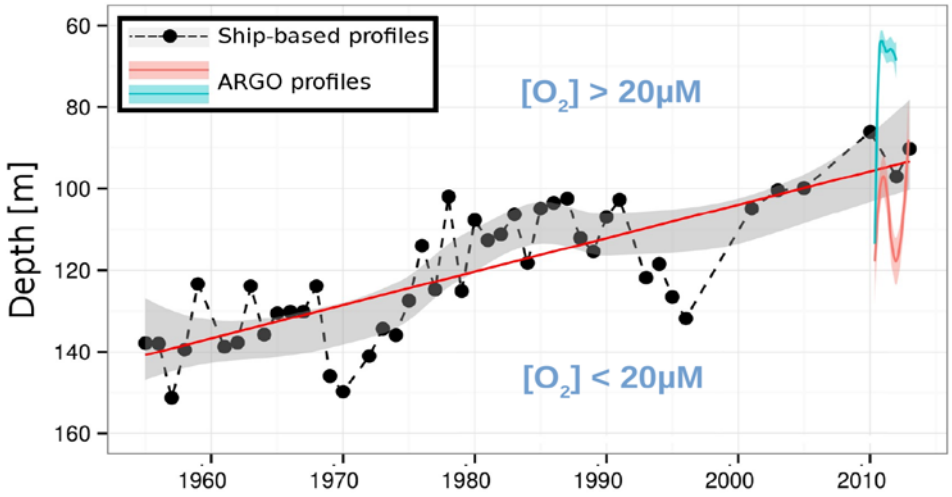

Illustration 1: Fig. 8 : Oxygen penetration depth derived from in-situ oxygen profiles. The ARGO profilers illustrates the spatial variability of oxygen vertical distribution and confirm the values derived from ship based casts for the most recent years.

Cold Intermediate Waters are dense waters formed in winter that sink to the level of the permanent halocline, bringing oxygen to the Black Sea intermediate levels. This convective ventilation has been identified has the main physical control on oxygen penetration depth (Konovalov et al, 2006). Here, we evidence that the deeper oxygen penetration depth observed after nutrient reduction (~1990) was induced by high CIW formation rates rather than lower oxygen consumption, thereby questioning the hypothesis of a quick Black Sea recovery from eutrophication.

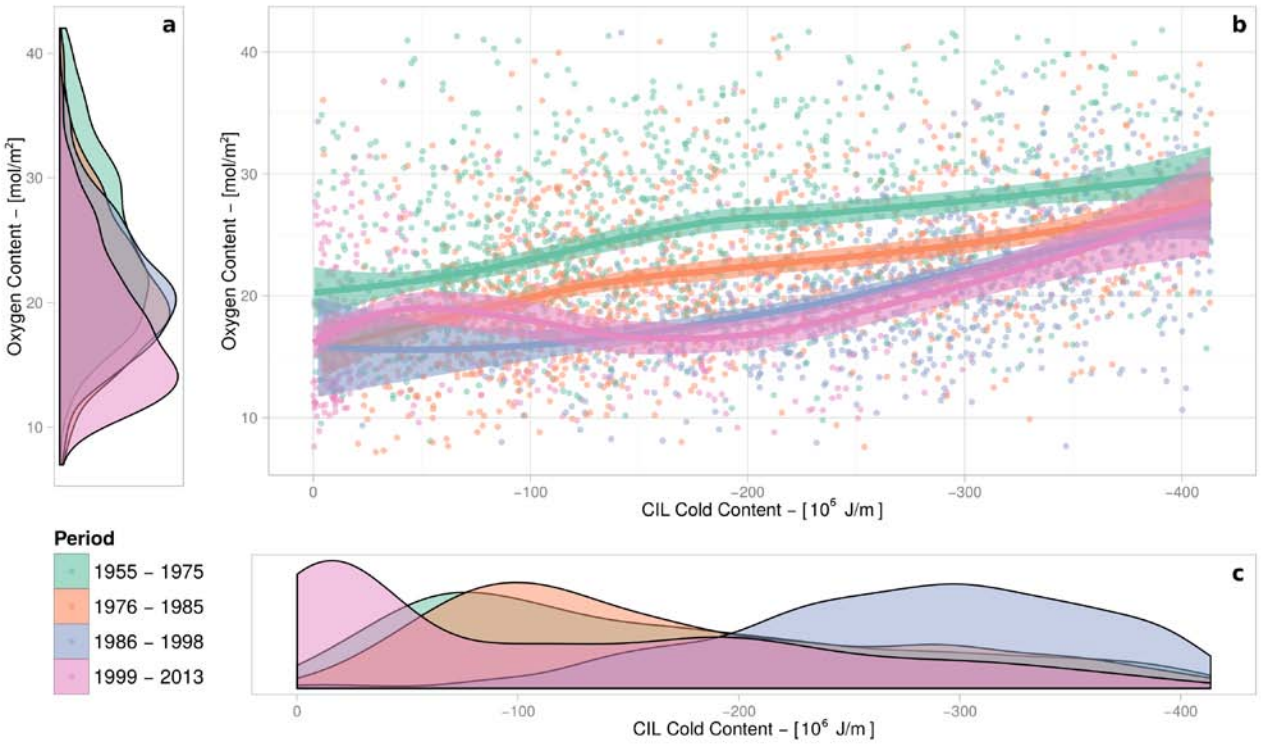

Fig. 9 : The comparison of Cold water and oxygen content from the profiles dataset evidences similar slopes for the different periods, illustrating the ventilation role of CIW formation. During the period 1985-1998, CIW content were significantly higher than in others periods, resulting in high Oxygen content. If nutrient reduction (after 1990) had entailed lower oxygen consumption in the intermediate depth, , then the general relationships between CIW and oxygen content after 1990 would appear above that of previous period. Instead, these relationships indicates higher oxygen consumption during the periods 1985-1998 and 1998-2013.

References

Capet, A., Troupin, C., J. Carstensen, J., Grégoire, M., Beckers, J.-M., *Untangling spatial and temporal trends in the variability of the Black Sea Cold Intermediate Layer and mixed Layer Depth using the DIVA detrending procedure,* Ocean Dynamics, 64(3), 2014

Capet, A., *Study of the multi-decadal evolution of the Black Sea hydrodynamics and biogeochemistry using mathematical modelling*, Phd Thesis, Univeristy of Liège, 2014

Capet, A., J.-M., Meysman, F., Soetaert, K., Grégoire, M., Beckers,: *Introducing spatial and temporal variability of benthic diagenesis in 3D biogeochemical models : A case study for the Black Sea North western shelf*, submitted to Ocean Modelling, 2015

Capet, A., Barth, A., Beckers, J.-M., Grégoire, M.: *Interannual variability of Black Sea's hydrodynamics and connection to atmospheric patterns*, Deep-Sea Research II 77-80(0), 128–142, 2012, Satellite Oceanography and Climate Change

Capet, A., Stanev, E.V., Beckers, J.-M., Murray, J.W., and Grégoire, M.: Recent decline of the Black Sea oxygen inventory, Biogeosciences Discuss., 12, 16233-16253, doi:10.5194/bgd-12-16233-2015, 2015.

Grégoire, M., Raick, C., Soetaert, K.: *Numerical modeling of the central Black Sea ecosystem functioning during the eutrophication phase*, Prodress in Oceanography, 76(3), 2008

Konovalov, S., Murray, J. W., Luther, G., and Tebo, B.: *Processes controlling the redox budget for the oxic/anoxic water column of the Black Sea*, Deep-Sea Research Part II : Topical Studies
in Oceanography, 53, 1817–1841, 2006

Oguz, T. (Ed.). *State of the Environment of the Black Sea (2001 - 2006/7)*. Publications of the Commission on the Protection of the Black Sea Against Pollution (BSC), 2008

NW-Black sea LTL coastal modelling (focus on Varna region) (USOF)

In this report we address the response of the Black Sea coastal phytoplankton variability during the last decade to climate change and anthropogenic inputs with a focus on Varna Bay region. The coastal area of Varna region is impacted by many interacting stressors due to extensive human activity (industry, tourism and urbanization) and recent global climatic changes. From 1934 to 2001 the population increased fourfold, the population density of Varna (1 350 km-2) far exceeding the country's coastal average. In 2000-2004 the number of hotels almost doubled, however the infrastructure development tailored to meet the direct tourist demands for leisure and entertainment facilities did not meet environmental protection needs. On the other side during the last decades summer temperatures showed extreme values which have never been measured before, the frequency and intensity of rain and storm events also increase drastically. The climate change is likely to further stress both the coastal ecosystem and resource management. Phytoplankton during 2000-2013 was featured by an overall decrease of total biomass (and chlorophyll-a), lower frequency of phytoplankton blooms although still observed, on the expense of pronounced alterations of community structure (increased dominance of species from not habitual for the Black Sea classes) introducing shifts in the taxonomic ratios of the phytoplankton assemblages. The phytoplankton related indicators classifying the ecological status of the coastal area between poor-good shown a very high variability.

To asses all those changes we will utilize observational data and coupled model simulations and provide an extensive analysis on the response of the ecosystem in the Varna coastal regions to nutrient loads and climatic changes. The results from observations and numerical simulations of the inter-annual and seasonal variability of the lower trophic levels are presented. Important climatologic features for the Black Sea, such as wind variability, changes of the stratification connected with the upwelling events near the coastal areas, the mixed layer and cold intermediate water variability are discussed. The synergy between the model simulations and observational data is demonstrated. We show that the variability in the biological system is strongly controlled by the variability of the meteorological forcing. A number of indicators were derived from marine ecological data, for assessing ecosystem status and trends for the coastal ecosystem, identifying vulnerability level and setting priorities for recovery measures. The indicators computed based on both observational data and modelling results can be used as a tool for socio-economic evaluation of the ecosystem status of the coastal waters.

Introduction

The coastal area of Varna region is impacted by many interacting stressors due to extensive human activity (industry, tourism and urbanization) and recent global climatic changes (NIAR, 2013). From 1934 to 2001 the population increased fourfold, the population density of Varna (1 350 km-2) far exceeding the country's coastal average. In 2000-2004 the number of hotels almost doubled, however the infrastructure development tailored to meet the direct tourist demands for leisure and entertainment facilities did not meet environmental

protection needs. On the other side during the last decades summer temperatures showed extreme values which have never been measured before, the frequency and intensity of rain events also increased. The climate change is likely to further stress both the coastal ecosystem and resource management. Varna coastal area is among the water bodies along the Bulgarian Black Sea coast reported at risk of not-achieving "good ecological state" by 2020. Marine phytoplankton plays a key role in the lower food web and in the transfer of energy to maintain the function and productivity at the level of a healthy ecosystem. As a fast response component of the marine biota it is a valuable indicator of the ecological/ environmental status of the coastal and marine waters (important element in WFD and component of several MSFD Descriptors). During the last 14 year phytoplankton related indicators showed a very high variability, classifying the ecological status of the coastal area between poor-good (Moncheva et al., 2015) To asses all those changes we utilize observational data and coupled model simulations and provide an extensive analysis on the response of the ecosystem in the Varna coastal region to nutrient loads and climatic changes.

To assess all those changes we will utilize observational data and coupled model simulations and provide an extensive analysis on the response of the ecosystem in the Varna coastal regions to nutrient loads and climatic changes. The results from observations and numerical simulations of the inter-annual and seasonal variability of the lower trophic levels are presented. Important climatologic features for the Black Sea, such as wind variability, changes of the stratification connected with the upwelling events near the coastal areas, the mixed layer and cold intermediate water variability are discussed. The synergy between the model simulations and observational data is demonstrated. We show that the variability in the biological system is strongly controlled by the variability of the meteorological forcing. A number of indicators were derived from marine ecological data, for assessing ecosystem status and trends for the coastal ecosystem, identifying vulnerability level and setting priorities for recovery measures. The indicators computed based on both observational data and modelling results can be used as a tool for socio-economic evaluation of the ecosystem status of the coastal water.

Materials and methods

The analysis was based on 13 years spring-summer data sets (2001 - 2014) of meteorological, hydrological, chemical and biological (phytplankton) variables. The assessment of the ecological status was based on classification system of the WFD National monitoring program (Regulation No 4 /14/09/2012).

The physical model

The hydrodynamical model is based the three-dimensional GFDL MOM. Solid boundaries are non-slip and insulating for temperature and salinity. Convection is parameterized by convective adjustment that is often used to remove static instabilities. The model has 24 vertical levels; mixing and diffusion in the horizontal are parameterized with biharmonic operators. The coefficients for momentum and tracers are: Ah=Kh=0.1x1019 cm4 s-1. The vertical mixing coefficient is Av=1.5 cm2 s-1. The vertical diffusion in the model is

parameterized as stability dependent: Kv=aN-1, where N is the Vaaisaala frequency, a=0.004 cm2 s-2. The bottom is insulating:

The biogeochemical model

The structure of the BIOGEN model (state variables and processes linking them) is schematically illustrated in the figure 1. The BIOGEN model (Lancelot et al., 2002, Staneva et al, 2007)-describes the cycling of carbon, nitrogen, phosphorus and silicon through aggregated chemical and biological compartments of the planktonic and benthic systems. Each biological component represents a set of di.erent organisms grouped together according to their trophic level and functional ecological behaviour. BIOGEN thus includes 34 state variables assembled in five models. These describe: (1) the growth physiology (photosynthesis, growth, exudation, respiration) of phototrophic flagellates (NF), diatoms (DA) and opportunistic non-siliceous microphytoplankton (OP); (2) the dynamics (grazing, growth, nutrient regeneration, egestion) of thedominant micro- (MCZ) and meso- (COP) zooplanktonpopulations; (3) the feeding and growth activity of the omnivorous giant dinoflagellate Noctiluca (NOC) and the carnivorous Aurelia (AUR) and Mnemiopsis (MNE) gelatinous organisms; (4) the dynamics of organic matter (particulate, POM anddissolved, DOM; each with two classes of biodegradability) degradation by bacteria (BAC) and its coupling with nutrient regeneration; and (5) the benthic diagenesis and nutrient release by local sediments. The model is closed by gelatinous organism mortality and by fish pressure. The latter is indirectly included in the model through the mortality of mesozooplankton (COP) and is described as first-order kinetics. Sediment biogenic material is pooled as benthic particulate organic matter (BPOM) with two classes of biodegradability. Benthic nutrient exchanges are calculated from organic matter degradation, oxygen consumption and nutrient release and transformation (nitrification/ denitrification), taking into account PO4 and NH4 adsorption on particles and mixing processes in the interstitial and solid phases of the sediment.). BIOGEN innovation is the representation of the feeding mode of the gelatinous organisms NOC, AUR and MNE. The omnivorous Noctiluca (NOC) feed on all auto- and heterotrophic micro-organisms and detrital POM. The gelatinous carnivores AUR and MNE eat mesozooplankton (COP). nThe impact of vertical stratification and forcing with different time scales on the functioning of biological system has been studied by Staneva et al. (1998). The results of coupling between different physical models (mixed layer model, box-like model and 3-D basin-wide general circulation model) and ecosystem model (Lancelot et al., 2002) demonstrate that simulated phytoplankton evolution compares well with the SeaWiFS and CSCZ satellite data. The impact of natural and anthropogenic matter from the land to the coastal environment and identifying limitations on the nutrient capacity of the coastal waters by studying extreme events for the north-western Black Sea have been studied (Staneva at al., 2007 and Kourafalou et al, 2005).

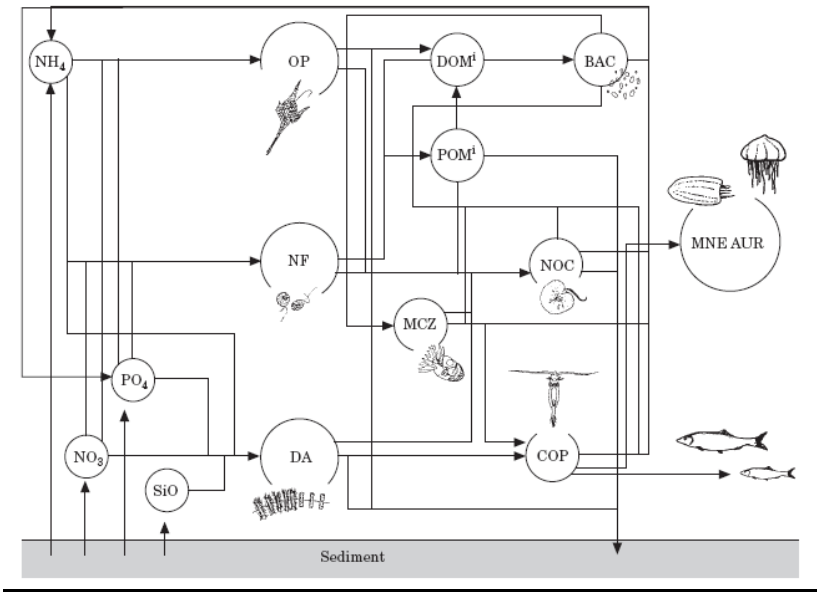

Fig. 1 Diagrammatic representation of the structure of the BIOGEN model.

Results

Figure 2 demonstrates the nutrient variability for several locations within the Varna Bay over the spring-summer seasons for the period from 2000 to 2013. Linear trends of observational data are plotted as well. It is clearly seen that for most of the nutrient there is a general decrease of the concentration during the last decade (except for the silicate concentration for Chanal area. The trend of decreasing of nutrient concentrations over Varna Bay coastal areas is even more pronounced for the summer season (Fig. 2). Phytoplankton during 2000-2013 (Fig. 3) was featured by an overall decrease of total biomass (and chlorophyll-a), lower frequency of phytoplankton blooms although still observed, on the expense of pronounced alterations of community structure (increased dominance of species from not habitual for the Black Sea classes) introducing shifts in the taxonomic ratios of the phytoplankton assemblages.

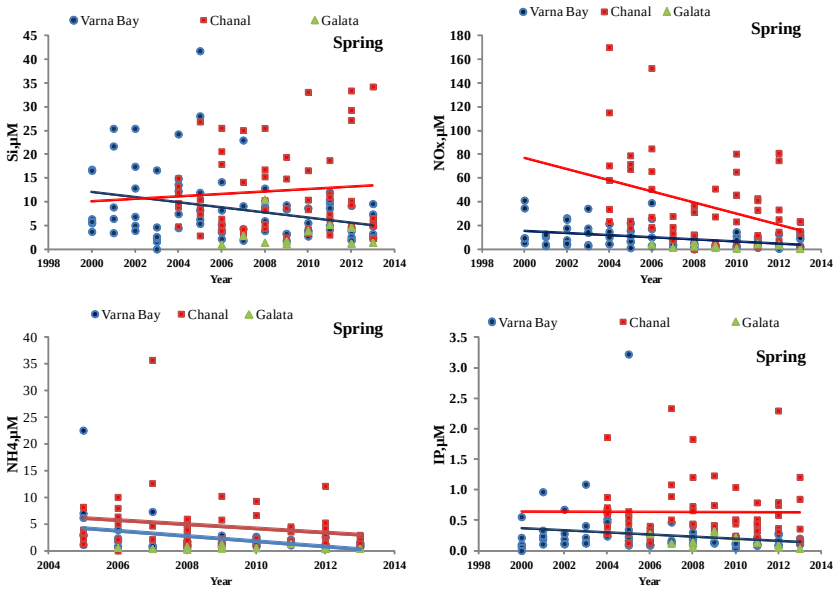

Fig. 2 Times series of Nutrients averaged over spring for different Varna Bay location

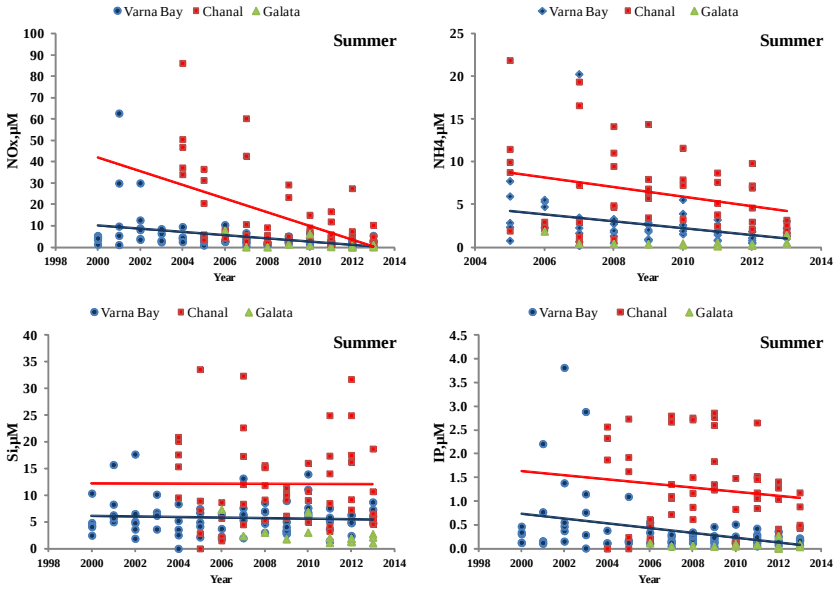

Fig. 3 Times series of Nutrients averaged over summer for different Varna Bay location

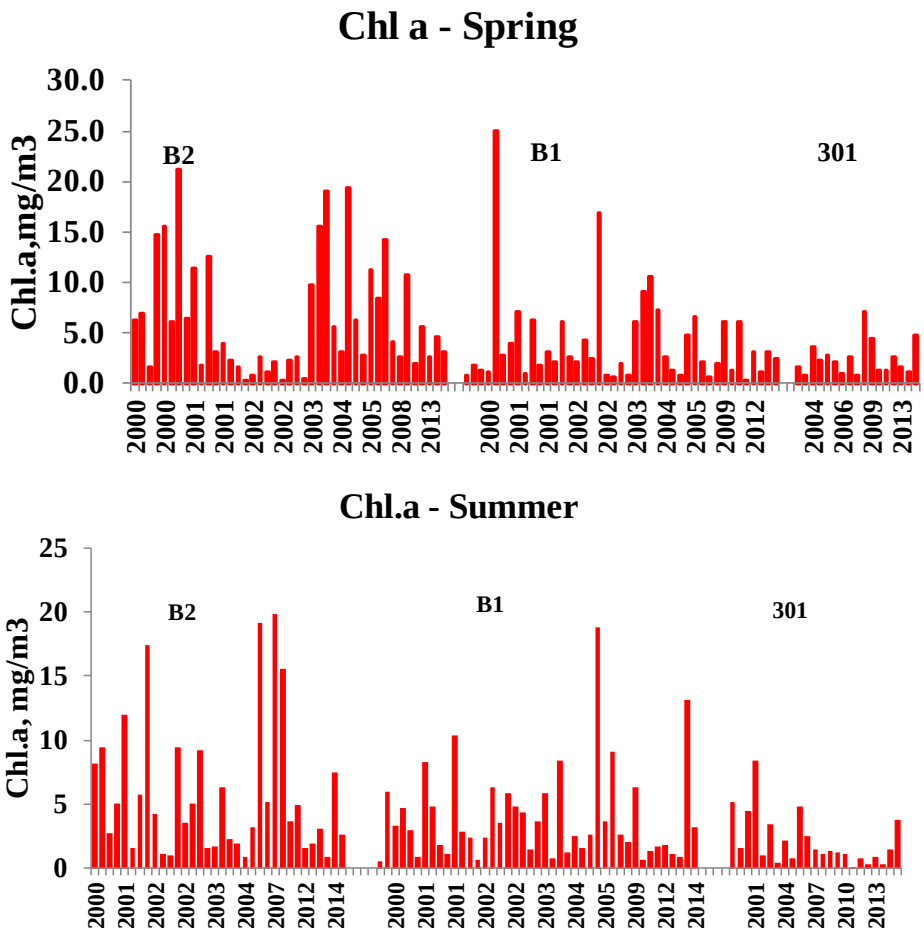

Fig. 4. Long-term (2000-2014) variability of chl.a time series in spring (Left) and summer (right) (B2-Chanal, B1- Varna bay, 301- Galata stations in Varna area)

The Phytoplankton concentration for spring season as an indicator for the Black Sea ecological state (Tables 1 and 2) is demonstrated on Figures 5 and 6: The classification of the values for this indicator and five ecological states is presented in the table on the bottom-left site. Temporal variability of the phytoplankton concentration is analyzed from 2001 until 2014 taken from the observations (left) and model simulations (right). The shadings correspond to the ecological state as defined by Table 1 for spring and Table 2 for summer: bad (red), poor (orange), moderate (yellow), good (green) and high (blue) state of the sea. The data from the numerical simulations have been extracted for the same locations and time as the observational ones. From the Control Run tt is clearly seen that there is a good agreement between model and observations giving the confidence that the model simulations could be used as a powerful tool for assessing the Black Sea ecosystem status. The interannual variability of the phytoplankton is relatively well reproduced by the model simulation compared with observations. Both patterns show a clear trend of improving the ecological status for the Varna Bay region from moderate to good during the last decade. Only for the period 2009-2010 the ecological status has been again shifted to moderate-

poor due to the increase of the nutrients. Several scenario has been performed in order to study the response of the Varna Bay ecosystem to both climate change and nutrient variability and this will be discuss as well. The ecological situation during the last decades have been significantly improved by Scenario 2 where for most of the years the simulated phytoplankton concentrations lays in good to moderate range. On the other hand, for scenario 1 all years showed moderate and poor status and no one of the simulations fall into good one. It is important also to notice that in all simulations a trend of improving the ecological status is simulated for both spring and summer period. It corresponds also with the observational evidence (see bottom left patterns of Figures 5 and 6)
This trend is more pronounced during the summer.

	Spring			
High	Good	Moderate	Poor	Bad
1.8-2.3	2.3-3.3	3.3-5.5	5.5-9.6	>9.6

Table 1: The Chlorophyll-a related indicator during **Spring** classifying the ecological status of the coastal area

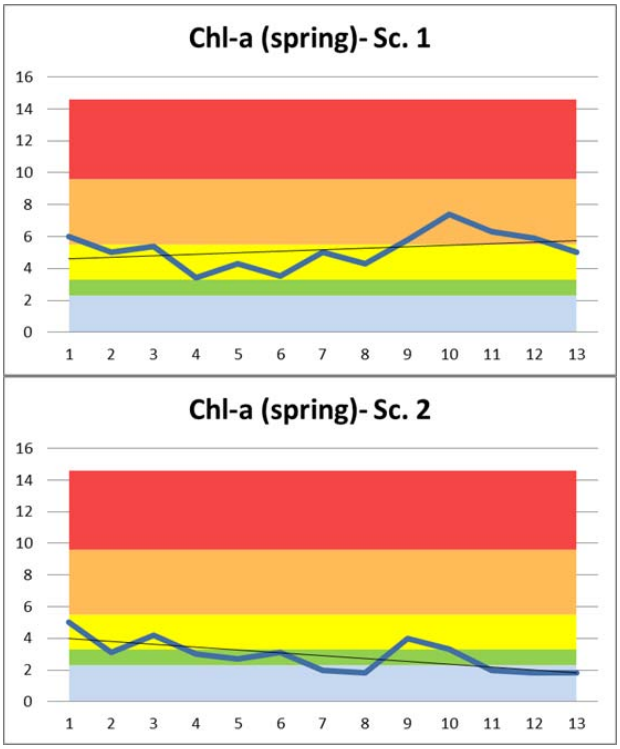

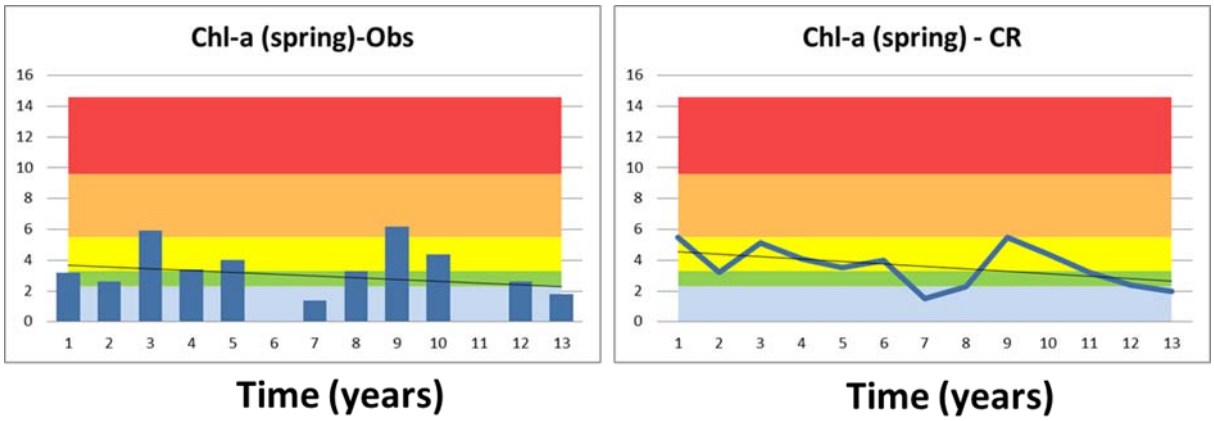

Fig. 5 Chlorophyll concentration during spring as an indicator for the Black Sea ecological state: Temporal variability of this indicator from 2001 until 2013- from the model simulations and observations (bottom-left). The shadings correspond to the ecological state as defined by Table1: bad (red), poor (orange), moderate (yellow), good (green) and high (blue) state of the sea

Summer				
High	Good	Moderate	Poor	Bad
<0.9	0.9-1.5	1.5-3.1	3.1-7.0	>7.0

Table 2: The Chlorophyll-a related indicator during summer classifying the ecological status of the coastal area.

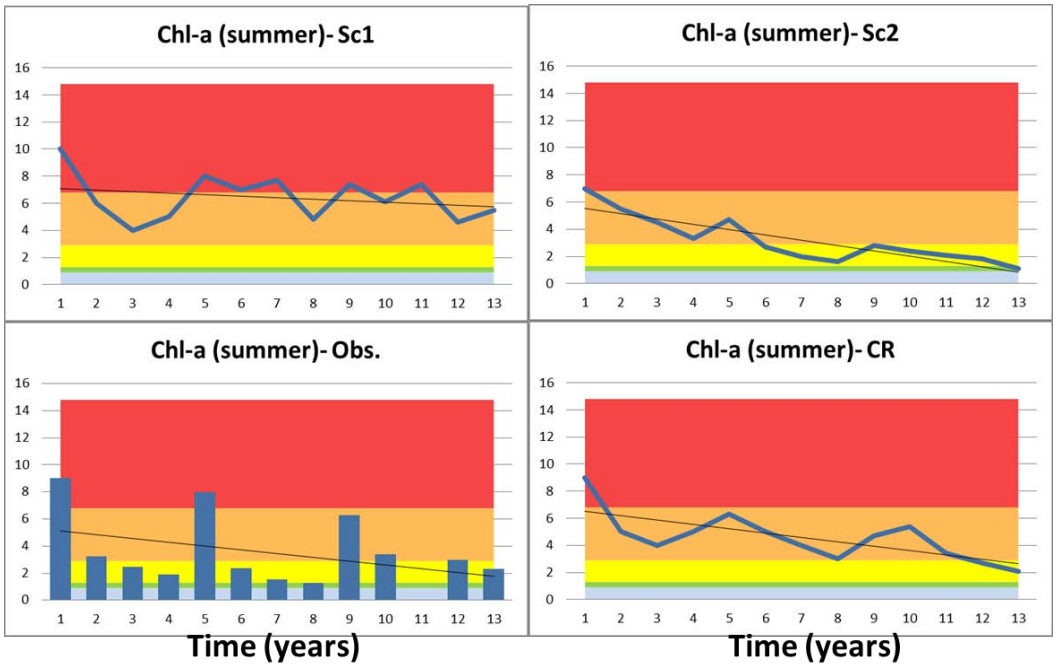

Fig. 6 Chlorophyll concentration during spring as an indicator for the Black Sea ecological state: Temporal variability of this indicator from 2001 until 2013- from the model simulations and observations (bottom-left). The shadings correspond to the ecological state as defined by Table1: bad (red), poor (orange), moderate (yellow), good (green) and high (blue) state of the sea

Conclusion/discussion

Among the main challenges in the implementation of WFD and MSFD is the growing demand for robust and reliable methodological approaches in selecting indicators for diagnose of the ecological state taking into account the complexity of multifactor drivers/pressures. The indicators computed based on both observational data and modelling results will be further used as a tool for socio-economic evaluation of the ecosystem status of the coastal waters. The aim of this study was to support for the policy advice to stakeholders/ governments on the need to invest in nutrient reduction projects. We aim to answer on which are the driving forces and responses of the marine systems to both anthropogenic and/or climate changes? Developing integrated tools for assessing marine ecosystem status is one the major outcomes of such a study.Text

References

Kourafalou, V., K. Tsiaras and J. Staneva (2004), Numerical studies on the dynamics of the Nortwestern Black Sea shelf, Med. Mar. Sci., Vol.5/1, 133-142.

Lancelot, C. L., J. V. Staneva, D. Van Eeckhout, J.-M. Beckers, and E. V. Stanev, 2002. Modelling the Danube-influenced North-Western continental shelf of the Black Sea. Ecosystem response to changes in nutrient delivery by the Danube River after its damming in 1972. *Estua. Coast and Shelf Sci*., 54, 473-499.

Moncheva S., Stefanova K, Doncheva V., Hristova O., Dzhurova B. and Racheva E., 2015. Plankton indicators to inform eutrophication management. Proceedings MEDCOAST Conference, 06-10 October 2015, Varna, Bulgaria (in press).

Staneva, J., V.H. Kourafalou and E.V. Stanev, 2003. The response of the Black Sea ecosystem to changes of nutrient discharge from the Danube River. In: "Oceanography of the Eastern Mediterranean and Black Sea," A. Yilmaz (ed.), Tubitak publ., Ankara, Turkey, pp. 307-313.

Staneva, J.V., V.H. Kourafalou and K. Tsiaras, 2007. Modeling the seasonal cycle of the Northwestern black Sea ecosystem. *Mediterranean Marine Systems.*

Staneva J.V. , E.V. Stanev and T. Oguz, 1998. The Impact of Atmospheric Forcing and Water Column Stratification on the Yearly Plankton Cycle, NATO- in: T. Oguz and L. Ivanov (eds.) NATO-ASI Kluwer academic publisher, 301-323.

Basin scale HTL Modelling

Introduction

For more than a decade, end-to-end (E2E) models have increased the understanding of ecosystems at a broader scale including the feedbacks and interactions between coupled physical, chemical and biological systems (Fulton, 2010; Shin et al., 2010; Rose et al., 2010; Travers et al., 2007). These models were considered as integrated ecosystem models that included ecosystem components from primary producers up to top predatory organisms and their interactions with the abiotic environment (Fulton, 2010). With such models, not only were the impacts of anthropogenic activities such as fishing and pollution examined, but long-term effects of climate variability and its consequences on the ecosystem scale could have also been investigated.

The Black Sea ecosystem is of great interest for its six riparian countries two of which are EU member states. Therefore, investigation of possible future changes in this ecosystem and impacts of them on the goods and services it provides, i.e. commercial fish and shellfish, is crucial. In this research, utilising an E2E modelling tool, the near-future changes that could be observed in the Black Sea ecosystem under the influence of variable fisheries exploitation conditions were investigated.

Materials and Methods

The Black Sea EwE model used in this research is based on Akoglu et al. (2014). The EwE model of the Black Sea was built to represent the general food web structure of the inner Black Sea basin, avoiding the extremely variable conditions of the Northwestern Shelf (NWS). The model covered an area of 150 000 km^2 where fisheries operated intensively (Oguz et al., 2008) in the vicinity of the exclusive economic zones (EEZs) of the six riparian countries. The geographical representation of the model did not include depths greater than 150 m in the open Black Sea where anoxia prevails.

The coupled E2E model was set-up according to Libralato and Solidoro (2009) with Ecopath with Ecosim (EwE) utilising BIMS-ECO biogeochemical model simulation of the Black Sea between 2000-2010. The lower-trophic-level compartments of the EwE Black Sea model were adjusted and re-parameterised according to the long-time averaged outputs from the hindcast (2000-2010) simulation of the BIMS-ECO model run. The final coupled model scheme is shown in **Figure 1**.

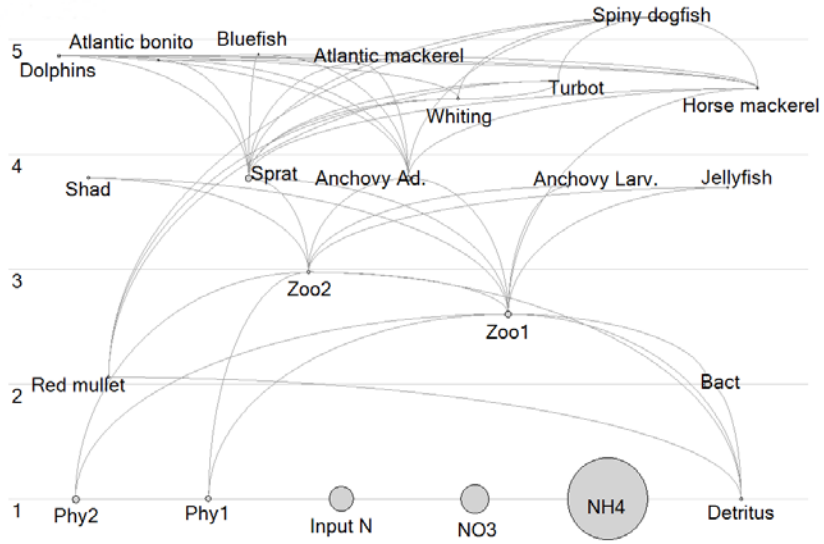

Figure 11. The structure of the BIMS-ECO - EwE coupled model of the Black Sea ecosystem.

A set of fisheries scenarios was run to test the impact of changing fisheries exploitation levels on the ecosystem structure and functioning. The scenarios and their descriptions are given in

Table 1.

Table 6. Fisheries model scenarios simulated for the years 2010-2020.

Scenario	Description
P10All	Increased fishing effort by 10% for all the fleets for the period 2010-2020 compared to 2009
M10All	Decreased fishing effort by 10% for all the fleets for the period 2010-2020 compared to 2009
P10Btwl	Increased fishing effort by 10% for trawls for the period 2010-2020 compared to 2009
M10Btwl	Decreased fishing effort by 10% for trawls for the period 2010-2020 compared to 2009
P10SPF	Increased fishing mortality by 10% for small pelagic fish species (sprat, anchovy, shad and horse mackerel) for the period 2010-2020 compared to 2009
M10SPF	Decreased fishing mortality by 10% for small pelagic fish species (sprat, anchovy, shad and horse mackerel) for the period 2010-2020 compared to 2009
P10LPF	Increased fishing mortality by 10% for large pelagic fish species (bluefish, bonito and Atlantic mackerel) for the period 2010-2020 compared to 2009
M10LPF	Decreased fishing mortality by 10% for large pelagic fish species

	(bluefish, bonito and Atlantic mackerel) for the period 2010-2020 compared to 2009

For comparison between scenarios, a set of metrics and indicators was derived utilising flows and biomasses of the coupled model simulations between the years 2010 and 2020 (**Table 2**). The time series results of these metrics and indicators were compared against the time series of metrics and indicators obtained in the BAU (business as usual, PERSEUS DoW) scenario using Kruskal-Wallis non-parametric one-way ANOVA (analysis of variance) test. Further, relative changes in the indicators and metrics in different scenarios compared to the BAU scenario were calculated utilising the formula

$$RelativeChange = \frac{(IndicatorValue_{Scenario} - IndicatorValue_{BAU})}{Indicatorvalue_{BAU}}$$

Table 7. Metrics and indicators used for assessing vigor, organisation and resilience of the Black Sea ecosystem under different fishing scenarios.

Vigor	Primary production (PP) Throughput (T) Catch
Organisation	Kempton's Q (Q) Fishing in Balance (FiB) Average Mutual Information (AMI) Ascendency (A) Finn's Cycling Index (FCI) Mean Path Length (mPL)
Resilience	Entropy - Average Mutual Information (H-AMI) Scope for Growth (SfG = Total production – Total primary production)

Results and discussions

Hindcast

The skill of the coupled model is shown in Figure 2 comparatively against statistical data (for catches), biogeochemical model simulated data (biomasses of the LTL and concentrations of the non-living groups) and other conventional model derived biomass estimates (Virtual Population Analysis (VPA) estimates for fish groups).

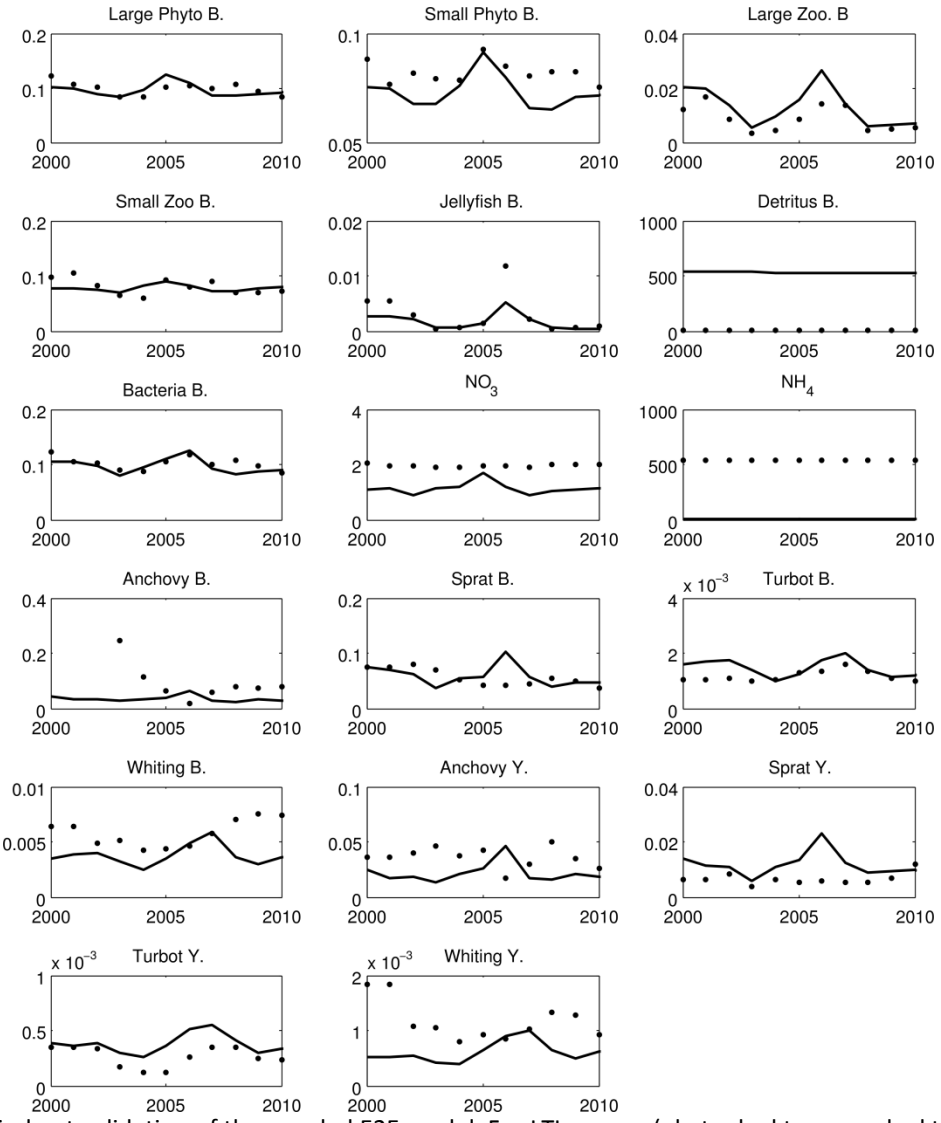

Figure 12. Hindcast validation of the coupled E2E model. For LTL groups (phytoplankton, zooplankton, jellyfish, bacteria, detritus, NH_4 and NO_3), dots represent model (standalone biogeochemical model BIMS-ECO) simulated data. For fish groups, dots represent VPA (virtual population analysis) estimated biomass values (abbreviated as "B.") and catch statistics (abbreviated as "Y."). All black lines denote E2E model simulated biomasses, concentrations or yields in gN m^{-2} y^{-1} where appropriate.

Vigor, Organisation, Resilience

The comparative summary of the indicators and metrics of the fisheries scenarios against BAU scenario is given in Table 3. Statistically significant (Kruskal-Wallis test @ p = 0.1) differences calculated in indicators and metrics compared to the BAU scenario are marked in red. The comparisons of the primary production (PP) metric between scenarios were calculated as nil because the primary production in the coupled model set-up was forced and identical in all scenarios. As can be inferred from the table, only a handful of indicators and metrics which are directly related to the fisheries (catch (Figure 3), catch/biomass (Figure 6) and FiB (Figure 4)) were found to be statistically different for certain scenarios. Many of the indicators and metrics were found to be similar between scenarios. Indicators especially related to the flows and the energetic capacity of the ecosystem did not differ significantly between scenarios because the LTL structure and its related flows were

identical and based on BAU scenario in all fishing scenarios. As can be inferred, changes in the exports from the system (different levels of fisheries exploitation) did not suffice to contrast these indicators and metrics between the fisheries scenarios.

Significant changes were observed for three catch-related indicators in scenarios where fishing pressure/effort was increased 10% for all fish species (P10All) and small pelagic fish (P10SPF) (Table 3). Acknowledging that the Black Sea fisheries dwell on small pelagic fish stocks, any increase in the fishing pressure/effort of the fleet(s) targeting small pelagic fish (i.e. purse seiners, which is one of the two fleets defined in the model) introduced significant changes in catch-related metrics; i.e. catch (Figure 3), and hence, catch/biomass (Figure 6), and indicator FiB (Figure 4). However, it is worth noting that FiB was found to be significantly different only in P10All scenario but not in P10SPF scenario contrary to the previous two metrics. This could be the result of the fact that small pelagic fish has already been exploited to its limits in the Black Sea ecosystem and a 10% increase did not suffice to create a significant change in the catches of its stocks. Contrastingly, FiB was found to be significantly different in P10Btwl, where effort of bottom trawlers was increased by 10%. This suggested that in the Black Sea, fisheries targeting benthic fish still bear a potential for development that could lead to increased catches. The increases of fishing effort/pressure in other scenarios did not introduce any fluctuations in yield so as to be reflected with a significant change in the FiB indicator. Considering large pelagic fish, scenarios (P10LPF and M10LPF) did not differ compared to the BAU scenario. This could be justified with the fact that fisheries on large pelagic fish in the Black Sea is marginal since the onset of 1970s due to the overexploitation of their stocks during 1960s, and since then, a very high exploitation level is applied on these stocks leaving no possibility for recovery of their stocks let alone significant changes in their catches (Akoglu et al., 2014).

From a holistic (ecosystem-based) point of view, all these scenarios did not introduce a change in the Black Sea ecosystem's resilience but only in its vigor (through catch) and organisation (through FiB). However, with the only changes reflected in exploitation-related indicators and metrics, it is not possible to evaluate and infer the status of its ecosystem's health. To do so, these analyses should also be complemented with LTL scenarios of RBE, REB, BA and MFA.

Table 8. Relative change in indicators between different fisheries scenarios. Red cells indicate statistically significant changes at p = 0.1 according to the Kruskal-Wallis test.

Fractional Change	PP	T	Catch	Q	FiB	AMI	A	FCI	mPL	H-AMI	SfG	C/B	mTLc
P10All	0	-0.00003	0.18186	-0.03642	0.15884	-0.00003	-0.00006	-0.00026	-0.00001	0.00001	-0.00036	0.18279	0.00133
M10All	0	0.00000	-0.00109	0.00018	-0.00104	0.00000	0.00000	0.00000	0.00000	0.00000	0.00000	-0.00109	-0.00001
P10Btwl	0	-0.00001	0.00817	-0.00922	0.13540	0.00000	-0.00001	-0.00008	-0.00001	0.00006	-0.00012	0.00957	-0.00119
M10Btwl	0	0.00000	-0.00006	0.00002	-0.00092	0.00000	0.00000	0.00000	0.00000	0.00000	0.00000	-0.00006	0.00001
P10SPF	0	-0.00002	0.17198	0.00205	0.02375	-0.00003	-0.00004	-0.00017	-0.00001	-0.00004	-0.00021	0.17114	0.00223
M10SPF	0	0.00000	-0.00168	0.00013	-0.00019	0.00000	0.00000	0.00000	0.00000	0.00000	0.00001	-0.00175	-0.00002
P10LPF	0	0.00000	0.00065	-0.02776	-0.00029	0.00000	-0.00001	0.00000	0.00000	0.00001	-0.00004	0.00070	0.00008
M10LPF	0	0.00000	0.00000	0.00036	0.00000	0.00000	0.00000	0.00000	0.00000	0.00000	0.00000	-0.00001	0.00000

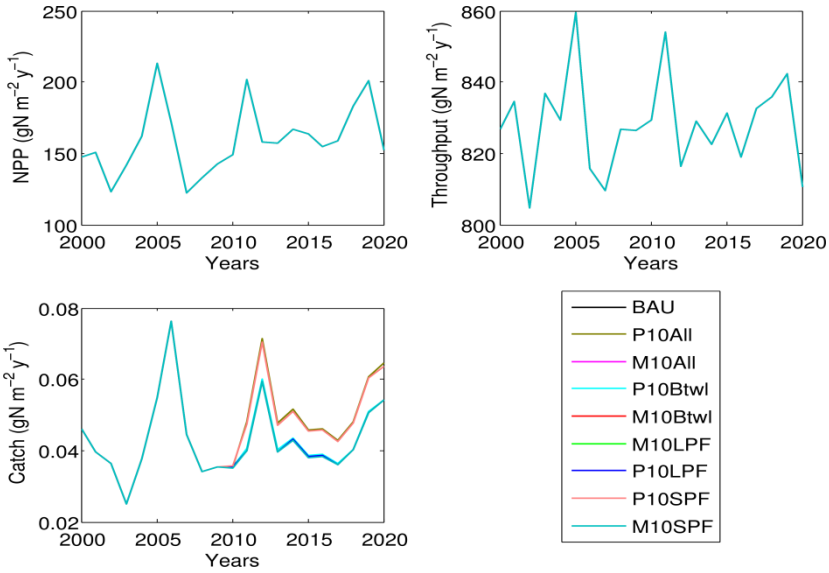

Figure 13. Indicators and metrics related to the ecosystem's vigor.

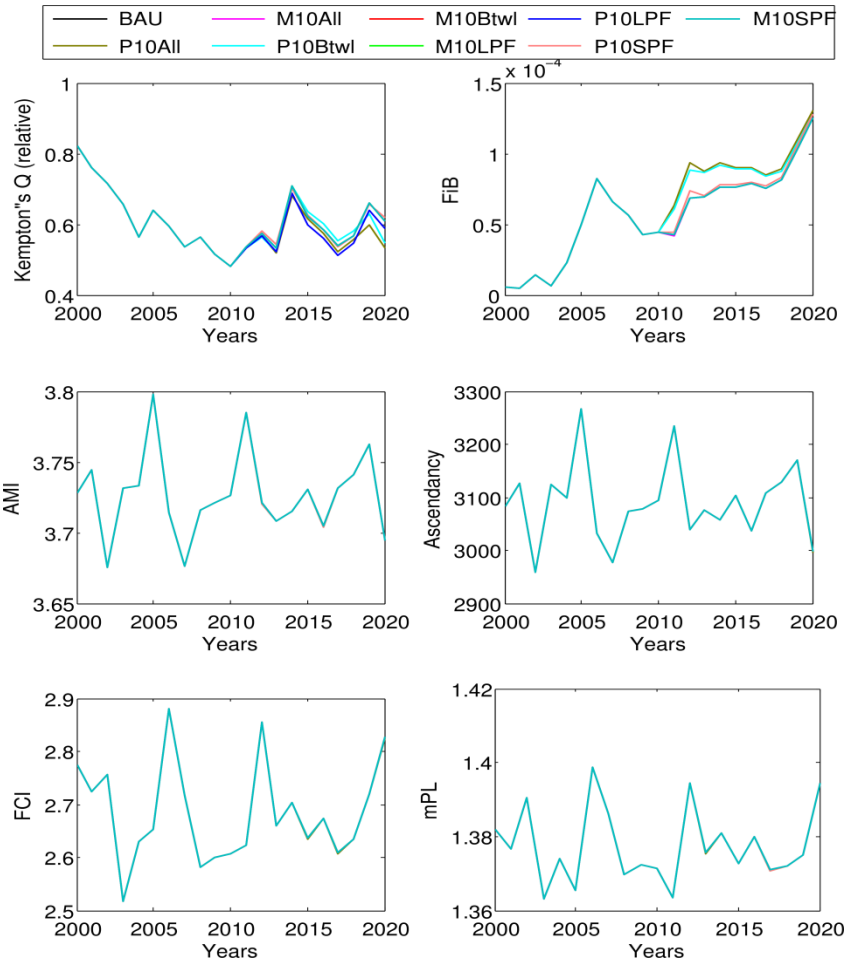

Figure 14. Indicators and metrics related to the ecosystem's organisation.

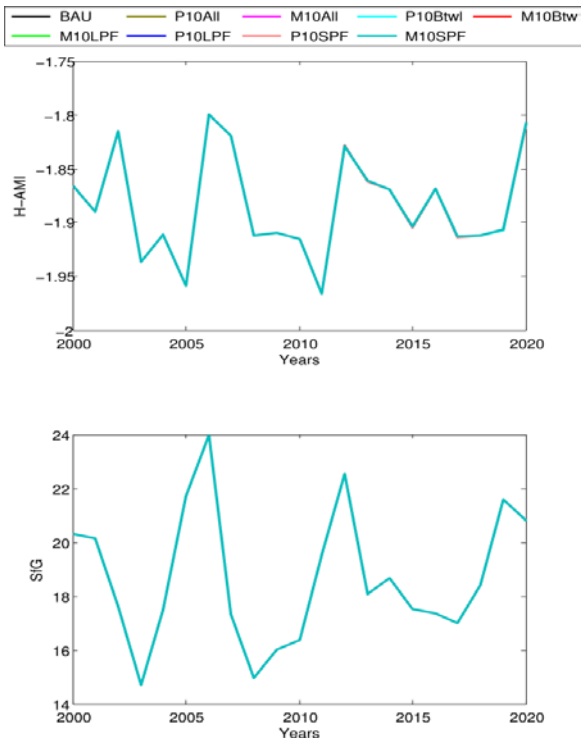

Figure 15. Indicators and metrics related to the ecosystem's resilience.

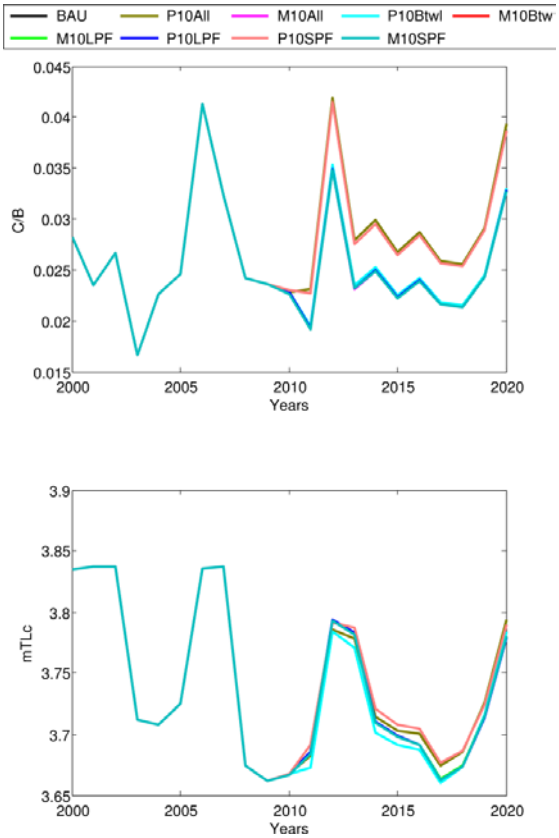

Figure 16. Other commonly used indicators and metrics.

References

Akoglu, E., Salihoglu, B., Libralato, S., Oguz, T., Solidoro, C., 2014. An indicator-based evaluation of the Black Sea food web dynamics during 1960 - 2000. Journal of Marine Systems, 134, 113 – 125.

Fulton, E. A., 2010. Approaches to end-to-end ecosystem models. Journal of Marine Systems, 81, 171–183.

Oguz, T., Fach, B., Salihoglu, B., 2008. Invasion dynamics of the alien ctenophore *Mnemiopsis leidyi* and its impact on anchovy collapse in the Black Sea. Journal of Plankton Research, 34(II), 1385-1397.

Rose, K. A., Allen, J. I., Artioli, Y., Barange, M., Blackford, J., Carlotti, F., Cropp, R., Daewel, U., Edwards, K., Flynn, K., Hill, S. L., HilleRisLambers, R., Huse, G., Mackinson, S., Megrey, B., Moll, A., Rivkin, R., Salihoglu, B., Schrum, C., Shannon, L., Shin, Y. –J., Smith, S. L., Smith, C., Solidoro, C., St. John, M., Zhou, M., 2010. End-To-End Models for the Analysis of Marine Ecosystems: Challenges, Issues, and Next Steps, Marine and Coastal Fisheries: Dynamics, Management, and Ecosystem Science, 2, 115-130.

Shin, Y. –J., Travers, M., Maury, O., 2010. Coupling low and high trophic levels models: Towards a pathways-orientated approach for end-to-end models. Progress in Oceanography 84, 105–112.

Travers, M., Shin, Y. –J., Jennings, S., Cury, P., 2007. Towards end-to-end models for investigating the effects of climate and fishing in marine ecosystems. Progress in Oceanography, 75, 751–770.


PERSEUS
POLICY-ORIENTED MARINE
ENVIRONMENTAL RESEARCH IN
THE SOUTHERN EUROPEAN SEAS